# THERMO-MECHANICALLY COUPLED NUMERICAL AND EXPERIMENTAL STUDY ON 7075 ALUMINUM FORGING PROCESS AND DIES

A THESIS SUBMITTED TO
THE GRADUATE SCHOOL OF NATURAL AND APPLIED SCIENCES
OF
MIDDLE EAST TECHNICAL UNIVERSITY

BY

MEHMET CİHAT ÖZCAN

IN PARTIAL FULFILLMENT OF THE REQUIREMENTS
FOR
THE DEGREE OF MASTER OF SCIENCE
IN
MECHANICAL ENGINEERING

SEPTEMBER 2008

Approval of the thesis:

THERMO-MECHANICALLY COUPLED NUMERICAL AND EXPERIMENTAL STUDY ON 7075 ALUMINUM FORGING PROCESS AND DIES

submitted by **MEHMET CİHAT ÖZCAN** in partial fulfillment of the requirements for the degree of **Master of Science in Mechanical Engineering, Middle East Technical University** by,

Prof. Dr. Canan ÖZGEN
Dean, Graduate School of **Natural and Applied Sciences** _____

Prof. Dr. Kemal İDER
Head of the Department, **Mechanical Engineering** _____

Prof. Dr. Mustafa İlhan GÖKLER
Supervisor, **Mechanical Engineering Dept., METU** _____

Prof. Dr. Haluk DARENDELİLER
Co-Supervisor, **Mechanical Engineering Dept., METU** _____

**Examining Committee Members:**

Prof. Dr. Metin AKKÖK
Mechanical Engineering Dept., METU _____

Prof. Dr. Mustafa İlhan GÖKLER
Mechanical Engineering Dept., METU _____

Prof. Dr. Haluk DARENDELİLER
Mechanical Engineering Dept., METU _____

Prof. Dr. Haluk AKSEL
Mechanical Engineering Dept., METU _____

Prof. Dr. Ali KALKANLI
Metallurgical and Materials Engineering Dept., METE _____

Date: _____

I hereby declare that all information in this document has been obtained and presented in accordance with academic rules and ethical conduct. I also declare that, as required by these rules and conduct, I have fully cited and referenced all material and results that are not original to this work.

Name, Last Name: Mehmet Cihat ÖZCAN

Signature:

## ABSTRACT

THERMO-MECHANICALLY COUPLED NUMERICAL AND EXPERIMENTAL STUDY ON 7075 ALUMINUM FORGING PROCESS AND DIES

ÖZCAN, Mehmet Cihat

M.Sc., Department of Mechanical Engineering
Supervisor: Prof. Dr. Mustafa İlhan GÖKLER
Co-Supervisor: Prof. Dr. Haluk DARENDELİLER

September 2008, 142 pages

Combination of high strength with light weight which is the prominent property of aluminum alloy forgings has led aluminum forgings used in rapidly expanding range of applications.

In this study, to produce a particular 7075 aluminum alloy part, the forging process has been designed and analyzed. The forging process sequence has been designed by using Finite Volume Method. Then, the designed process has been analyzed by using Finite Element Method and the stress, strain and temperature distributions within the dies have been determined. Five different initial temperatures of the billet; 438 °C, 400 °C, 350 °C, 300 °C and 250 °C, have been considered in the thermo-mechanically coupled simulations. The initial temperatures of the dies have been taken as 200 °C for all these analyses. Finite volume analysis and finite element analysis results of the preform and finish part have been compared for the initial billet temperature of 400 $^{o}$C. Close results have been observed by these analyses. The experimental study has been carried out for the range of the initial billet temperatures of 251–442 $^{o}$C in METU-

BILTIR Center Forging Research and Application Laboratory. It has been observed that the numerical and the experimental results are in good agreement and a successful forging process design has been achieved. For the initial die temperature of 200 $^{o}$C, to avoid the plastic deformation of the dies and the incipient melting of the workpiece, 350 $^{o}$C is determined to be the appropriate initial billet temperature for the forging of the particular part.

**Keywords:** Aluminum Forging, Forging Process Design, Finite Volume Analysis, Finite Element Analysis, Thermo-Mechanically Coupled Analysis.

# ÖZ


7075 ALUMİNYUM DÖVME PROSESİ VE KALIPLARI ÜZERİNE TERMO-MEKANİK SAYISAL VE DENEYSEL ÇALIŞMA

ÖZCAN, Mehmet Cihat

Yüksek Lisans, Makina Mühendisliği Bölümü
Tez Yöneticisi: Prof. Dr. Mustafa İlhan GÖKLER
Ortak Tez Yöneticisi: Prof. Dr. Haluk DARENDELİLER

Eylül 2008, 142 Sayfa

Alüminyum dövme parçalarının seçkin özelliği olan yüksek mukavemetin ve düşük ağırlık ile kombinasyonu, alüminyum dövme parçalarının kullanım alanlarını hızlı bir şekilde yaygınlaştırmaktadır.

Bu çalışmada, 7075 alüminyum alaşımından yapılmış olan bir parçayı üretebilmek için dövme prosesi tasarlanmış ve analiz edilmiştir. Dövme uygulaması Sonlu Hacim Metodu kullanılarak tasarlanmıştır. Daha sonra; tasarlanan proses Sonlu Elemanlar Metodu kullanılarak analiz edilmiştir ve kalıplardaki gerilimler, gerinimler, sıcaklık dağılımları belirlenmiştir. Termo-mekanik simülasyonlar, 438 °C, 400 °C, 350 °C, 300 °C ve 250 °C olmak üzere iş parçasının beş farklı başlangıç sıcaklık değeri dikkate alınarak gerçekleştirilmiştir. Kalıpların başlangıç sıcaklık değeri bütün analizlerde 200 °C olarak alınmıştır. İş parçasının 400 °C başlangıç sıcaklığında gerçekleşen, sonlu hacim analizinin ve sonlu elemanlar analizinin önform ve son parça için elde edilen sonuçları karşılaştırılmıştır. Bu analizlerde yaklaşık sonuçlar elde edilmiştir. Deneysel çalışma, iş parçasının 251–442 $^{o}$C başlangıç sıcaklıkları arasında, ODTÜ-BİLTİR Merkezi Dövme Araştırma ve Uygulamaları

Laboratuarında yapılmıştır. Sayısal sonuçlarla deneysel sonuçların birbiriyle tutarlı olduğu gözlenmiştir ve başarılı bir dövme proses tasarımı gerçekleştirilmiştir. 200 $^{o}$C kalıp başlangıç sıcaklık değerinde, kalıplar üzerinde kalıcı deformasyonu ve iş parçasının anlık erimesini önlemek için iş parçasının 350 $^{o}$C başlangıç sıcaklığının parçanın dövülebilmesi için uygun sıcaklık olduğuna karar verilmiştir.

**Anahtar Kelimeler:** Alüminyum Dövme, Dövme Proses Tasarımı, Sonlu Hacim Analizi, Sonlu Elemanlar Analizi, Termo-Mekanik Analiz.

To My Family

**ACKNOWLEDGEMENTS**

I express sincere appreciation to my supervisor Prof. Dr. Mustafa İlhan Gökler and my co-supervisor Prof. Dr. Haluk Darendeliler for their great guidance, advice, criticism, systematic supervision, encouragements, and insight throughout the study.

I would like to thank to TÜBİTAK for providing support at the beginning of the thesis.

I wish to thank Mr.Cevat Kömürcü, Mrs.Tülay Kömürcü, Mrs.Tülin Özkan, from AKSAN Steel Forging Company, Mr. Melih Şahin from FNSS Defense Systems Inc. and Ahmet Kurt from ASELSAN Inc. The technical assistance of them is gratefully acknowledged. I also would like to thank to METU-BILTIR Research and Application Center for the facilities provided for my work.

My special thanks go to my colleagues, Arda Özgen, Özgür Cavbozar, Hüseyin Öztürk, Ulaş Göçmen, Derya Akkuş for their valuable support and aid; to my senior colleagues Sevgi Saraç, İlker Durukan, Mehmet Maşat and Kazım Arda Çelik for their support and guidance.

I also would like to thank to Halit Şahin, Ali Demir, Hüseyin Ali Atmaca, Tarık Öden, Filiz Güngör Sutekin, Arzu Öztürk, Halime Küçük and Mehmet Ali Sarıhan for giving me support.

I also want to thank my beloved family, my mother Kadriye Özcan, my father Yusuf Ziya Özcan, my sister Esra Güney and her husband Tekin Güney for their encouragement and faith in me.

**TABLE OF CONTENTS**

## LIST OF FIGURES

## LIST OF TABLES

# CHAPTER 1

# INTRODUCTION

## 1.1 Aluminum in Industry

Aluminum's unique properties which are light weight, high strength and resistance to corrosion make it an ideal material for use in conventional and novel applications. It is only one third as heavy as steel. Besides, the strength to weight ratio of aluminum is relatively higher than steel [1]. Although it costs much more per kilogram than steel because of its light weight it is cheaper per unit volume.

Aluminum has become increasingly important in the production of automobiles and trucks, packaging of food and beverages, construction of buildings, transmission of electricity, production of defense and aerospace equipment, manufacture of machinery and tools, and production of durable and consumer products. As demand for more technologically complex and ecologically sustainable products increases, opportunities for aluminum will continue to expand [2].

It must be noted that although the reduction by two thirds of the weight of an aluminum part compared with a similarly sized steel part generally seems attractive, this replacement is accompanied by a reduction by two thirds in the stiffness of the part. So although direct replacement of steel part with a duplicate made from aluminum may give acceptable strength to withstand peak loads, the increased flexibility will cause three times more deflection in the part. Therefore, when excessive flex is undesirable due to the design requirements, replacement of steel with similarly sized aluminum is generally not recommended.

Other important structural limitation of aluminum is its fatigue properties. While steel has a high fatigue limit (the structure can theoretically withstand an infinite number of cyclical loadings at this stress), aluminum's fatigue limit is near zero, meaning that it will eventually fail under even very small cyclic loadings, but for small stresses this can take an exceedingly long time [3].

### 1.2 Aluminum Alloys

Much work has been done to develop aluminum alloys which have much greater strength than pure aluminum and still retain the advantage of light weight, good conductivity and corrosion resistance. Aluminum alloys replaces the steel, in most cases, only where the need of lightness, corrosion resistance, or high thermal and electrical conductivity offsets the added cost.

While the majority of aluminum alloys are made from the heat treatable alloys produced by ingot metallurgy, advanced alloys have been developed for specific property improvements. The aluminum-lithium series, for example, provides high strength and increased elastic modulus with reduced density. Premium strength alloys have also been developed by consolidating rapidly solidified powders into forging stock [2]. These alloys are particularly resistant to corrosion. Aluminum alloy composites, reinforced with silicon carbide particulate, provide improved strength over conventional aluminum alloys.

More information about aluminum and aluminum alloys are given in Appendix A.

### 1.3 Aluminum Forging

There is an increasing demand for "strong" but "light weight" parts in industry. Aluminum forged parts consist of both properties and they are already being used in developed countries.

After 1960, aluminum forging was applied for automobile parts because it had a high strength to weight ratio and it was particularly applicable producing precise, intricate shapes with good surface finishes. For instance, pistons for racing motorcycles were forged from 4032 alloy at 400 °C and valve lifters for sport cars were forged at the room temperature. The amount of aluminum which was forged has increased since about 1970 after forging of aluminum wheels started. If much stronger aluminum alloy to be forged is found, for instance by increasing the silicon content, aluminum application to the motor car industry can be accelerated [2].

The main reasons for the use of aluminum forged products in automotive industry are as follows:

- Structurally most efficient products
- High damage tolerance and impact resistance
- Opportunity to produce products very close to end product
- High production volumes

Some application areas of aluminum alloy forgings are as follows:

- Used primarily for structural components such as the intake of gas turbine engines.
- Used in helicopters, piston-engine planes, commercial jets and supersonic military aircraft. Many aircrafts contain more than 450 structural forgings as well as hundreds of forged engine parts.
- Used as housings, casings, linkages for a variety of mechanical systems.
- Used in automotive applications where commonly shock and stress are critical such as: Connecting rods, pistons, crankshaft, gears, axle beams, steering arms, wheel spindles.

Figure 1.1 shows variety of aluminum forged parts.

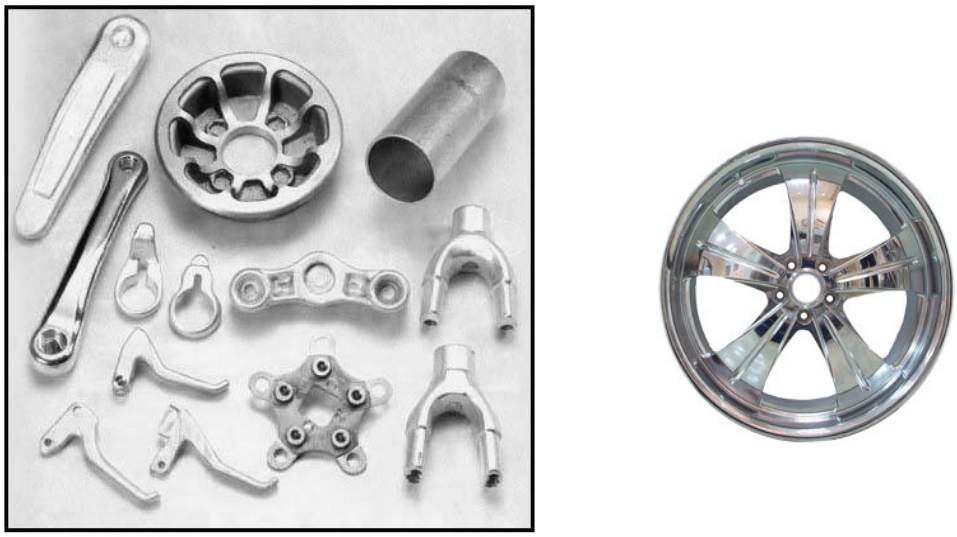

**Figure 1.1 Some Aluminum Forged Parts**

In USA, Europe, Asia and Australia, there is an increasing demand for aluminum alloy forgings. In Europe, especially in automotive industry, to decrease the weight of the cars and to reduce energy consumption, the tendency of use of aluminum alloy forgings has increased. In India, aluminum forging constitutes 14% of total forging and this ratio is continuously increasing. In Japan, although this ratio is about 2%, recently there have been important improvements [4]. Aluminum forging companies have started to cooperate with automotive companies and they have been working intensely to improve aluminum forged parts. For instance, Honda Legend, 2004 brand car of Honda, has 200 kg aluminum parts, 23% of which is aluminum forged parts [5]. In Turkey, there is little information and application about aluminum forging.

Despite these increments in aluminum forging, forgings still constitute a small percentage of total aluminum usage however; their importance in load transmission applications offsets their low numbers.

## 1.4 Usage of CAD/CAM/CAE in Forging

Today, in some of the forging companies, design of the dies and selection of the process conditions in forging process are still performed by trial and error methods to a large extend. In many cases, this approach causes waste of material, early die wear, increasing cost, etc. With the development of Computer-Aided-Design (CAD), Computer-Aided-Manufacturing (CAM) and Computer-Aided-Engineering (CAE) techniques, the reduced time and effort on design and manufacturing stages have become possible.

By using CAD/CAM softwares, 3-D models of the forgings, preform and finish dies can be created. So that parameters such as dimensions, drafts, fillet radii, the shrinking factor, etc. can be easily changed.

By using CAE programs, necessary information such as material flow in the dies, level of die fill, defects, strain, stress, temperature distribution on the workpieces and the dies, and working force can be easily obtained. CAE programs used in forging applications are based on Finite Element Method and Finite Volume Method.

In Finite Element Method (FEM), the deformation zone in an elastic-plastic body is divided into a number of elements interconnected at a finite number of nodal points. Applications of FEM include linear and nonlinear structural, thermal, dynamic, electromagnetic, and flow analysis. Since there is severe element distortion in metal forming operations, remeshing is necessary to follow the gross material deformation. MSC. SuperForm is based on this technology.

To be able to successfully apply the FEM to the metal forming operations, the following requirements should be fulfilled [6]:

1- The physical problem should be well-defined for the application of simulation.

2- The idealization of this problem should be done correctly: Simplifications and assumptions should be reasonable. Unnecessary details should be eliminated.

3- The idealized problem should have the correct spatial discretization: Type of elements used, topology of element mesh, and the density of element mesh should be constructed according to the nature of problem.

4- Boundary conditions of the physical model should be investigated and applied in the simulation: friction, heat transfer, machines, dies etc.

5- Correct material laws and parameters should be used in the simulation: flow curve, anisotropy, failure, etc.

6- Numerical parameters used in the simulation should be chosen accordingly: penalty factors, convergence limits, increment sizes, remeshing criteria, etc.

7- The simulation should be "economical": Computation times and the time required to prepare the model should be reasonable, storage requirements of the model and the results should also be within physical limits.

8- The results should be evaluated carefully and checked whether they are reasonable or not.

Finite element simulation of the forging process is complicated by the large displacements and the large strains that the material is subjected to. Because of the large displacements, the relationship between the strain and the displacement becomes nonlinear. There are other causes of nonlinearity in forging problems. Basically there are three types of nonlinearity [7]:

1- Material nonlinearity (physical)

2- Geometric nonlinearity (kinematic)

3- Changing boundary conditions

Material nonlinearity is due to the nonlinear relationship between stress and strain like in elastic-plastic (i.e. elastoplastic), elasto-viscoplastic materials, creep, composite and concrete structure problems etc. Geometric nonlinearity is aroused from nonlinear relationship between strains and displacements, and nonlinear relationship between stresses and forces. Changing boundary conditions also contribute to nonlinearity. If the loads on the structure vary with the displacements, nonlinearity occurs. Moreover, contact and friction problems lead to nonlinear boundary conditions.

Finite Volume Method (FVM) is particularly suited for simulating the gross material deformations inherent in forging operations. Unlike a traditional finite element mesh, which distorts while attempting to follow the deformation material, the mesh is a fixed frame of reference and material simply flows through the finite volume mesh completely. FVM eliminates the need for volume remeshing techniques and commonly considered as the main bottleneck in 3-D forging simulations based on the FEM [8]. MSC. SuperForge is based on this technology.

## 1.5 Some Previous Studies

Some previous studies have been conducted on different types of forgings in METU-BILTIR Research and Application Center [6-18].

As a Ph.D. study at University of Birmingham, Gökler [9] developed a computer program for the design of the operational sequences and the dies for horizontal forging machines.

Alper [10] developed a computer program for axisymmetric press forgings, which designs the forging geometry and the die cavity for preforms and finishing operation.

Elmaskaya [11] studied on upset forging process and the design limits for tapered preforms by using the elastic-plastic Finite Element Method.

Kutlu [12] studied on the design and analysis of preforms in hot forging for non-axisymmetric press forging. In this study, the importance of volume distribution along the length of part was shown for reducing the wear of finishing die and process of forging of gear fork was revised to reduce wear of dies and waste of material.

İsbir [6] studied on the finite element simulation of shearing using the element elimination method to examine trimming operation on forged parts.

Karagözler [13] studied on the analysis and preform design for long press forgings with non-planar parting surfaces.

Civelekoğlu [14] examined three different alloy steels, which had been hot forged in industry. The flow of the material, stress distribution, die filling and the effects of the process parameters on the forging were investigated. Three industrial forging parts; M20 and M30 eye bolts and a runner block were studied. The results of the simulations were compared with the findings of the experiments carried out in a forging company.

Gülbahar [15] studied on the preform design and analysis of hot forging process for a heavy vehicle steering joint. A method was proposed for the design of the preform dies to reduce the material wastage, number of applied strokes and production costs. The designed operations were examined by using commercially available finite volume analysis software. The designed process was verified by the experimental work in a forging company. As a result of this study, remarkable reduction in the flash was achieved with a reasonable number of forging operations.

Abachi [16] studied the analysis of die wear. Results from computer simulation were compared with the measurement on the worn die taken from industry and

evaluation of wear coefficient from comparison of computer simulation and the measurement from worn die were done.

Aktakka [17] studied hot and warm forging processes of a part which was used in automotive industry. The processes in different temperatures of the part, in which 1020 carbon steel was used, were analyzed by the finite volume analysis software, MSC. Superforge. The results of these analyses compared with the results of the experimental tests that were performed in a forging company.

Maşat [18] studied precision forging of a particular standard spur gear. A precision forging die design was done to produce near-net shape spur gears with hot forging process by a single forging stroke.

Saraç [7] studied on design and thermo-mechanical analysis of warm forging process and dies. Forging process of a part which was produced within the hot forging temperature range and which needed some improvements in accuracy, material usage and energy concepts, was analyzed. The forging process sequence design with a new preform design for the particular part was proposed in warm forging temperature range and the proposed process was simulated using Finite Element Method.

In aluminum forging, there are not many studies that have been made. Altan, F. W. Boulger, J. R. Becker, N. Akgerman and H. J. Henning [1] briefly explained the general characteristics and parameters of aluminum forging.

In the study prepared by ASM Handbook Committee [2], the general characteristics and parameters of aluminum forging was explained.

In the study of George E. Totten and D. Scott Mackenzie [2], design aspects of aluminum forging were described. Also the general characteristics of aluminum forging were mentioned.

In the study of Jensrud and Pedersen [20], cold forging of high strength aluminum alloys were investigated and a new thermo-mechanical processing for

the economical forging process by reducing the preform steps compared with cold forging was developed.

In the study of Tanner and Robinson [21], methods to reduce the residual stress in 2014 aluminum alloy forging were examined.

In the study of Yoshimura and Tanaka [22], precision forging of aluminum forging and their parameters were investigated and results were compared with precision forging of steels.

### 1.6 Scope of the Thesis

A combination of high strength with light weight which is the outstanding properties of aluminum alloy forgings has led to a rapidly expanding range of applications. Aluminum forging technology is also equally notable for the ease with which unusual shapes and extremely large components with excellent mechanical properties can be obtained. However, in Turkey, there is not much research about aluminum forging and there are not many applications of aluminum forging.

The scope of this study is to design and analyze of producing a particular 7075 aluminum alloy part by forging operation. This part is currently produced by machining operation in industry so an alternative method of producing this part is proposed in this study.

General characteristics of aluminum forging will be discussed in Chapter 2 to provide a basis for the study. The forging process sequence and die design for the sample part will be presented in Chapter 3. Results of the analysis of the designed process and the dies using FEM will be given in Chapter 4, in detail. Experimental study carried out in METU-BILTIR Center Forging Research and Application Laboratory will be presented in Chapter 5. Finally, conclusions and suggestions for future works will be given in Chapter 6.

# CHAPTER 2

# GENARAL CHARACTERISTICS OF ALUMINUM FORGING

## 2.1 Introduction

In Chapter 1, the use of aluminum in industry and the importance of aluminum forging have been discussed. In this chapter, general characteristics and parameters of aluminum forging will be explained in detail.

Since aluminum alloys are very ductile at hot working temperature range and do not develop scale during heating, forging of aluminum alloys is particularly applicable producing precise, intricate shapes with good surface finish. However, there are limitations to the geometric complexity that can be obtained. During the forging process, the force applied to the material by the forging equipment generates pressure that forces metal to flow into intricate cavities of the die. Long, thin cavities require high pressure to force the material into them. If excessive pressure is required, the total forging load may exceed the capacity of the forging equipment. In addition, localized stresses in the die due to high pressure in the die cavities may become large enough to cause overloading failure of the die, fatigue cracking due to repeated loading, and rapid die wear in high metal flow regions. An additional limitation to shape complexity is the possibility of defect formation in the material during forging. In particular as the material flows around small corner radii on the die (the result of small fillet radii on the part) laps and cracks may occur [2].

Although some of the low-strength aluminum alloys, such as 1100 and 6061 require considerably less forging pressure than 1020 steel, a high strength aluminum alloy, such as 7075, requires considerably more pressure to produce the same forged shape. Other aluminum alloys, such as 2219, require

approximately the same forging pressures as required by low-carbon steels. Generally speaking, aluminum alloys are considered to be more difficult to forge than low-carbon steels and many alloy steels. Figure 2.1 compares the flow stresses of some commonly forged aluminum alloys at 350 °C to 370 °C and at a strain rate of 4 to 10 $s^{-1}$ to 1025 carbon steel forged at an identical strain rate but at a forging temperature typically employed for this steel [23].

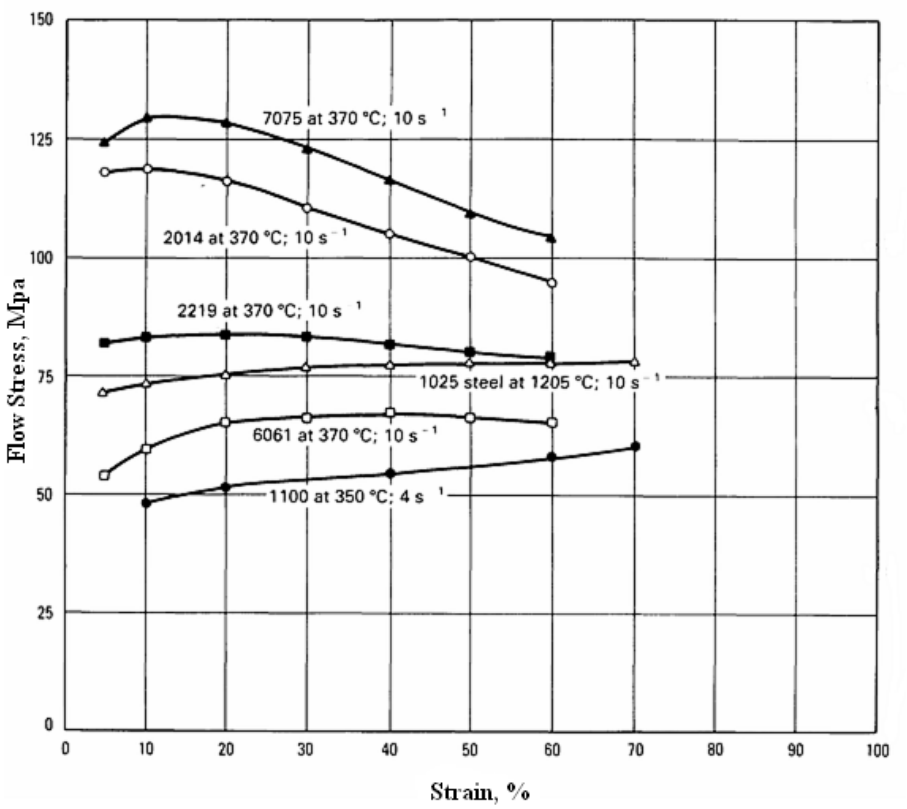


**Figure 2.1 Flow stresses of Commonly Forged Aluminum Alloys and of 1025 Steel at Typical Forging Temperatures and Various Levels of Total Strain [23]**

Methods used for forging aluminum alloys include open die, closed die, upset and roll forging, and ring rolling [19]. Two types of these are sometimes used in sequence to obtain a desired shape.

*Open die forging:* This method often used to produce small quantities, for which the construction of expensive closed dies is not justified. Open die forging is also used to make preforms, which are later completed in closed dies.

*Closed die forging:* By far the greatest tonnage of aluminum forgings is produced in closed dies. Three types of aluminum forgings are shaped in closed dies: blocker type, conventional, and close tolerance.

*Upset Forging:* This method is sometimes the sole process used in forging a specific shape from aluminum. Large bolts are an example. For other products, upset forging is used as preliminary operation.

*Roll Forging:* This method can be used as preliminary operation to save metal or to reduce the number of closed die operations. The decision as to whether or not roll forging is to be used as a preliminary operation is based on cost.

*Ring Rolling:* This method is being used successfully to produce ringlike parts from aluminum. The technique used for ring rolling of aluminum is essentially the same as that used for steel.

## 2.2 Forgeability of Aluminum Alloys

Forgeability represents the ability of a metal to be deformed without failure, regardless of the magnitude of load and stresses required for deformation. Although all aluminum alloys have good forgeability from the standpoint of ductility, the energy and load requirements vary appreciably with composition [19]. Figure 2.2 illustrates the relative forgeability of the ten alloys that comprise the major tonnage of aluminum alloy forgings [19]. The arbitrary units shown on the vertical axis of Figure 2.2 are based principally on deformation per unit of energy absorbed at the various temperatures ordinarily used for forging these alloys.

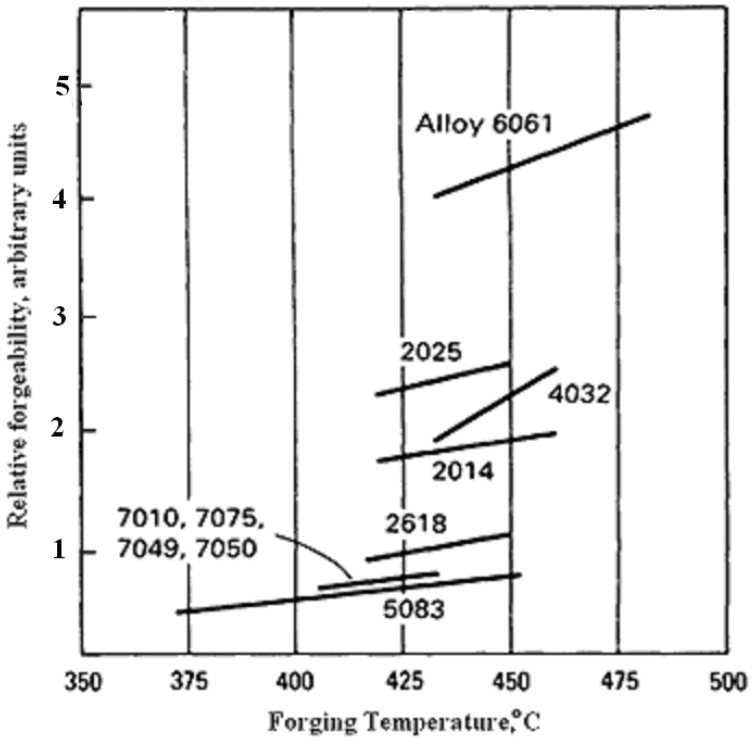


**Figure 2.2 Forgeability and Forging Temperatures of Ten Aluminum Alloys [19]**

There are wrought aluminum alloys, such as 1100 and 3003, whose forgeability would be rated significantly above those presented; however, these alloys have limited application in forging because they cannot be strengthened by heat treatment [23].

## 2.3 Effect of Temperature in Aluminum Forging

As shown in Figure 2.2, forgeability of alloys is affected by forging temperature. But there is considerable variation in the effect of temperature on forgeability. Alloy 4032 shows the most marked response while 7000 series alloys show the least effect.

Flow stress curves at different temperatures of two aluminum alloys; 6061 and 7075 are shown in Figure 2.3. This figure shows the significant effect of

temperature on the flow stress; decreasing the forging temperature by 100 °C from 350 °C, more than doubles the flow stress, while increasing the forging temperature by 100 °C from 350 °C, decreases the flow stress by approximately one-half [2]. Therefore, selection of the forging temperature has a critical effect on the ease of the flow of materials, and resulting precision and detail that can be formed in the forged part.

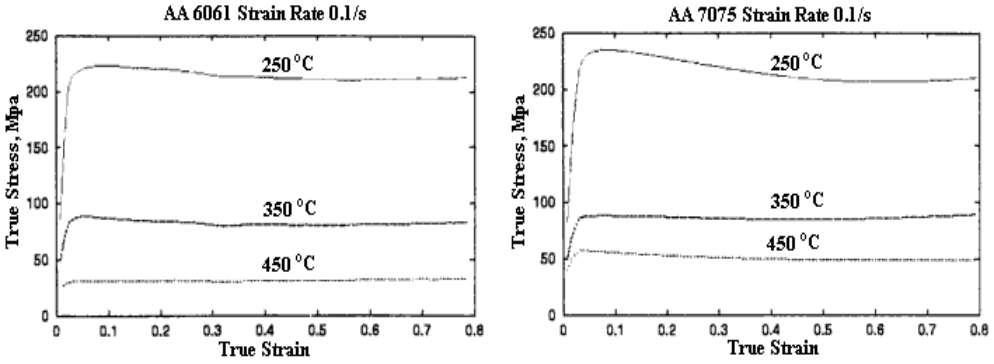


**Figure 2.3 Flow Stress Curves of Aluminum Alloy 6061 and Aluminum Alloy 7075 at Different Temperatures [2]**

The comparison of typical forging temperatures of some metals with that of aluminum alloys are tabulated in Table 2.1 [19]. Actual temperatures may vary 40 °C or more from those listed in Table 2.1, depending on the composition of the particular alloy being forged.

**Table 2.1 Typical Forging Temperatures for Various Metals [19]**

| Metals | Temperature (°C) |
|---|---|
| Magnesium Alloys | 370 |
| Aluminum Alloys | 425 |
| Copper Alloys | 815 |

**Table 2.1 Typical Forging Temperatures for Various Metals [19] (Continued)**

| Metals | Temperature (°C) |
|---|---|
| Tool Steels | 1035 |
| Stainless Steels | 1200 |
| Carbon and Alloy Steels | 1260 |

Temperatures which have been recommended for forging aluminum alloys are tabulated in Table 2.2 [1]. These temperatures are at about 70 °C below the solidus temperature of these alloys. This can cause the risk of incipient melting when conditions of forging promote significant temperature increases. Such increases are caused by either too rapid or too large forging reductions. Because, the heat generated has little time to diffuse into the dies. If incipient melting occurs; forgings will sometimes rupture and will be permanently damaged. This possibility is greatest in mechanical and hammer forging.

**Table 2.2 Temperatures Recommended for Forging Aluminum Alloys [1]**

| Temperatures Recommended for Forging Aluminum Alloys | |
|---|---|
| Alloy | Forging Temperature °C |
| 2025 | 420-450 |
| 2218 | 405-450 |
| 2219 | 427-470 |
| 3003 | 315-405 |
| 4032 | 415-460 |
| 5083 | 405-460 |
| 6061 | 432-482 |

**Table 2.2 Temperatures Recommended for Forging Aluminum Alloys [1] (Continued)**

| Temperatures Recommended for Forging Aluminum Alloys | |
|---|---|
| **Alloy** | **Forging Temperature °C** |
| 6151 | 432-482 |
| 7039 | 382-438 |
| 7075 | 382-438 |
| 7079 | 405-455 |

## 2.4 Effect of Deformation Rate in Aluminum Forging

Although, aluminum alloys are generally not considered to be as sensitive to strain rate as other materials, such as titanium and nickel/cobalt-base superalloys, selection of the strain rate in a given forging process affects the flow stress seriously. As shown in Figure 2.4, increasing the strain rate from 0.1 per sec to 20 per sec increases the flow stress of aluminum alloy 7075 by one-half at the typical forging temperature of 350 °C [2].

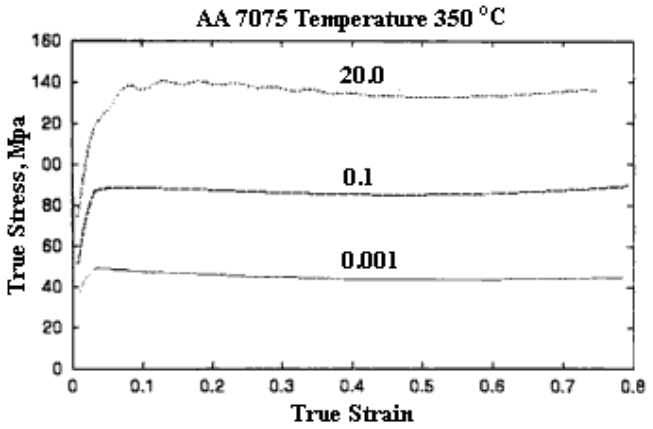


**Figure 2.4 Flow Stress of Aluminum Alloy 7075 at Different Strain Rates [2]**

## 2.5 Cutting of Aluminum Alloys

Two methods which are usually used for cutting aluminum alloys are sawing and shearing. Abrasive cut-off may be used, but it is slower than sawing for aluminum.

Sawing with a circular saw having carbide-tipped blades is the fastest, and generally the most satisfactory method. However, sawing produces burrs that may trigger defects when the stock is forged in closed dies.

Shearing is less used for aluminum than steel. Because the aluminum billets are softer, most likely mutilated in shearing and generally have more ragged sheared ends than steels. If shearing is done to cut the aluminum alloy then the ends of the billets should be conditioned to remove the rough edges and torn areas.

## 2.6 Heating of Aluminum Alloys

Gas-fired furnaces are the most widely used for heating aluminum for forging, mainly because gas is widely available and is usually the least expensive source of heat. Furnace design and construction necessarily vary with the requirements of the operation.

Oil-fired furnaces may be used if gas is not available. The oil must be low in sulfur content to avoid high-temperature oxidation, especially if used in a semimuffle furnace rather than a fullmuffle furnace.

Electric furnaces are entirely satisfactory for heating aluminum alloys, but in most areas they cost more to operate than fuel-fired types, and hence they are seldom used.

Aluminum alloys form a very strong oxide coating upon heating. Because of this coating, aluminum alloys do not have scale to the same extent as steel does.

However, most aluminum alloys are susceptible to hydrogen pickup during heating.

Excessive hydrogen pickup in forged aluminum alloys shows itself in two ways. The first is high-temperature oxidation, which is usually indicated by blisters on the surface of the forging. The second is bright flakes, or unhealed porosity, which is usually found during the high-resolution ultrasonic inspection of final forgings [23]. Both types of hydrogen pickup are influenced by furnace equipment in which water vapor as a product of combustion is the primary source of hydrogen. Fullmuffle gas-fired furnaces or low relative humidity electric furnaces provide the least hydrogen pickup.

Because of the relatively narrow temperature ranges for forging aluminum alloys, good control of temperature is important. The furnace should be equipped with pyrometric controls that can maintain temperature within ± 5 °C [23].

Heating time for aluminum alloys varies, depending on the section thickness of the stock and the furnace capabilities. However, in general, because of the increased thermal conductivity of aluminum alloys, the required heating times are shorter than with other forged materials.

## 2.7 Cleaning and Surface Finish of Aluminum Forgings

Aluminum products should be cleaned as soon as possible after forging. In general, the following type of treatment will remove oxide and lubricant residue and produce smooth surface with a natural luster [1]:

- Immerse in a 4 to 8 weight percent aqueous solution of NAOH at 71 °C for 0.5 to 5 minutes.
- Rinse in 77 °C water for same length of time.

- Immerse in aqueous solution of nitric acid, 10 percent by volume, at a temperature of 88 °C of higher to remove black deposit.

- Rinse in hot water.

Surface finish after forging is generally good for aluminum forgings, although it is likely to vary considerably from one portion of a forging to another [19].

Surface finish of 125 micro-inches or better is considered normal for forged aluminum alloys [19]. Under closely controlled production conditions, surfaces smoother than 125 micro-inches often can be obtained.

## 2.8 Heat Treatment of Aluminum Forgings

To achieve highest level of mechanical properties 2000, 6000 and 7000 series aluminum alloys are subjected to heat-treatment. These alloys are strengthened slightly during forging as the hot working reduces the grain size. Appropriate mechanical properties of the part are developed subsequently through heat treatment. In this post operation, the materials are solution heat treated at a temperature just below the solidus temperature, then water quenched and artificially aged above room temperature for several hours.

Distortions of the part geometry may occur during heat treatment because of nonuniform cooling. This is largely due to adjoining geometric features that have different area to mass ratios. Designer can minimize this type of distortions by avoiding designs that lead to non-uniform cooling.

## 2.9 Aluminum Forging Dies

For the closed die forging of aluminum alloys, die materials selection, die design, and manufacturing of dies are critical elements in the overall aluminum forging process because the dies are a major element of the final cost of such

forgings. Further, forging process parameters are affected by die design, and the dimensional integrity of the finished forging is considerably controlled by the die cavity. Therefore, the forging of aluminum alloys requires the use of dies which are specifically designed for aluminum for at least three reasons [23]:

- The deformation behavior of aluminum alloys differs from that of other materials; therefore, the intermediate and final cavity die design must optimize metal flow under given forging process conditions and provide for the fabrication of defect-free final parts.

- Allowances for shrinkage in aluminum alloys are typically greater than those for steels.

- Temperature control of the dies used to forge aluminum alloys is critical; therefore, the methods used for heating and maintaining die temperatures during forging must be considered in the design.

The die materials used in the closed die forging of aluminum alloys are identical to those employed in forging steels except that, because of the forces applied in aluminum alloy forging and the sophistication of the parts produced; such materials are typically used at lower hardness levels in order to improve their toughness. For instance, if a die block with hardness 388 to 429 BHN is used for forging a specific size and shape from steel, a block with hardness of 341 to 375 BHN is used for aluminum alloys [24].

Die for lower hardness can be used for aluminum alloys because die wear is seldom a problem. Available die materials were primarily designed for the forging of steels and are not necessarily optimized for the demands of aluminum alloy forgings. However, with advanced steelmaking technology, such as argon oxygen decarburization refining, vacuum degassing, and ladle metallurgy, the transverse ductility and fracture toughness of available standard and proprietary die steel grades have been improved dramatically [24]. As a result, the

performance of these grades in the forging of aluminum alloys has also improved dramatically.

Although die wear is less problem with aluminum alloy forgings than with steel and other high temperature materials, high volume aluminum alloy forgings can present die wear problems in cases in which die blocks have reduced hardness in order to provide improved toughness. Therefore, higher hardness die inserts and surface treatments are often used to improve wear characteristics in order to maintain die cavity integrity. The surface treatments employed include carburizing, nitriding, carbonitriding, and surface alloying [24].

Aluminum alloy forgings are produced by a number of machining techniques, including hand machining, electrical discharge machining (EDM) and computer numerically controlled (CNC) machining. These techniques reduce the cost of the dies, perhaps more important; increase the accuracy of the dies. The finish on the dies used for the forging of aluminum alloys is more critical than that on dies used for steel because surface marks are more easily transferred to the surfaces of aluminum. Therefore, cavities are highly polished, frequently with automated equipment, by a variety of techniques in order to obtain an acceptable finish and to remove the disturbed surface layer resulting from such die-sinking techniques as electrodischarge machining. A finish of 6 micro-inches is usually specified on dies for forging aluminum [19].

Since forging temperature of aluminum alloys is relatively low, the dies can be heated nearly the same temperature as the workpiece, which prevents cooling of the workpiece and facilitates flow of metal into small cavities in the die. Therefore, die temperature is another critical element for aluminum forging. Table 2.3 summarizes the die temperature ranges typically used for several aluminum forging processes [23]. The criticality of die temperature in the optimization of the process depends on the forging equipment being employed, the alloy being forged, and the severity of the deformation or the sophistication of the forging design. For slower deformation processes, such as hydraulic press

forging, die temperature frequently controls the actual metal temperature during deformation, and in fact, aluminum alloys forged in hydraulic presses are isothermally forged; that is, metal and dies are at the same temperature during deformation. Therefore, the die temperatures employed for hydraulic press forging exceed those typical of more rapid deformation processes, such as hammers and mechanical presses.

**Table 2.3 Die Temperature Ranges for Forging of Aluminum Alloys [23]**

| **Forging Process/Equipment** | **Die Temperature (°C)** |
|---|---|
| **Open Die Forging** | |
| Ring rolling | 95-205 |
| Mandrel forging | 95-205 |
| **Closed Die Forging** | |
| Hammers | 95-150 |
| Upsetters | 150-260 |
| Mechanical presses | 150-260 |
| Screw presses | 150-260 |
| Rotary Presses | 150-260 |
| Spin forging | 150-315 |
| Roll forging | 95-205 |
| Hydraulic presses | 315-430 |

Dies are always heated for the forging of aluminum alloys, with die temperature for closed die forging being more critical. As shown in Table 2.3, the die temperature used for the closed die forging of aluminum alloys varies with the type of forging equipment being employed and the alloy being forged. Both

remote and on-press die heating systems are employed in the forging of aluminum alloys. Remote die heating systems are usually gas fired die heaters capable of slowly heating the die blocks. These systems are used to preheat dies to the desired temperature prior to assembly into the forging equipment.

On-press die heating systems range from relatively rudimentary systems to highly engineered systems designed to maintain very tight die temperature tolerances. On-press die heating systems include gas fired equipment, induction heating equipment, and resistance heating equipment. In addition, presses used for the precision forging of aluminum alloys frequently have bolsters that can be heated or cooled as necessary. On-press aluminum die heating equipment can hold die temperature tolerances within ±15 °C or better [23]. Specific on-press die heating systems vary with the forging equipment used, the size of the dies, the forging process, and the type of forging produced.

Since aluminum rich materials have a pronounced tendency to adhere to steel at elevated temperatures, die lubrication is very critical for aluminum forging process so dies are always lubricated for forging aluminum. Lubricants must be capable of modifying the surface of the die to achieve the desired reduction in friction, withstand the high die and metal temperatures and pressures employed, and yet leave the forging surfaces and forging geometry unaffected [23]. The major active element in aluminum alloy forging lubricants is graphite; however, other organic and inorganic compounds are added to in order to achieve the desired results. If metal flow is a problem, as in forging metal into narrow rib sections, soap is added to the graphite mixture.

Excess lubricant may become a problem in forging aluminum, especially in dies which have intricate cavities. The preferred method to eliminate this problem is to blow off excess lubricant with an air nose.

## 2.10 Cost Aspects of Aluminum Forging

The cost of aluminum forgings depends strongly on the quantity of parts to be produced, shape complexity of the part and the amount of machining required to reach the finished shape, dimensions and tolerances. Blocker, conventional and precision types are the classifications, respectively, of forgings that are progressively closer to the final part geometries. Blocker type forgings, which are only a rough approximation of the desired part shape, are produced with inexpensive, simple shape dies, but they require extensive machining to reach the final shape. In contrast, precision forgings use very expensive, complex dies, but they require little machining to reach the final part dimensions. Blocker type forgings are economical for parts in small quantities, and precision forgings are economical for producing large quantities of parts over which the high die costs can be amortized.

Process and equipment limitations also affect the forging cost. As mentioned before, aluminum alloy billets are heated somewhat below their solidus temperature because heat generated during forging deformation causes a temperature rise in the material. If the material temperature plus the temperature rise during forging exceeds the solidus temperature, incipient melting occurs, leading to severe cracking. This reduces the complexity of the shapes that can be produced on high speed forging equipment, and potentially increases the amount of machining required. Thus, increasing the production rate by using a high speed forging operation also reduces the shape complexity that can be obtained and may increase the amount of machining required to reach the final shape.

# CHAPTER 3

# PROCESS DESIGN USING FINITE VOLUME METHOD

## 3.1 Case Study for Aluminum Forging

As case study, forging of road wheel bearing housing which is used in military trucks and has been made of aluminum alloy 7075 will be analyzed and forged. Photographs of the part are given in Figure 3.1 [25].

**Figure 3.1 Photographs of the Part [25]**

Aluminum alloy 7075 is one of the highest strength aluminum alloys available. This alloy in heat treated condition has yield strength higher than that of low-alloy-high-yield-strength structural steel. Its strength to weight ratio is excellent when heat treated. It also has excellent properties at low temperatures. Its ductility, however, is not quite as good [6].

7075 is commonly used in manufacturing aircraft and aerospace parts and other highly stressed structural applications where high strength and good resistance

to corrosion are required [26]. The success of very large modern aircraft is to a considerable extent due to the development of this high strength aluminum alloy. Chemical composition of aluminum alloy 7075 is tabulated in Table 3.1 [26]. Mechanical and physical properties of aluminum alloy 7075-0, where "0" represents for without heat treatment, are tabulated in Table 3.2 [27].

**Table 3.1 Chemical Composition of Aluminum Alloy Aluminum Alloy 7075 [26]**

| **7075** | **Cu %** | **Mg %** | **Mn %** | **Si %** | **Fe %** | **Cr %** | **Zn %** | **Ti %** |
|---|---|---|---|---|---|---|---|---|
| | 1.2-2.0 | 2.1-2.9 | Max. 0.3 | Max. 0.4 | Max. 0.5 | 0.18-0.28 | 5.1-6.1 | Max. 0.2 |

**Table 3.2 Mechanical and Physical Properties of Aluminum Alloy 7075-0 [27]**

| | |
|---|---|
| **Hardness** | 60 BHN |
| **Ultimate Tensile Strength** | 228 MPa |
| **Tensile Yield Strength** | 103 MPa |
| **Elongation at Break** | 16% |
| **Modulus of Elasticity** | 71.7 GPa |
| **Poisson's Ratio** | 0.33 |
| **Shear Strength** | 152 MPa |
| **Shear Modulus** | 26.9 MPa |
| **Density** | 2810 $kg/m^3$ |
| **Thermal Conductivity** | 173 W/m*K |
| **Specific Heat and Heat Capacity** | 960 J/kg*K |
| **Coefficient of Thermal Expansion** | $2.52x10^{-5}$ 1/K |
| **Solidus Temperature** | 477 °C |
| **Liquidus Temperature** | 635 °C |

The case part is modeled by using Pro-Engineer Wildfire 3.0 [28]. 3-D model of the part from different views are given in Figure 3.2.

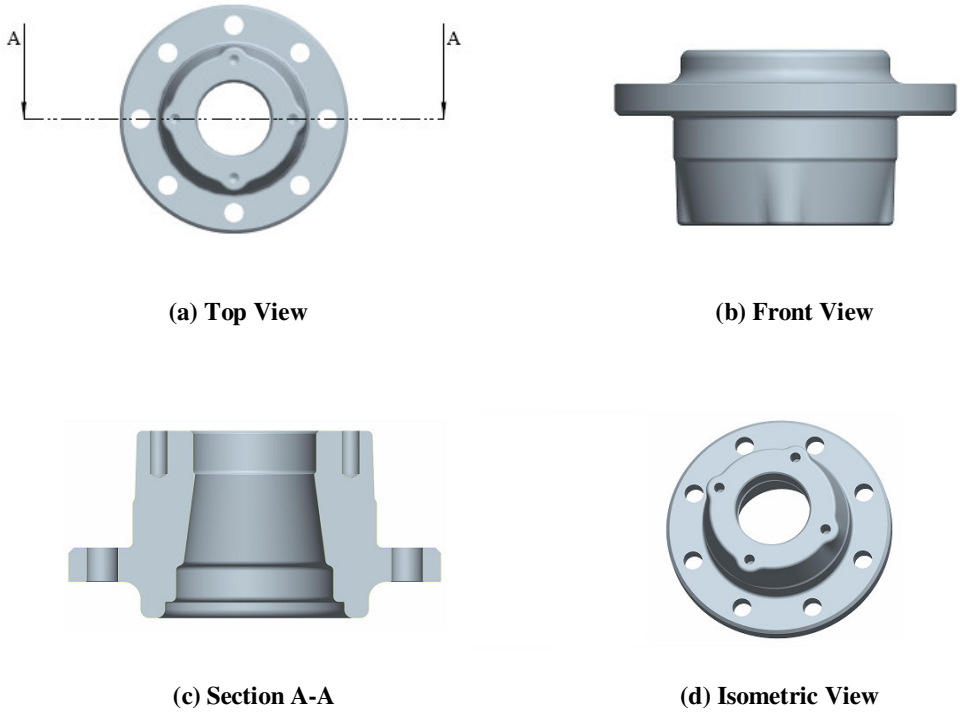


**(a) Top View** **(b) Front View**

**(c) Section A-A** **(d) Isometric View**

**Figure 3.2 Views of 3-D Model of the Part**

## 3.2 Design of the Forged Part

In order to produce the part shown in Figure 3.2 by forging operation, some modifications have to be done on the current part. First of all, Ø5.7 mm through holes located on the flange of the part and pre-holes of M3 tapped holes located on the top of the part are too small to be produced by forging operation, so these holes are left to be produced by machining after forging. Besides, obtaining through hole is very difficult by forging operation because of the tolerances between upper and lower die. For this reason, 2.5 mm thickness is left where

upper and lower dies meet. 3-D Model of the modified part from different views is given in Figure 3.3.

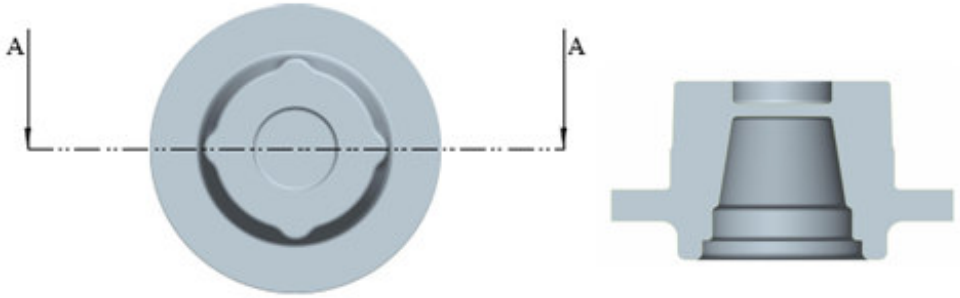


**(a) Top View** **(b) Section A-A**

**Figure 3.3 Views of 3-D Model of the Modified Part**

Parting plane generally is the plane having the maximum cross-sectional area perpendicular to the forging direction. So for this part, the parting plane will be the plane that passes from the middle of the flange and it is shown in Figure 3.4.

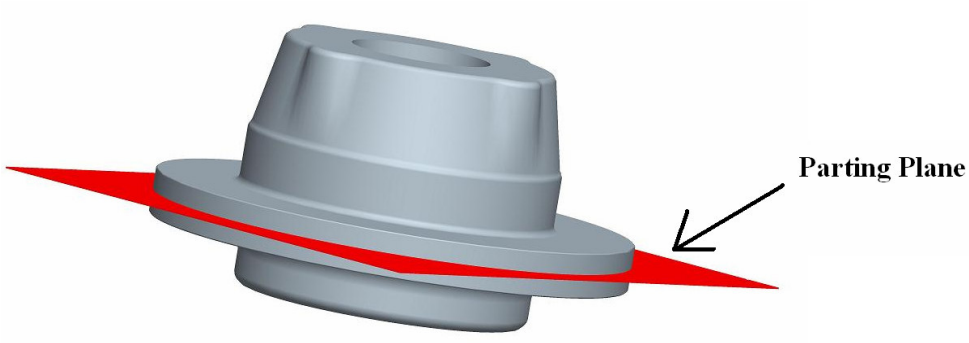


**Figure 3.4 View of Parting Plane**

A primary consideration in forging is that the forged part has to be removed from the die after the forging process is completed. Because geometries that would interlock with the dies cannot be forged net. Furthermore, surfaces

parallel to the forging axis will often generate high frictional forces with the tooling during ejection. So draft angles are given to these surfaces to facilitate ejection. Recommended draft angles for different materials are tabulated in Table 3.3 [29]. Based on Table 3.3, 2° draft angle is given to the upper and the lower finish dies.

**Table 3.3 Recommended Draft Angles for Materials [29]**

| **Material** | **Draft Angle** (°) |
|---|---|
| Aluminum | 0-2 |
| Copper Alloys | 0-3 |
| Steel | 5-7 |
| Stainless Steel | 5-8 |

Generous fillets and corner radius should be provided to aid in material flow during the forging process. Small corner radii in the dies (i.e. sharp fillet radius in the parts) corners are stress-risers in the forgings, and lead to number of problems including laps, cracks and excessive die wear. Recommended corner radius limits for aluminum alloy forgings are given in Figure 3.5 [2].

Flash thickness has great influence on forging pressure. Essentially, forging pressure increases with decreasing flash thickness. Since the forces applied in aluminum alloy forging are considerably less than those of steel forging, the small flash tolerances are used for aluminum forging. Mass and material based on flash thicknesses are tabulated in Table 3.4 [29].

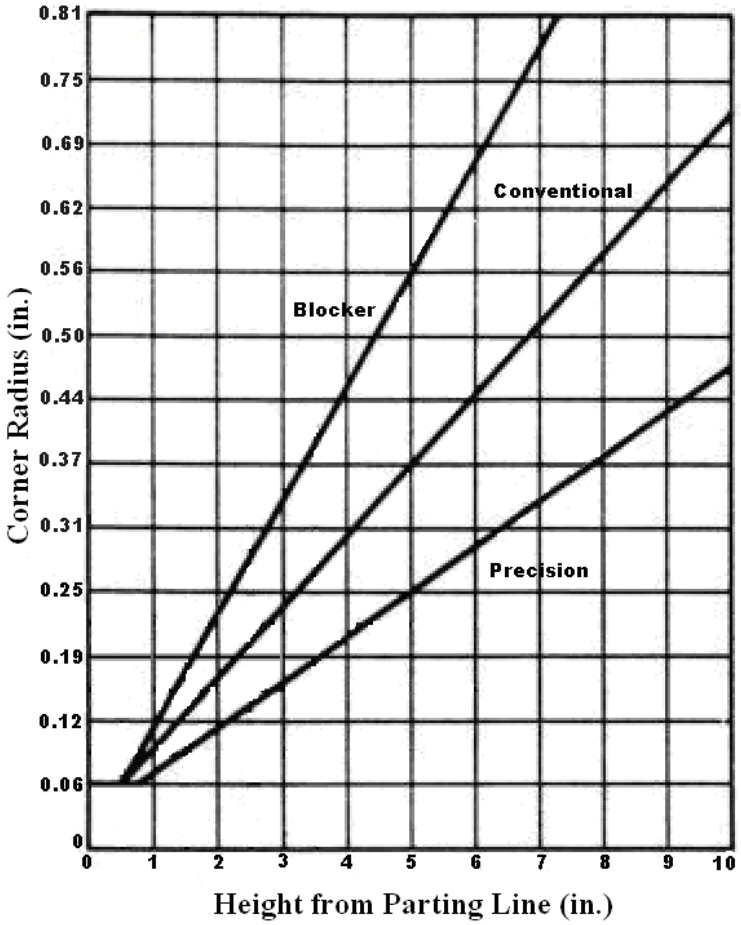


**Figure 3.5 Recommended Corner Radius Limits for Aluminum Alloy Forgings [2]**

**Table 3.4 Recommended Flash Thicknesses for Materials [29]**

| **Material** | **Finished Forging Mass (Trimmed kg)** | | |
|---|---|---|---|
| | <10 | <50 | <500 |
| | **Die Match Tolerance (mm)** | | |
| Aluminum Alloys, Copper Alloys | 0.8 | 3.25 | 10 |
| Steel, Stainless Steel, Titanium | 1.60 | 5 | 12.50 |

Steel forgings are coated on the surface with a thin layer of iron oxide or scale, which is caused by contact of the heated steel with air [15]. Because of this scale formation problem, a scale allowance has to be applied to the calculations of the billet volume. But as mentioned in Chapter 2, scale is not a problem for aluminum forging because aluminum alloys do not have scale to the same extent as steel does. So no scale allowance is given to the billet volume for the scale formation. However, since the workpieces contract after forging due to cooling, the dies scaled up 1.6% in Pro-Engineer Wildfire 3.0. The value 1.6 is calculated such that the billets will be forged at the initial temperature of 400 °C.

After all these steps, designed part's 3-D model from different views is shown in Figure 3.6.

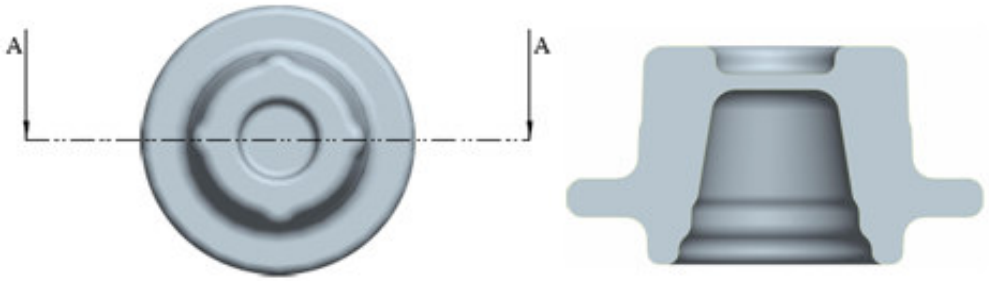


**(a) Top View** **(b) Section A-A**

**Figure 3.6 Views of 3-D Model of the Final Part**

### 3.3) Preform Design of the Forged Part

The forging operation of the particular part will be done in two stages. So a preform has to be designed. Design of preforms is one of the most important aspects of the closed die forging process in order to achieve adequate metal distribution. With proper preform design, defect-free metal flow and complete die fill can be achieved in the final forging operation and metal losses into flash can be minimized.

In design of preform, three basic rules must be followed [23]:

- The area of each cross section along the length of the preform must be equal to the area of the finish cross section augmented by the area necessary for flash. Therefore, the initial stock distribution is obtained by determining the areas of cross sections along the main axis of the forging.

- All the concave radii (including fillet radii) of the preform should be larger than the radii of the forged part.

- When practical, the dimensions of the preform should be greater than those of the finish part in the forging direction so that metal flow is mostly of the upsetting type rather than the extrusion type. During the finishing operation, the material will then be squeezed laterally toward the die cavity without additional shear at the die material interface. Such conditions minimize friction and forging load and reduce wear along the die surfaces.

Based on these rules, the preform geometry is designed. 3-D model of the designed preform and comparison of the preform and the finish part are shown in Figure 3.7 and Figure 3.8, respectively.

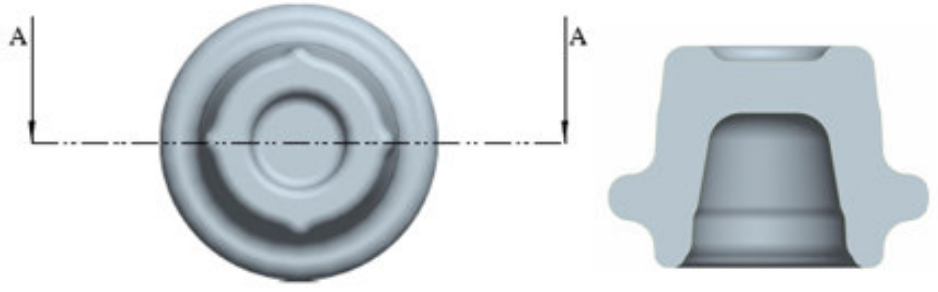


**(a) Top View** **(b) Section A-A**

**Figure 3.7 Views of 3-D Model of the Preform**

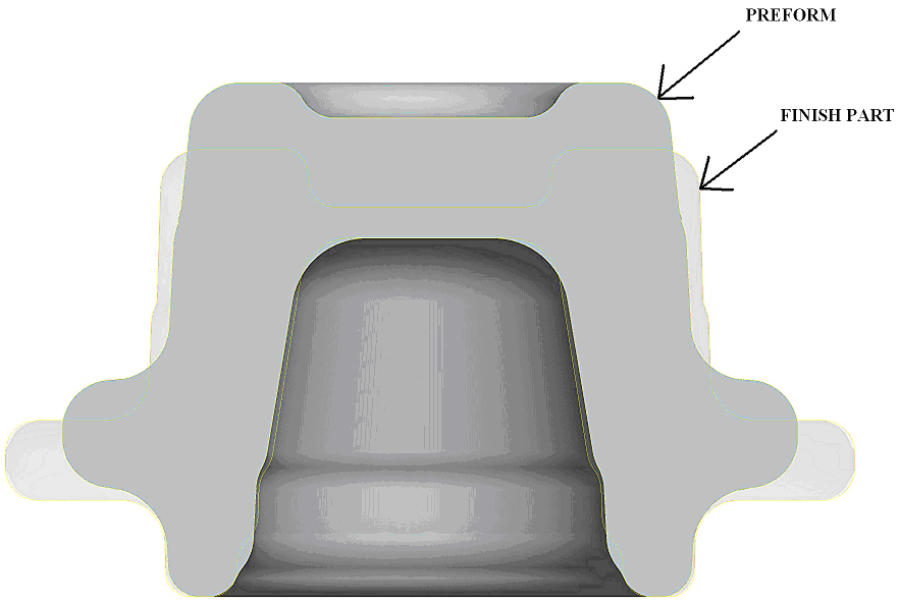


**Figure 3.8 Comparison of Preform and Finish Part**

### 3.4) Selection of the Billet and Design of the Dies

Main criterion for the determination of the billet geometry is the final geometry of the part. Another restriction for the decision of the right billet geometry is the commercially existence of raw materials. In general, these raw materials are found in round or square cross-sections. In Turkey, round cross-sections can be found in the range of 15 to 125 mm in diameter with a step of 2 mm [15].

Cylinder having a diameter of 37 mm is chosen as the billet material so that billet can be located at the bottom of the lower preform die directly without much deviation on x and y axes. To decide the height of the billet first of all, the volume of the finish part is calculated by using Pro-Engineer Wildfire 3.0. Then the volume of the flash is added to the calculated volume and finally the height of the part is calculated from the volume of the cylinder having the diameter of 37 mm.

Based on the preform and finish part, the upper and lower dies are modeled by using Pro-Engineer Wildfire 3.0. 3-D model of the preform and finish die assemblies from different views are given in Figure 3.9 and Figure 3.10, respectively.

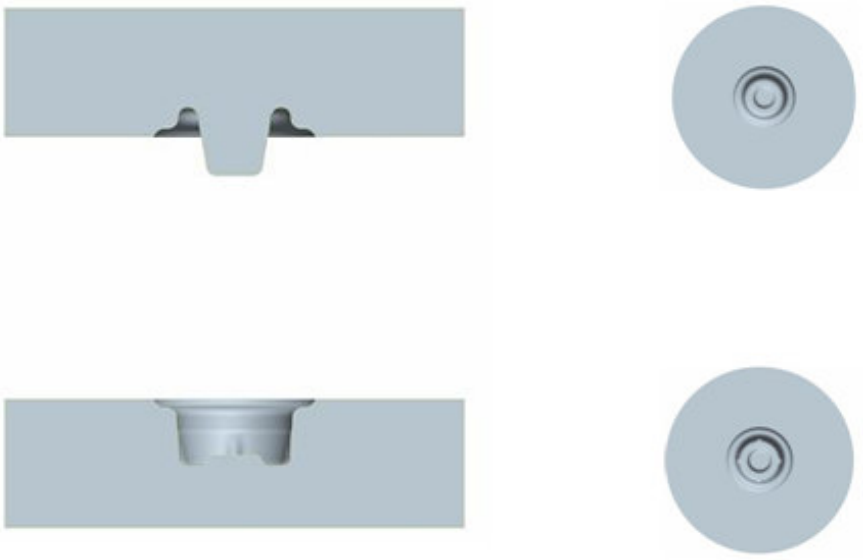

**Figure 3.9 Views of 3-D Model of Preform Die Assembly**

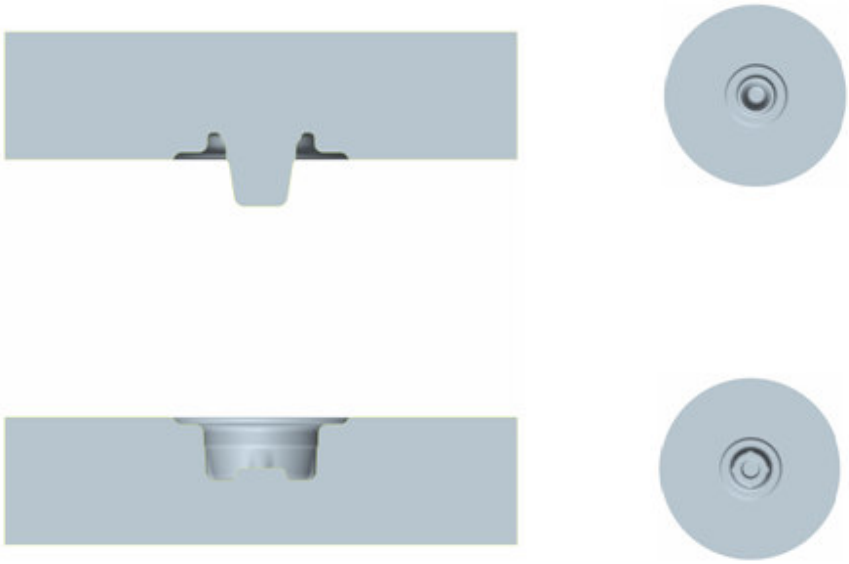

**Figure 3.10 Views of 3-D Model of Finish Die Assembly**

### 3.5) Analysis of Forging Process Using Finite Volume Method

Although in Chapter 4, to analyze the dies MSC. SuperForm, a finite element solver, will be used; to examine the material flow, die filling success, flash formation and possible fold/lap formation MSC. SuperForge, a finite volume solver, is used. The reason using MSC. SuperForge instead of MSC. SuperForm for the process design is that [18]:

- In order to optimize designs in the assembly such as; draft angles, round diameters in the dies, billet diameters and preform geometries, the user must be able to perform parameter studies that require relatively short calculation times. However, FEM is relatively time consuming to use.

- The prediction of metal flow, stress, strain and temperature distributions requires accurate and robust algorithms in FEM. Since the process of forging is typically characterized by gross 3-D material deformation and continuously changing boundary conditions, its complexity requires much simulator expertise and sometimes "tricks and tweaks" to produce a full solution.

- Finite element meshes usually get over-distorted; auto-remeshing is then necessary to complete the simulation. But the auto-remeshing technology for three-dimensional problems is not so robust and also very time consuming.

In MSC. SuperForge, to define a complete thermo-mechanical analysis following steps have to be completed:

*a) Importing Models:* The dies and the billet which are modeled by using Pro-Engineer Wildfire 3.0 are converted to “stl” (stereolithography) format because dies and workpiece will consist of triangular shaped facets only.

*b) Positioning of Models:* The objects are aligned along the vertical axis by moving option bar. Once the objects are aligned along the vertical axis, the position the dies against the workpiece is aligned by using positioner option.

*c) Material Definition:* Since dies are considered to be rigid bodies in forging process design, a material model is only defined for the workpiece. MSC. SuperForge has a material database that includes physical and mechanical properties of certain metals like aluminum, copper, magnesium, steel, tool steel, etc [8]. For aluminum alloy 7075, the material properties given in the database are shown in Figure 3.11 [30]. These material properties are valid between the temperature ranges of 400 °C and 550 °C.

*d) Press Definition:* The press available in METU-BILTIR Center Forging Research and Application Laboratory is 1000 ton SMERAL mechanical press, so crank press option is selected in the software. The software needs crank radius, rod length, and angular speed to define the mechanical press. The required properties of available press are:

- Crank radius (R): 110 mm
- Rod length (L): 750 mm
- Angular speed: 100 rpm

*e) Friction Model:* Since two bodies (i.e. die and billet) that are in contact have rough surfaces and are forced to move tangentially with respect to one another, frictional shear stresses will develop at the interface. MSC. SuperForge provides two alternative models for friction which are coulomb friction, plastic shear friction. For forging operations involving relatively high contact pressures, it is generally more appropriate to use the law of plastic shear friction [31].

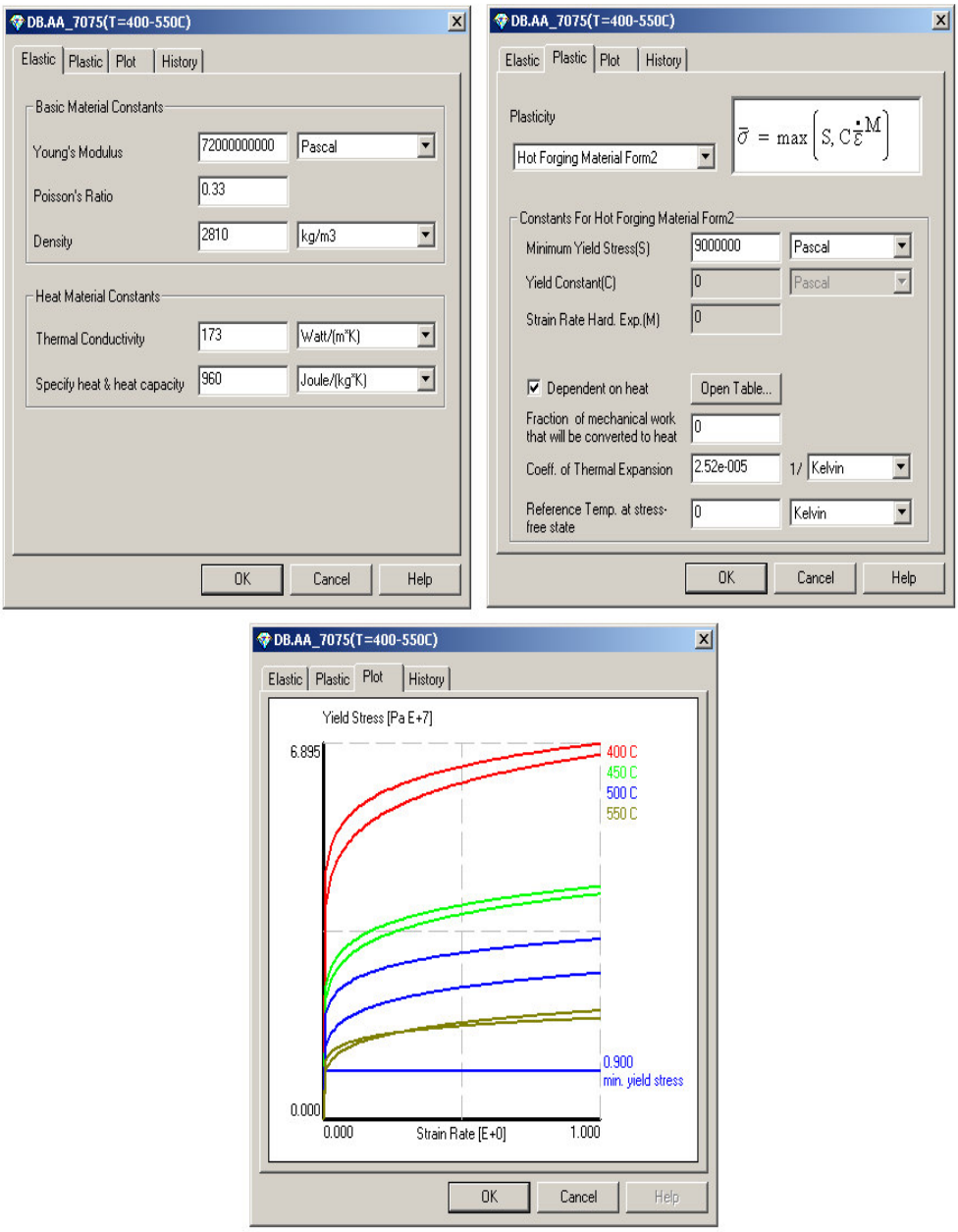


**Figure 3.11 Material Database of Aluminum Alloy 7075 in MSC. SuperForge [30]**

*f) Thermal Properties:* Based on Table 2.1 and Table 2.2, the initial temperature taken for the billet is 400 °C and the initial temperature taken for the dies is 200 °C. Properties like heat transfer coefficient and emissivity for heat radiation to

ambient are taken automatically by the software according to the predefined material.

*g) Simulation Control:* In this step, stroke of the operation, size of the finite volume workpiece and die element sizes, output step size, results wanted to be visualized and problem type (i.e. closed-die, open die, bending, forward extrusion, backward extrusion, rolling and also hot or cold forging) are defined. The workpiece and the die element size are taken as 1 mm. As the element sizes are reduced results become more accurate but process time increases.

*h) Visualization of Results:* After all the steps mentioned above have completed, the processes started successfully. With the completion of the process, the die filling success, flash geometry and flash thickness of the preform and finish dies are examined and shown in Figure 3.12 and Figure 3.13, respectively. The geometry of the part at the end of each stage of the process is shown in Figure 3.14.

As seen from Figures 3.12 and 3.13, the dies are filled successfully both at preform and finish stages. From Figure 3.14, it is seen that the flash distribution is uniform around the periphery of the finish part and the flash amount is as expected. Although not shown here, the fold and lap formation of preform and finish stages are also examined by animating the results step by step and it is seen that no fold or laps occurs throughout the analysis.

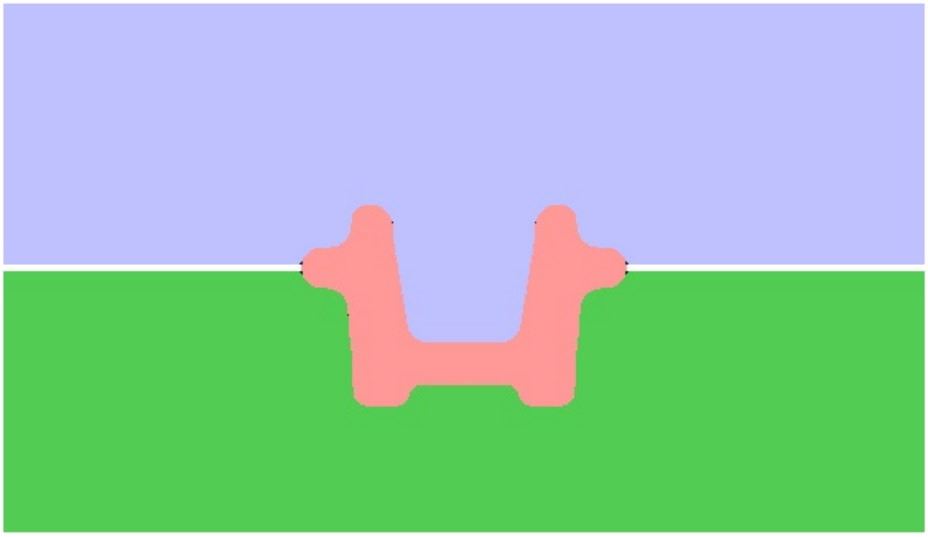

**Figure 3.12 Die Filling Success of Preform Stage**

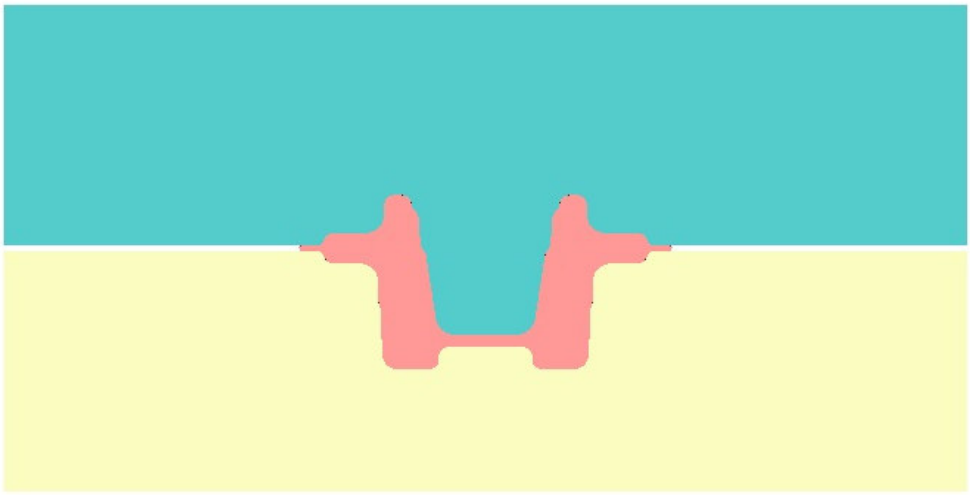

**Figure 3.13 Die Filling Success of Finish Stage**

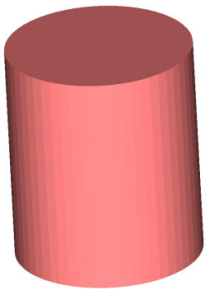

**(a) Initial Billet**

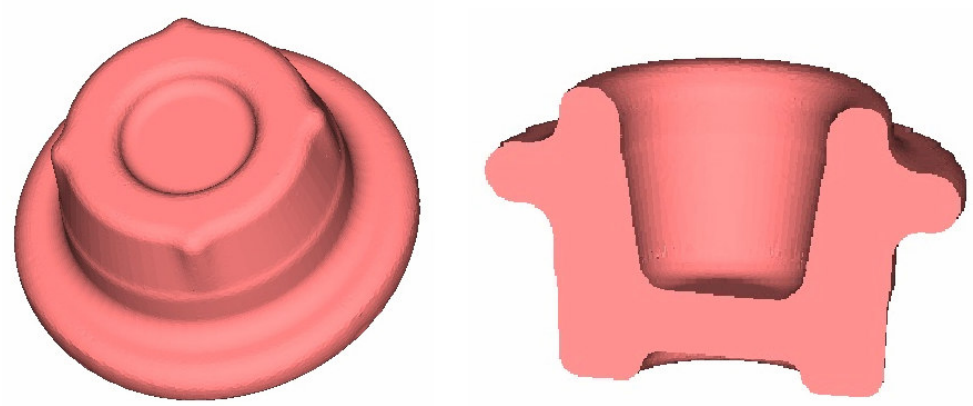

**(b) Preform**

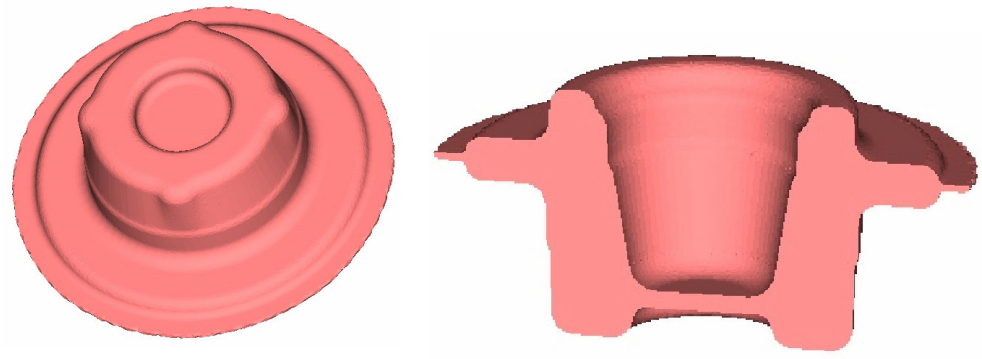

**(c) Finish Part**

**Figure 3.14 Geometry of the Part at Each Stage of the Process**

# CHAPTER 4

# THERMO-MECHANICALLY COUPLED FINITE ELEMENT ANALYSIS OF THE FORGING PROCESS AND THE DIES

Material flow, die filling success, flash formation, possible fold and lap formation have been examined by using MSC. SuperForge as discussed in Chapter 3. In this chapter, MSC. SuperForm which is based on FEM is used to analyze the process and the dies.

Finite element simulation of the forging process is very complex because of the large displacements and the large strains that the material is subjected to. These severe element distortions make the equations highly non-linear and require frequent remeshing to follow the gross material deformation. Friction between contact bodies, modeling the analysis as thermo-mechanically coupled, modeling the geometries in 3-D, modeling the dies as deformable bodies also increase the complexity of the analysis, as discussed in Chapter 3. Therefore, FEM is used to realize the die analysis which includes stress, strain and thermal analyses during the forging process.

## 4.1 Using FEM to Simulate the Process with Die Analysis

In MSC. SuperForm software, the main steps which are involved in the modeling process are [33]:

- Choosing the type of analysis
- Defining geometries and mesh
- Defining material properties

- Applying initial conditions
- Defining contact bodies
- Choosing remeshing scheme and parameters
- Defining forming presses and stages using loadcases
- Submitting the job
- Postprocessing the results

Choosing the type of simulation that will be performed is the first step in MSC. SuperForm. The choice depends on the geometry involved and the tool motions. For the particular analysis, thermo-mechanically coupled analysis option is chosen because in forging operations, following conditions are present [33]:

- The body undergoes large deformations such that there is a change in the boundary conditions associated with the heat transfer problem.
- Deformation converts mechanical work into heat through an irreversible process, which is large relative to other heat sources.

In either case, a change in the temperature distribution contributes to the deformation of the body through thermal strains and influences the material properties.

The coupled analysis is realized in a so called “loose sense” described in Figure 4.1 [34]. At a given time step, say t, the mechanical equilibrium equations are solved using the flow curve corresponding to the known temperature distribution at this time step. The geometry at the time step $t+\Delta t$ is updated using the velocity of step t. Then, knowing the latent heat, a purely thermal analysis is performed at time $t+\Delta t$ supplying a new temperature distribution for this time increment. For the new increment at time $t+\Delta t$ a velocity field is computed using the flow curve at the updated temperature field.

This supplies a new latent heat input, from which a new temperature field at the updated geometry at time t+2Δt with a purely thermal analysis is obtained and so on.

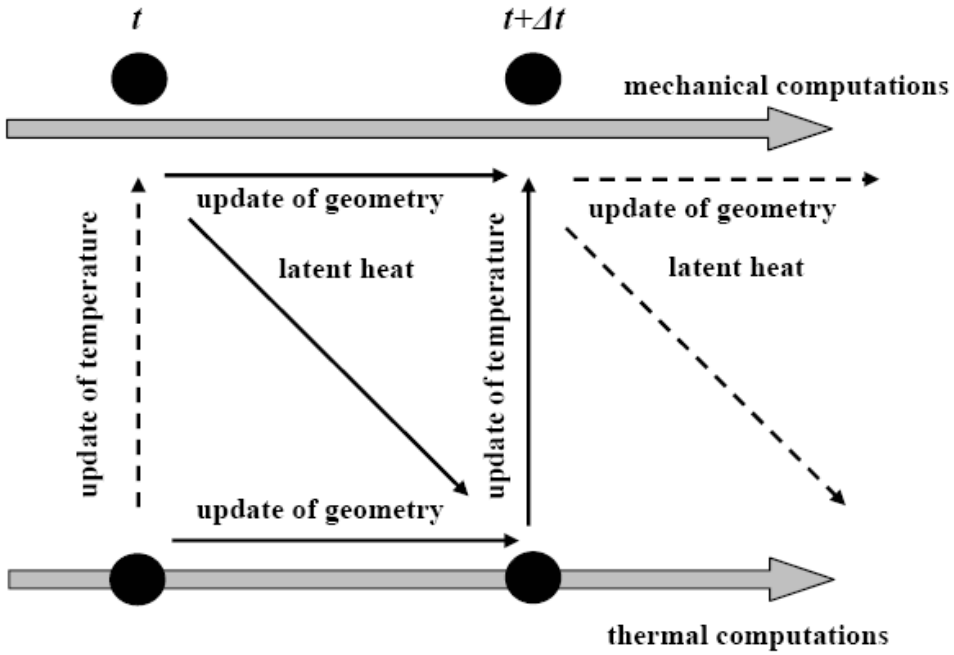


**Figure 4.1 Loosely Coupled Thermo-Mechanical Analysis [34]**

## 4.2 Defining Geometries and Mesh in FEM

The geometry representation involves both defining the sizes and shapes of the workpiece and dies, as well as creating a mesh on these entities. The dies and the billet are modeled by using Pro-Engineer Wildfire 3.0. Due to symmetry of the workpiece, only a quarter of the dies and the billet are modeled in order to reduce complexity and time of the analysis.

After modeling, the billet is exported to MSC. SuperForm. The mesh of the billet is created by the automesh feature of the MSC. SuperForm. First 2-D planar mesh is created by 2-D planar meshing feature of the software. These

elements are 4-nodes quadlateral elements having 1 mm edge lengths. Quadlateral elements are then converted to 3-D 8-nodes hexahedral elements by expanding them in the direction perpendicular the planer surface. 12900 elements are created in the quarter of the billet but the number of elements increases through the analysis according to the remeshing parameters which will be described in Section 4.5.

The meshes of the dies are created in MSC. Patran [35]. The reason is that for complex bodies, creating mesh in MSC. Patran is simpler than creating mesh in MSC. SuperForm. In Patran, 4-node tetrahedral elements are created for the dies. As the number of elements increases, the difficulty and time of the analysis increases. For this reason small elements having average edge length of 2 mm are created for the critical sections of the dies, while bigger elements having average edge length of 8 mm are created for the rest. Total number of elements is 10474 for quarter of the preform dies where the smallest element has 1 mm edge length and the greatest element has 20 mm edge length and total number of elements is 13371 for the quarter of the finish dies where the smallest element has 1 mm edge length and the greatest element has 20 mm edge length. The dies having hexahedral elements are then exported to MSC. SuperForm in “out” format.

After creation of the mesh, the billet and the dies are shown as in Figure 4.2 and 4.3, respectively.

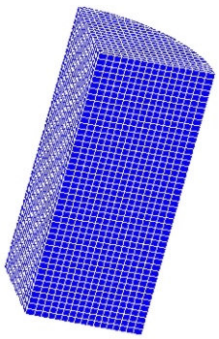

**Figure 4.2 View of the Billet after Creation of Mesh Using Hexahedral Elements**

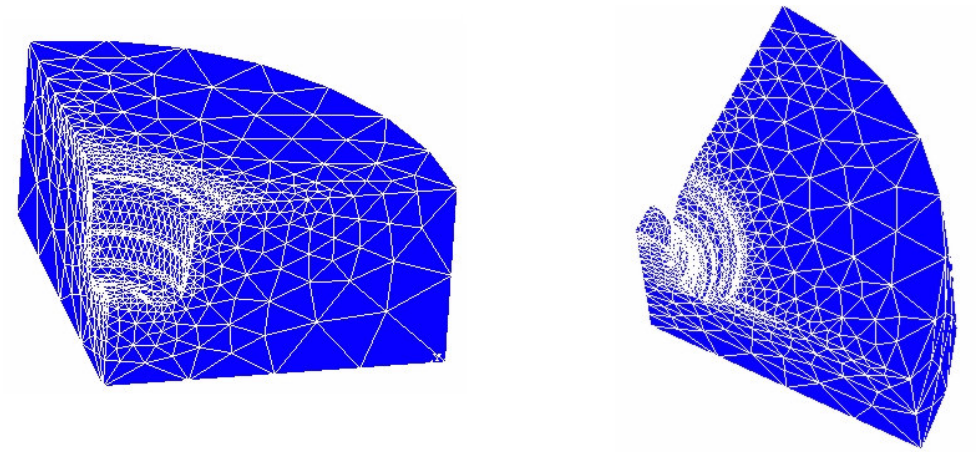

**(a) Lower Preform Die** **(b) Upper Preform Die**

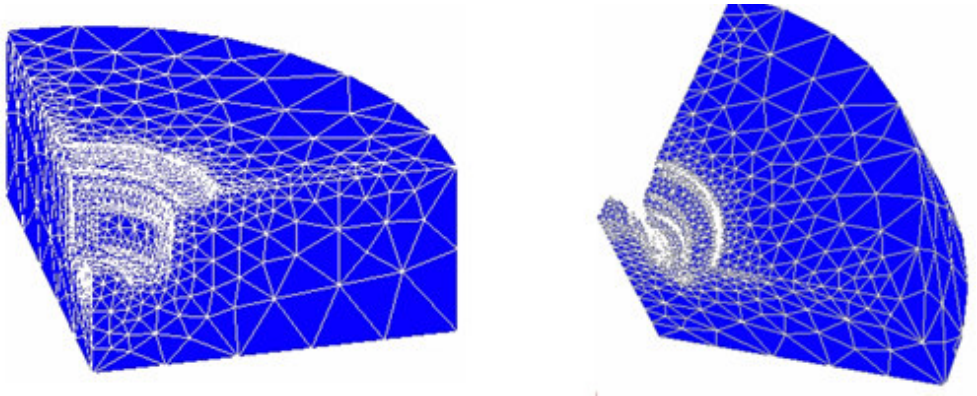

**c) Lower Finish Die** **(d) Upper Finish Die**

**Figure 4.3 View of the Dies after Creation of Mesh Using Tetrahedral Elements**

## 4.3 Defining Material Properties in FEM

After the geometry has been input, the material properties of the workpiece and the dies are defined. MSC. SuperForm simplifies this process by providing a material database. The material library contains 198 different materials. In a thermo-mechanically coupled analysis, once material is read from the material

library, temperature dependent mechanical and thermal properties of the material are defined by software automatically. But if the required material is not one of those that MSC. SuperForm offers, the program allows user to input the material's properties manually.

Defining Material Properties of the Workpiece:

MSC. SuperForm has two plasticity options for the deformable bodies which are rigid-plastic and elastic-plastic flow. In rigid-plastic flow analysis, elastic deformation is neglected, so it is assumed that material is deformed only plastically. The rigid-plastic flow analysis is a good approach to large deformation analysis and decreases the analysis time considerably by neglecting the elastic strains. But this approach has disadvantages. Physical behaviors that depend on elasticity, such as spring back or residual stresses cannot be observed in the solution so that the exact final shape and characteristics of the specimen may not fulfill the accuracy requirements [8]. In elastic-plastic material option elastic deformation is taken into consideration. For the analysis, elastic-plastic material option is selected for the workpiece to obtain more reliable results.

The workpiece material which is aluminum alloy 7075 is included in the material database of MSC. SuperForm, so material properties of the workpiece are read from the database. For aluminum alloy 7075, MSC. SuperForm has only a flow stress material database for different temperature values. Flow stress curves of 7075 at 250 $^{o}$C are shown in Figure 4.4 [32]. As seen, the flow stress of 7075 is a function of effective plastic strain and strain rate. The other mechanical and thermal properties of aluminum alloy 7075 (i.e. Young's modulus (E), Poisson's ratio ($\nu$), thermal conductivity, coefficient of thermal expansion, etc.) are entered manually. The values of these properties have been given in Section 3.1.

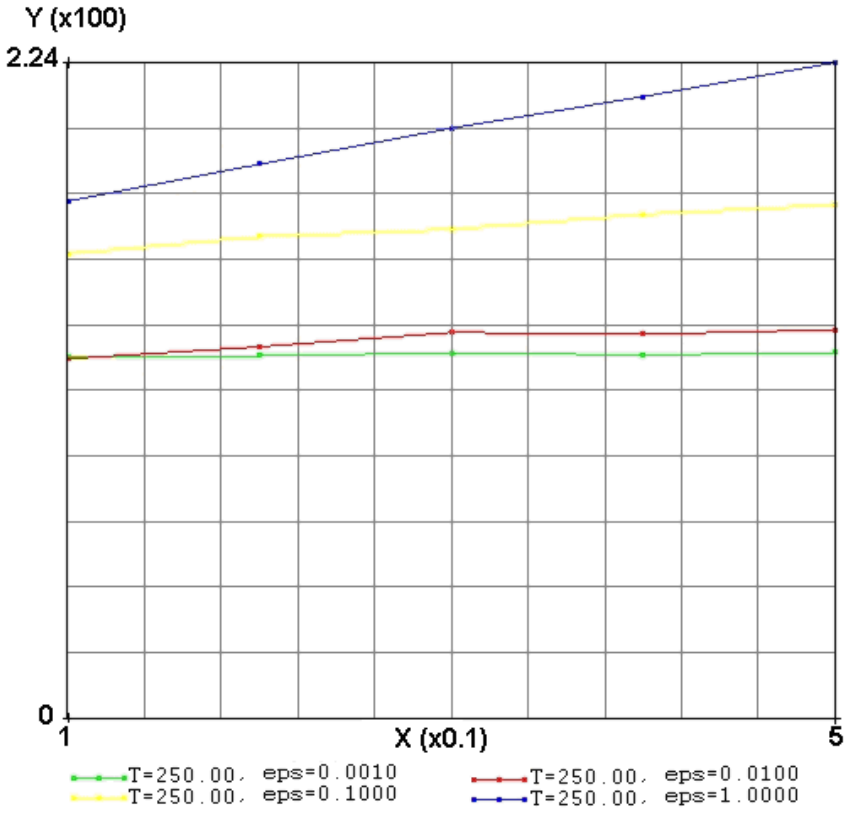


**Figure 4.4 Flow Stress Curves of Aluminum Alloy 7075 at 250 °C as Function of Strain and Strain Rate [32]**

Defining Material Properties of the Dies

The die material used in the experiments is DIEVAR [37]. DIEVAR a is high performance chromium-molybdenum-vanadium alloyed hot work tool steel which offers a very good resistance to heat checking, gross cracking, hot wear and plastic deformation. DIEVAR is characterized by:

- Excellent toughness and ductility in all directions
- Good temper resistance
- Good high-temperature strength
- Excellent hardenability

- Good dimensional stability throughout heat treatment and coating operations

The physical properties of DIEVAR at room and elevated temperatures are shown in Table 4.1 [37].

**Table 4.1 Physical Properties of DIEVAR [37]**

| **Temperature** | **20 °C** | **400 °C** | **600 °C** |
|---|---|---|---|
| **Density, kg/m$^3$** | 7800 | 7700 | 7600 |
| **Modulus of Elasticity, MPa** | 210000 | 180000 | 145000 |
| **Coefficient of Thermal Expansion, per °C from 20 °C** | – | 13.3x $10^{-6}$ | 13.3x $10^{-6}$ |
| **Thermal Conductivity, W/m °C** | – | 31 | 32 |

The dies are modeled as elastic-plastic bodies in the analyses. The elastic behavior of the die material is defined by using Young's Modulus (E) at different temperatures and Poisson's ratio (ν) which is taken as a constant, having a value of 0. 3.

To define the inelastic behavior, the flow curve of the material in the inelastic region has to be specified. For this reason, uniaxial tension tests have been performed with the specimens shown in Figure 4.6. Specimens are tested by using a 40 tons hydraulic tensile test machine which is available at METU Central Laboratory. The available test machine is shown in Figure 4.5. The material of these specimens is DIEVAR and same heat treatment used for the dies has been applied to these specimens. Since the analysis is thermo-mechanically coupled, flow stress curve has to be defined as a function of temperature. For this reason, each four specimen has been tested at different temperatures. These temperatures are the ones which the dies are thought to

reach during the analyses. After the tension tests, the obtained true stress versus true plastic strain curves of DIEVAR at different temperatures are shown in Figure 4.7.

**Figure 4.5 40 tons Tensile Test Machine (left), Displacement Sensor (right)**

**Figure 4.6 View of Test Specimens**

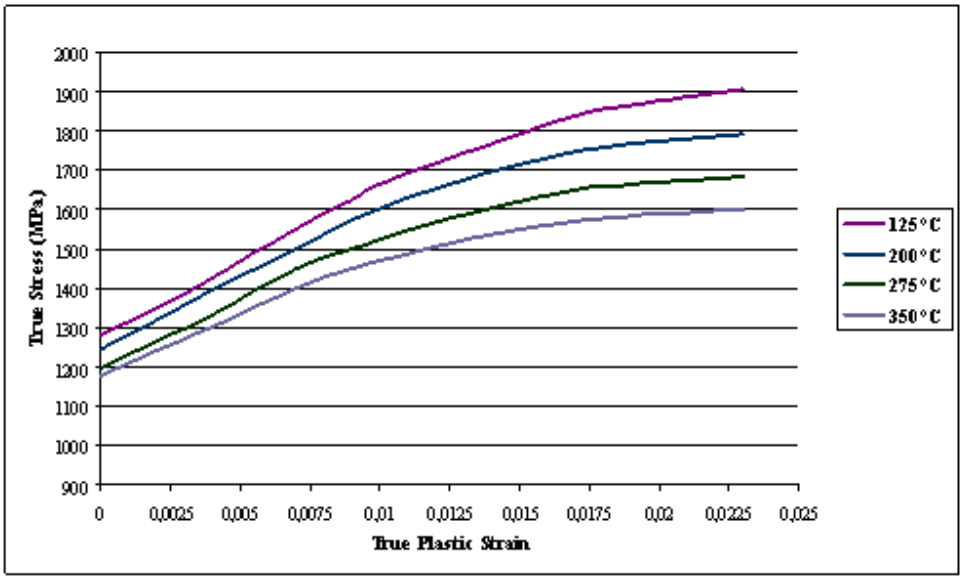


**Figure 4.7 True Stress versus True Plastic Strain Curve of DIEVAR**

The modulus of elasticity (E) versus temperature and true stress versus true plastic strain curves which have been drawn according to Table 4.1 and Figure 4.6 are shown in Figure 4.8 and Figure 4.9, respectively.

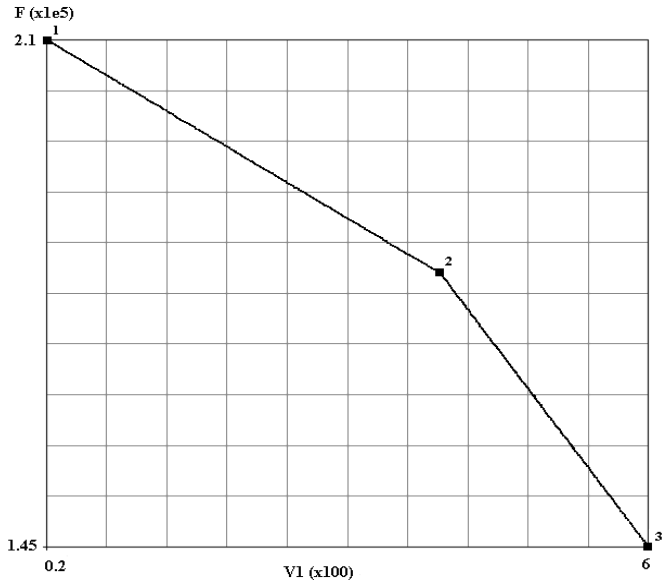


**Figure 4.8 Modulus of Elasticity versus Temperature Curve of DIEVAR after Insertion into the Analysis**

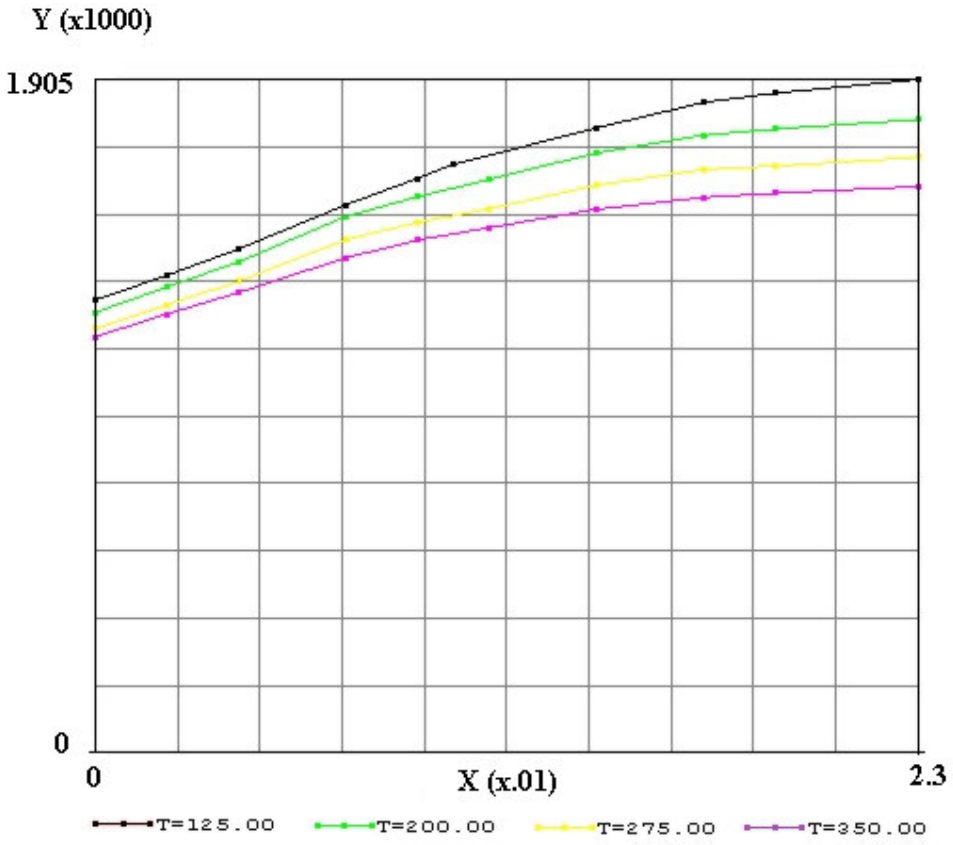


**Figure 4.9 True Stress versus True Plastic Strain Curve of DIEVAR after Insertion into the Analysis**

In MSC. SuperForm, there are two types of initial conditions which are temperature and displacement. For the analysis performed, as the initial conditions, the initial temperatures of the workpiece and the dies are specified. Since material properties of the workpiece and the flow stress of the dies are temperature dependent, the software decides the values to be used initially according to these initial temperatures.

The initial temperature of the preform and the finish dies are specified as 200 °C. The initial workpiece temperatures are given as 438 °C, 400 °C, 350 °C, 300 °C and 250 °C for five different set of analyses to be discussed in Section 4.7.

### 4.4 Defining Contact Bodies in FEM

Metal forming is a contact problem in which workpiece, dies and punches are in contact during the deformation. The software needs to know which body is the workpiece and which body is the punch that is moving. Therefore it is important to define these geometry bodies with special class, such as “workpiece”, “rigid tools”, “deformable tools”, etc. The workpiece is always modeled as a deformable body. The dies are represented as either rigid contact bodies or deformable bodies. If they are modeled as deformable bodies, the stress, strain can be analyzed. In the analysis performed contact body types are defined as:

- Workpiece as deformable body
- Upper and lower dies as deformable bodies
- Symmetry planes as rigid surfaces
- Upper and lower fixing surfaces as velocity controlled rigid surfaces

To set correct contact relationship between contact bodies contact tables are used. Since preform and finish forging simulations are implemented in a single job, two contact bodies are defined in the analysis, the first one for the preform stage and the second one for the finish stage. In the contact tables, contact type “touching” is defined between the bodies that will touch each other throughout the analysis so that there will be a continuous check on contact between these bodies. For the bodies that will not touch each other, contact type “no contact” is defined between them.

In the analyses, four symmetry planes are defined as shown in Figure 4.10. The reason is that when two symmetry planes are used, nodes of the workpiece could have contact on the symmetry plane itself and on the side of the tool that has contact with the symmetry plane at the same time [38]. That means the node slides along the symmetry plane and outside of the tool. Only solution is the usage of four symmetry planes with a small gap of about 0.1 mm which is

greater than contact tolerance between each pair of parallel planes. The tools must become little bigger so that an overlap between tools and original symmetry planes appears. Workpiece only contacts to the symmetry planes 1 and 2, all the deformable tools contact to the symmetry planes 3 and 4. Defined contact bodies in the analysis for the preform and finish stages are shown in Figure 4.11 and Figure 4.12, respectively.

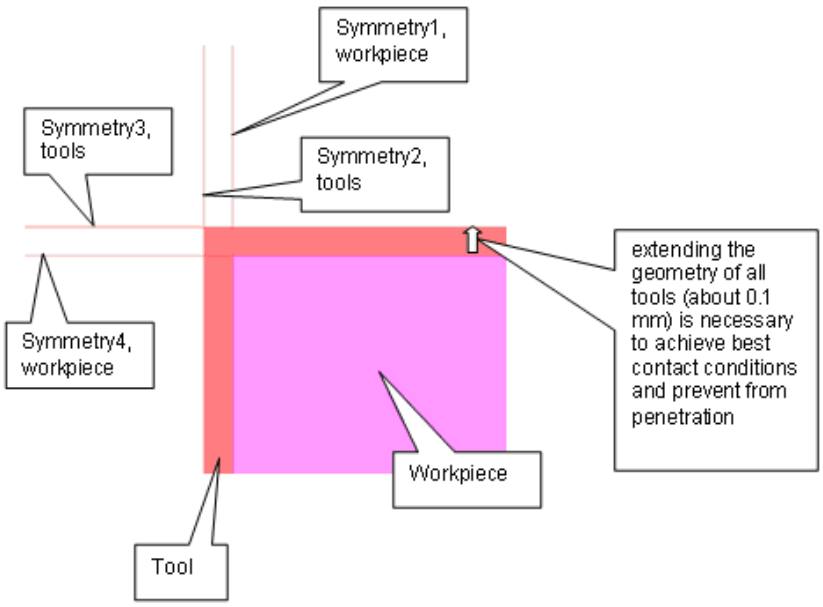


**Figure 4.10 Symmetry Planes Defined in the Analysis**

For a coupled analysis, information between contact bodies, such as, friction coefficient, film coefficient to environment, heat transfer coefficient and environment sink temperature are also specified in this step [33]. Friction coefficient, convection heat transfer coefficient, heat conductivity values can be read from the database of the software. The friction coefficient for the analyses is taken as 0.3 which is the recommended value for medium level graphite lubrication for aluminum parts in the database of MSC. SuperForm. In the database of the software, different convection heat transfer coefficient and heat

conductivity values are recommended for hot forging, warm forging and cold forging operations. As convection heat transfer coefficient, 0.35 W/m$^2$ /°C and 0.20 W/m$^2$ /°C are the recommended values for hot forging and warm forging operations, respectively. As heat conductivity, 30 W/m/°C and 25 W/m/°C are the recommended values for hot forging and cold forging operations, respectively. The recrystallization temperature of aluminum alloys is about 315 °C [39]. So for the analyses conducted at the initial billet temperatures of 438°C, 400 °C and 350 °C, the values recommended for hot forging operation are chosen while for the analyses conducted at the initial billet temperatures of 300 °C and 250 °C, the values recommended for warm forging operation are chosen.

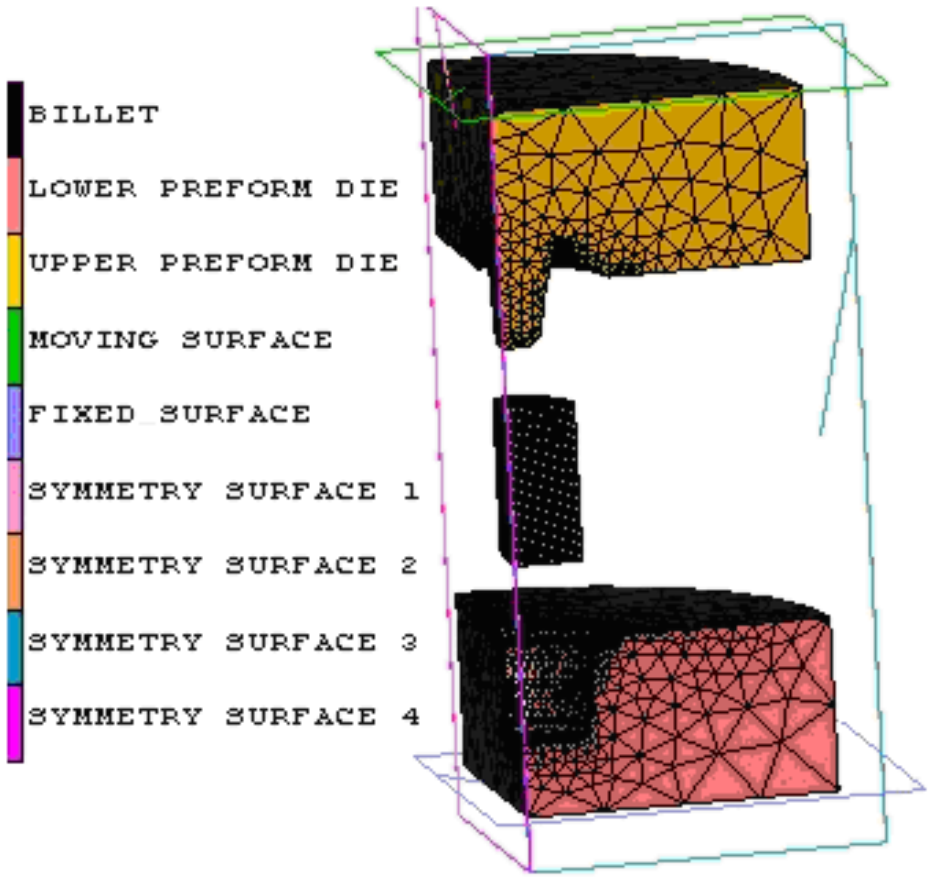


**Figure 4.11 View of Contact Bodies in Preform Stage**

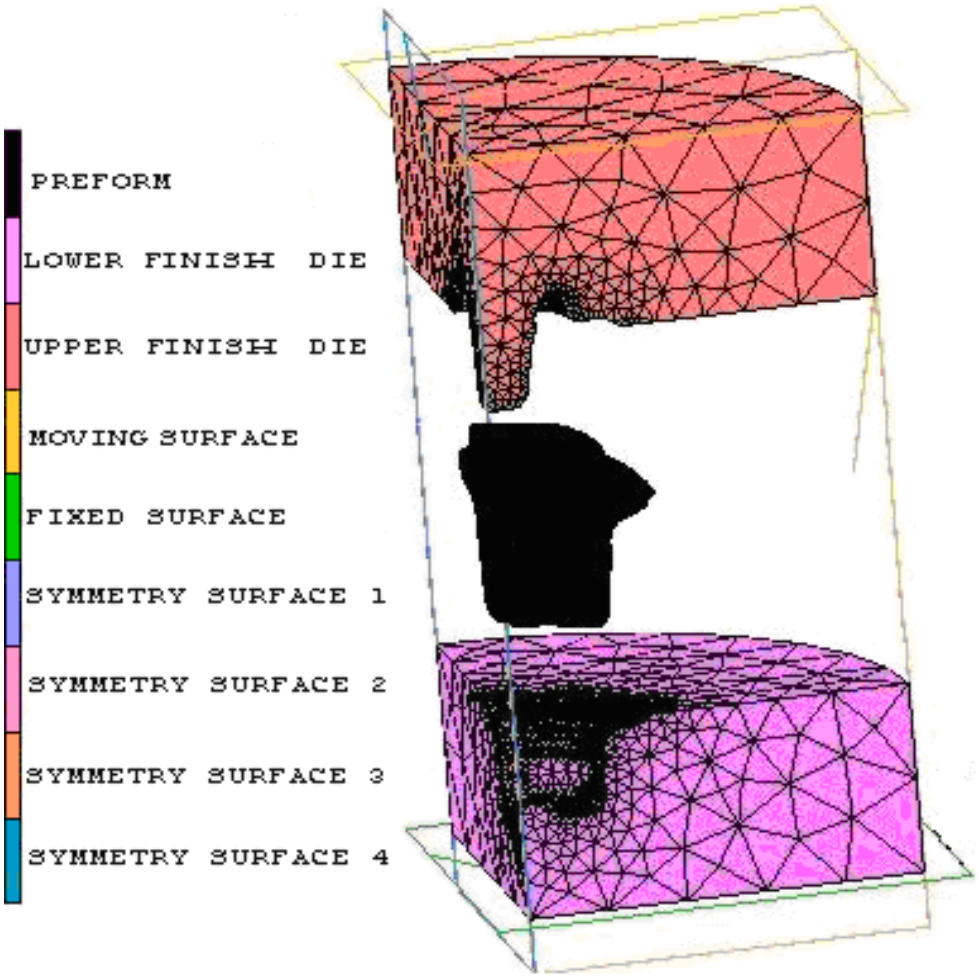


**Figure 4.12 View of Contact Bodies in Finish Stage**

## 4.5 Choosing Remeshing Scheme and Parameters in FEM

Very often, due to excessive deformation, the finite element mesh becomes distorted and may cause the simulation predictions to become inaccurate or the deformation is so great that the mesh can no longer be used for the simulation without a remesh. To remedy this, the software automatically remeshes the workpiece when it becomes necessary, both in two and three dimensions. To define when and how the workpiece will be remeshed during the analysis, remeshing criteria must be defined.

There are two types of remeshing procedures available for 3-D problems in MSC. SuperForm:

- *Overlay Hex* creates a mesh of hexahedral elements on the deforming body.
- *Patran Tetra* creates a mesh composed of tetrahedral elements on the deforming body.

The remeshing criteria have to be decided after choosing the remeshing procedure. MSC. SuperForm offers four remeshing criteria:

- *Increment:* Remeshing occurs at specified increment frequency.
- *Strain Change:* Remeshing occurs when any element of the body has a strain change greater than the control limit since the last remesh.
- *Contact Penetration:* Remeshing occurs when a tool penetrates the workpiece over a considerable length.
- *Immediate:* The identified body is remeshed before performing any analysis.

In the analyses, since the workpiece consist of hexahedral elements, "overlay hex" is chosen as the remeshing procedure. As the analysis progress, more intricate sections of the dies start to be filled by the material flow so frequency of remeshing has to be increased and edge lengths of the new elements have to be decreased. This is accomplished by decreasing the strain change factor from 0.6 to 0.4 and decreasing the edge lengths of new elements from 0.5 mm to 0.4 mm. The number of elements of workpiece has increased up to 81727 at the end of the particular analysis.

### 4.6 Defining Forming Presses and Stages Using Loadcases in FEM

The experiments will be done using the 1000 ton SMERAL mechanical press available in METU-BILTIR Center Forging Research and Application Laboratory. For this reason, "crank press" type is used as the machine in the loadcases. For crank press, velocity of moving tools calculated from the crank length, the rod length, and 360 degrees cycle time and press direction. The required properties of SMERAL press are:

- Crank radius: 110 mm
- Rod length: 750 mm
- Angular speed: 100 rpm

Five sub-stages are present in the crank press type [33]:

1- Workpiece Positioning: Workpiece is moved to the fixed tool.

2- Tools Moving In: Crank rotates such that the moving tool touches the workpiece. The required rotation angle is calculated automatically.

3- Workpiece Deformation: The crank rotates until the reference point of the moving tool reaches the bottom dead center at an angle of 180 degrees.

4- Tools Moving Out: Punch is removed such that elastic spring-back can be calculated.

5 -Workpiece Release: Fixed tool is removed from the workpiece.

In these sub-stages "workpiece deformation" is the most critical one because this substage controls the actual forging of the workpiece. For this substage stepping procedure has to be defined. The available stepping procedures are:

1- Fixed Time Steps

2- Fixed Displacement Steps

3- Adaptive Steps (Plastic Strain)

4- Adaptive Steps (Auto Step)

In the analyses, “adaptive steps (plastic strain)” is used so that steps are determined according to the plastic strain change. Although using “fixed time steps”, faster solutions can be obtained and probability of convergence can be increased, more accurate results are obtained using “adaptive steps (plastic strain)” procedure.

Two loadcases are defined for the preform stage. First loadcase starts the preform stage and it is completed at the crank angle of 165°. At this angle a new loadcase should start because remeshing criteria need to be changed for convergence. At the second loadcase remeshing occurs more frequently and finer meshes are created. For the finish stages, two loadcases are defined. The first loadcase starts the finish stage and it continues up to the crank angle of 176°. At this angle the second loadcase starts with new remeshing criteria.

### 4.7 Results of FEM

Five analyses have been performed by giving different initial temperatures to the billet. These temperatures are 438 °C, 400 °C, 350 °C, 300 °C and 250 °C while the dies initial temperatures are taken as 200 °C for all these analyses. The first analysis performed at 438 °C because as shown in Table 2.1, this temperature is the maximum recommended temperature for forging aluminum alloy 7075.

The following results are examined in the postprocess:

- The maximum equivalent stress distribution on the preform and finish dies
- The maximum equivalent plastic strain distribution on the preform and finish dies

- The maximum temperature distribution on the preform and finish dies
- The maximum temperature distribution on the preform and finish part
- The residual stress distribution on the preform and finish part

In the following subsections, the results will be presented for different initial billet temperatures. In the figures which show the results of the finite element simulations, the views on the right side are the enlarged views of the sections which are encircled by the red ellipse.

### 4.7.1 Results for Initial Billet Temperature of 438 °C

The maximum equivalent stress and the maximum temperature distributions on the preform and finish dies for the initial billet temperature of 438 $^{o}$C, are given in Figures 4.13–4.20. The maximum values are tabulated in Table 4.2 and Table 4.3.

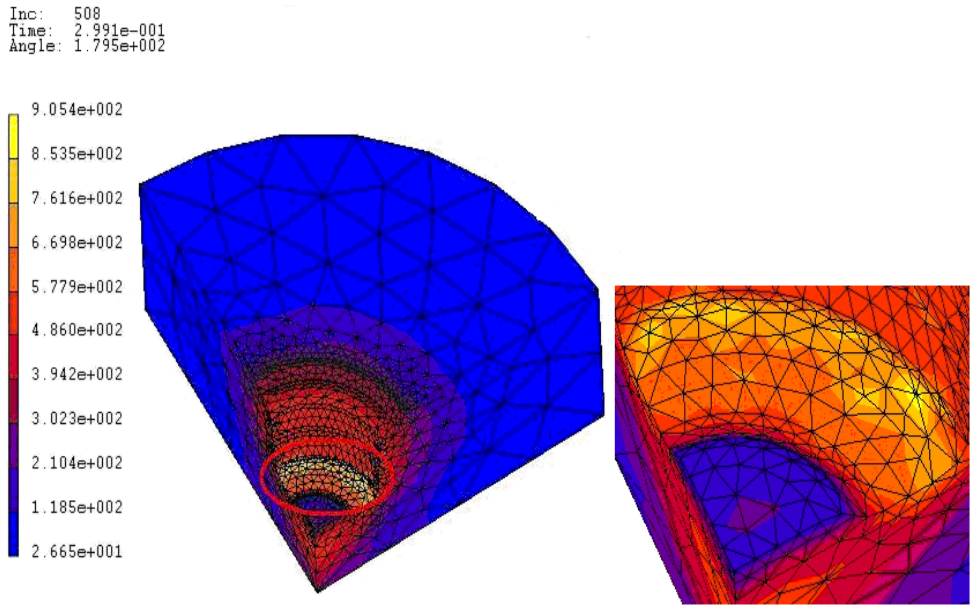


**Figure 4.13 Maximum Equivalent Stress Distribution on Lower Preform Die for Initial Billet Temperature of 438 $^{o}$C**

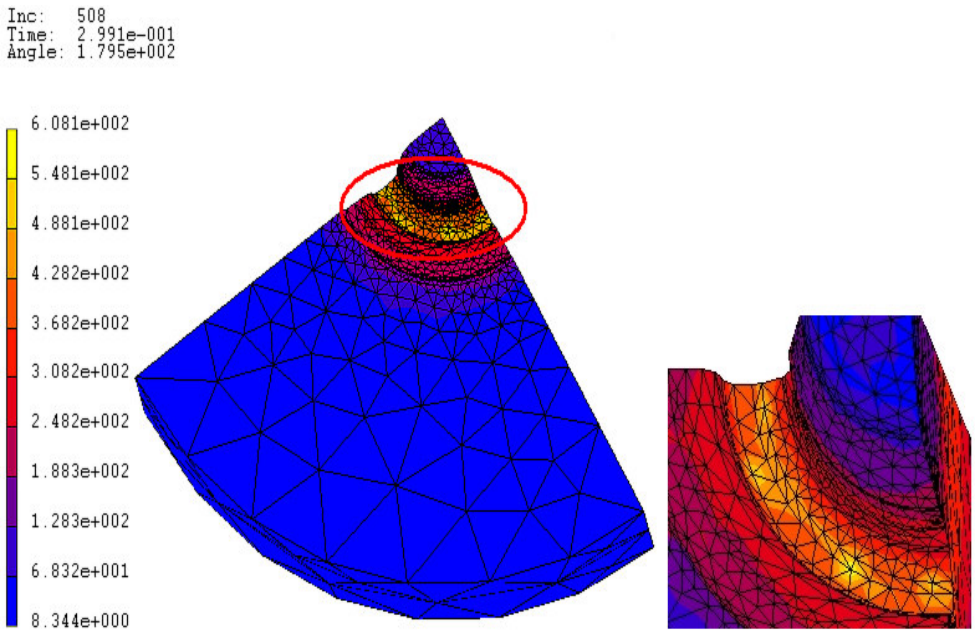


**Figure 4.14 Maximum Equivalent Stress Distribution on Upper Preform Die for Initial Billet Temperature of 438 $^{o}$C**

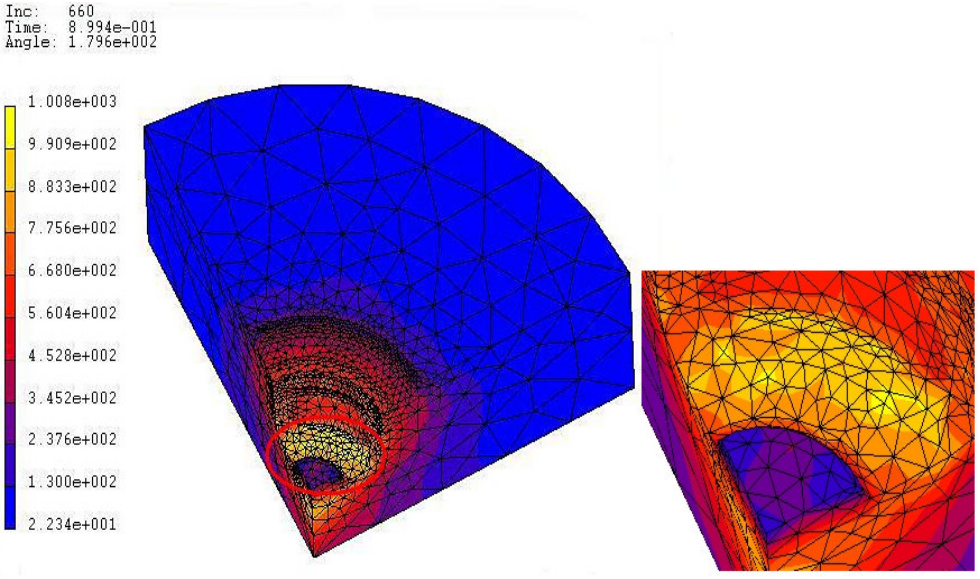


**Figure 4.15 Maximum Equivalent Stress Distribution on Lower Finish Die for Initial Billet Temperature of 438 $^{o}$C**

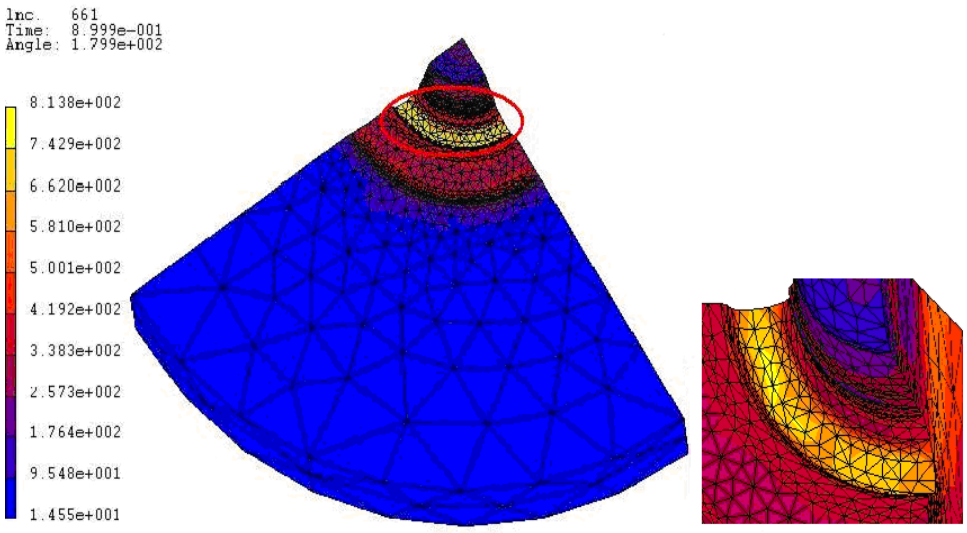


**Figure 4.16 Maximum Equivalent Stress Distribution on Upper Finish Die for Initial Billet Temperature of 438 $^{o}$C**

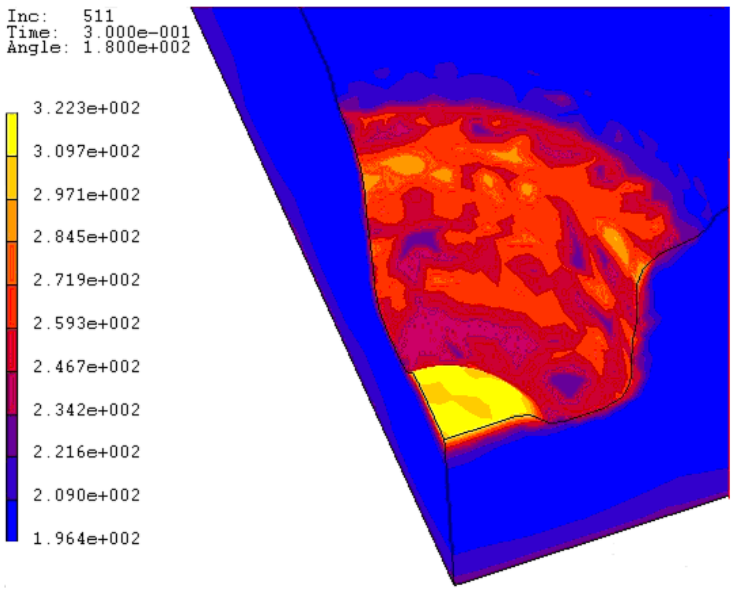


**Figure 4.17 Maximum Temperature Distribution on Lower Preform Die for Initial Billet Temperature of 438 $^{o}$C**

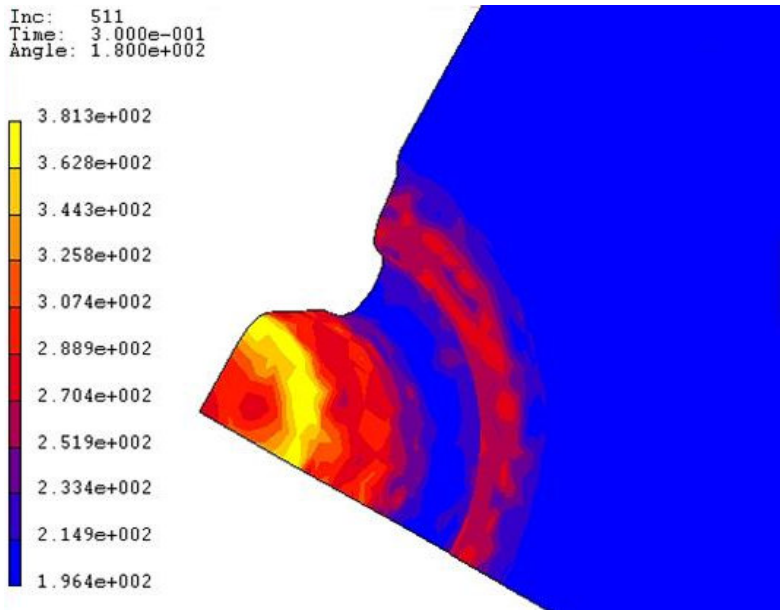


**Figure 4.18 Maximum Temperature Distribution on Upper Preform Die for Initial Billet Temperature of 438 °C**

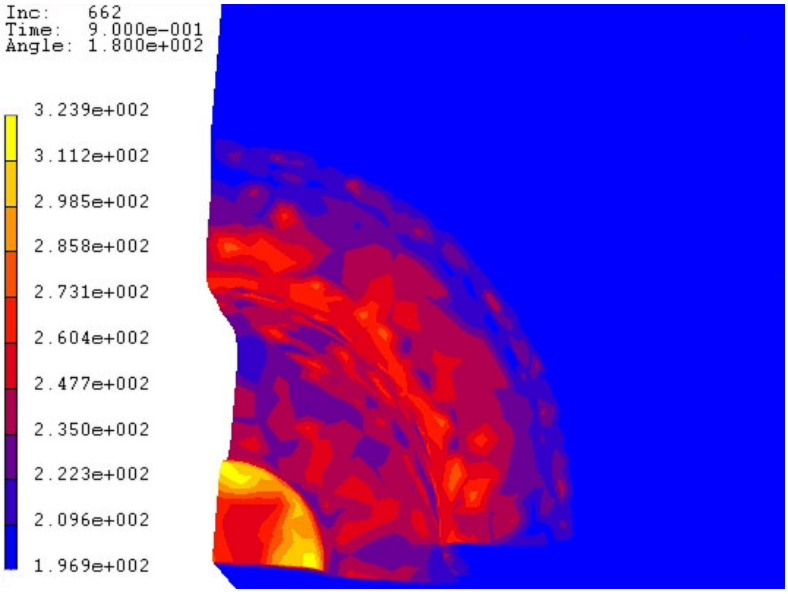


**Figure 4.19 Maximum Temperature Distribution on Lower Finish Die for Initial Billet Temperature of 438 °C**

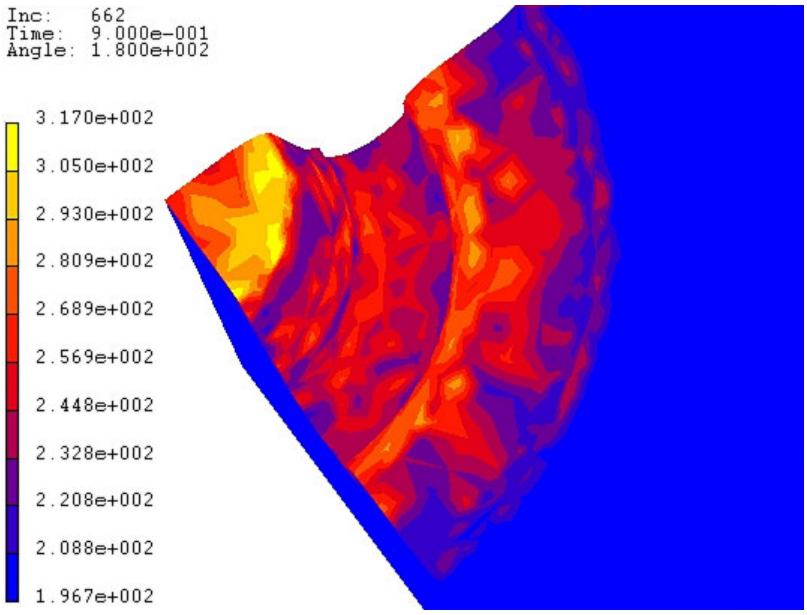


**Figure 4.20 Maximum Temperature Distribution on Upper Finish Die for Initial Billet Temperature of 438 °C**

**Table 4.2 Maximum Equivalent Stress and Maximum Temperature Values on Preform and Finish Dies for Initial Billet Temperature of 438 °C**

| | Max. Equiv. Stress (MPa) | Max. Equiv. Plastic Strain | Max. Temp. (°C) | Max. Equiv. Stress. at the Region of Max. Temp. (MPa) | Max. Temp. at the Region of Max. Equiv. Stress (°C) | Angular Pos. of Crank at Max. Equiv. Stress (°) |
|---|---|---|---|---|---|---|
| **Lower Preform Die** | 905 | 0 | 322 | 220 | 250 | 179.5 |
| **Upper Preform Die** | 608 | 0 | 381 | 200 | 235 | 179.5 |
| **Lower Finish Die** | 1008 | 0 | 323 | 300 | 255 | 179.6 |
| **Upper Finish Die** | 813 | 0 | 317 | 270 | 240 | 179.9 |

The maximum equivalent stresses on lower and upper preform dies are about 905 MPa and 608 MPa, respectively. The maximum equivalent stress is about 1008 MPa for the lower finish die and 813 MPa for the upper finish die. The maximum stresses occur at the bottom regions of the dies as seen in Figures 4.13-4.16. When the simulations are examined, it is seen that the stresses on the preform and finish dies increase as the upper die moves towards to lower die and reach to their peak values at the increments very close to the end. The maximum stress values for finish dies are greater than the preform dies as expected because no flash is formed at the preform stage and as known flash formation greatly influences the pressure on the dies. It is also observed from the results, no plastic deformation occurs on the dies meaning that the deformations of the dies are elastic only.

The peak values of the temperature on the lower preform die, upper preform die, lower finish die and upper finish die are about 322 °C, 381 °C, 323 °C and 317 °C, respectively. Since the initial temperature of the dies is 200 °C, there is a large increase of the die temperatures, especially for the upper preform die, when the forging temperature of 438 °C is considered. The reason for this large increase could be that the locations where the temperature reaches to its peak values are in contact with the workpiece throughout the analysis. Besides, as mentioned in Chapter 2, second to copper, aluminum has excellent heat conductivity. So that high heat flux from workpiece to the dies could be another reason for high die temperatures. This increase in the die temperatures causes increase in the wear coefficient and decrease in the hardness of the die sharply [16]. However, as shown in Table 4.2, the equivalent stresses at the increments and regions where the temperature reaches to its peak values are very low when compared with maximum equivalent stresses and the temperatures at the regions of maximum stresses are quite low when compared with the peak temperature values. So it could be said that wear is not big a problem.

The maximum temperature and the residual stress values in the preform and finish part for the initial billet temperature of 438 $^{o}$C, are given in Figures 4.21–4.23. The maximum values are tabulated in Table 4.3.

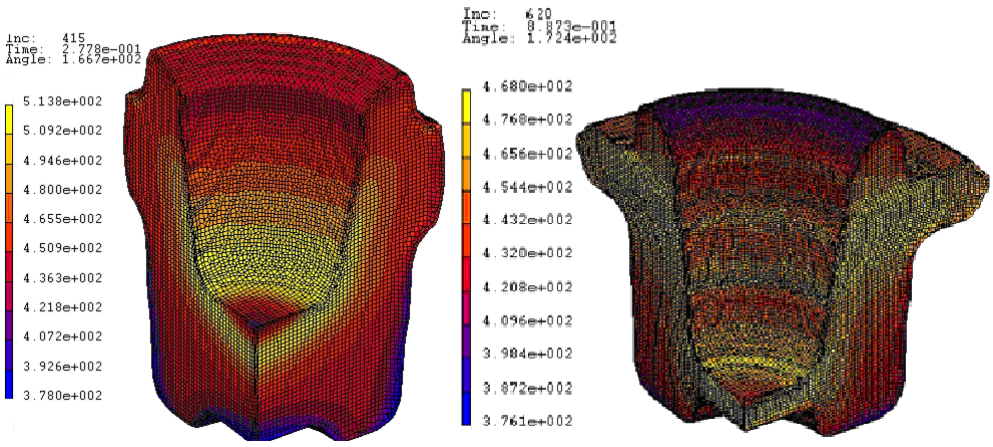


**(a)** **(b)**

**Figure 4.21 Maximum Temperature Distribution on (a) Preform (b) Finish Part for Initial Billet Temperature of 438 $^{o}$C**

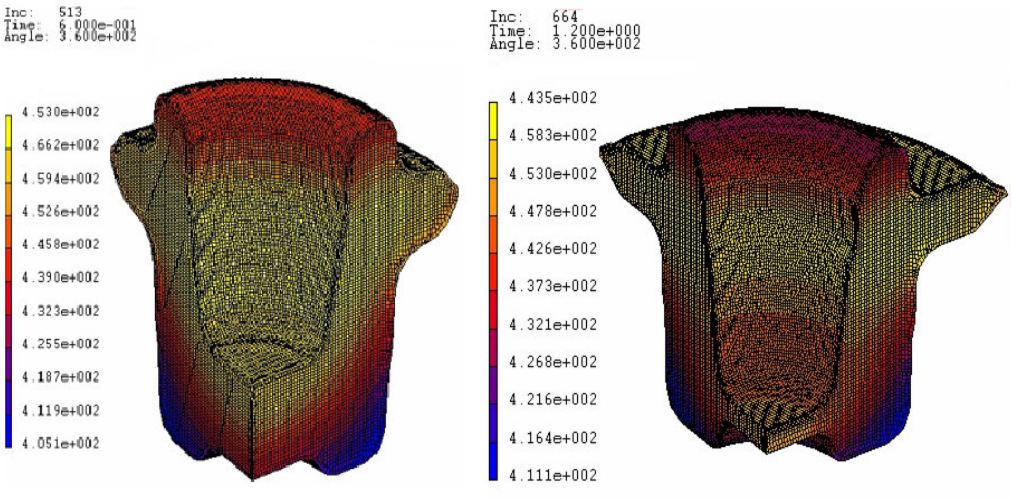


**(a)** **(b)**

**Figure 4.22 Temperature Distribution at the Last Increment on (a) Preform (b) Finish Part for Initial Billet Temperature of 438 $^{o}$C**

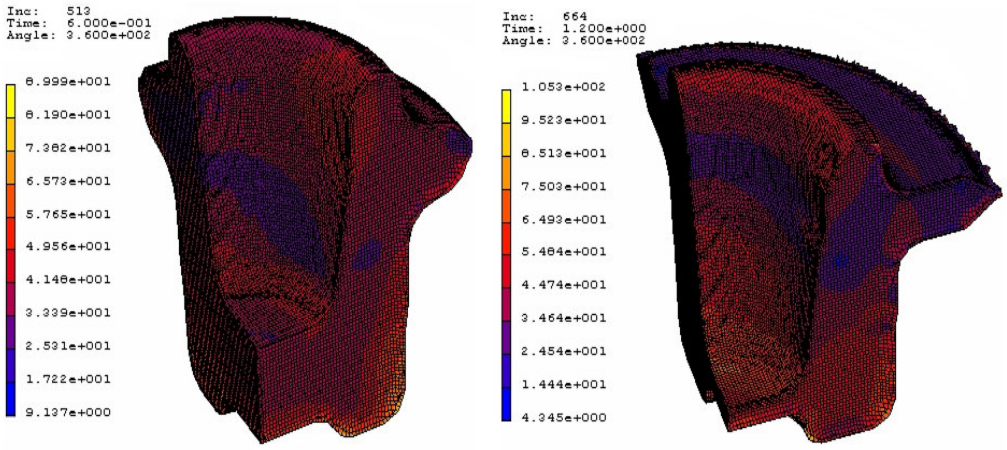


**(a)** **(b)**

**Figure 4.23 Residual Stress Distribution on (a) Preform (b) Finish Part for Initial Billet Temperature of 438 $^{o}$C**

**Table 4.3 Maximum Temperature and Residual Stress Values on Preform and Finish Part for Initial Billet Temperature of 438 °C**

| | Max. Temp. (°C) | Max. Residual Stress (MPa) | Temp. at the End of Forging (°C) | Angular Position of Crank at Max. Temp. (°) | Time at Max. Temp. (s) |
|---|---|---|---|---|---|
| **Preform Part** | 513 | 90 | 453 | 166.7 | 0.277 |
| **Finish Part** | 468 | 105 | 443 | 172.4 | 0.287 |

As mentioned in Chapter 2, while forging aluminum alloys, there is a risk of incipient melting when conditions of forging promote significant temperature increases because forging temperatures are very close to melting temperatures of alloys. As seen in Table 3.2, the solidus temperature of aluminum alloy 7075 is 477 °C. As shown in Table 4.3, maximum temperatures of preform and finish part are about 513 °C and 488 °C, respectively. These values are greater than the solidus temperature of aluminum alloy 7075 that means incipient melting of the workpiece occurs during both preform and finish forgings which can be resulted in rupture, cracks and permanently damage of the workpiece.

### 4.7.2 Results for Initial Billet Temperature of 400 °C

The maximum equivalent stress and the maximum temperature distributions on the preform and finish dies for the initial billet temperature of 400 °C are given in Figures 4.24–4.31. The maximum values are tabulated in Table 4.4.

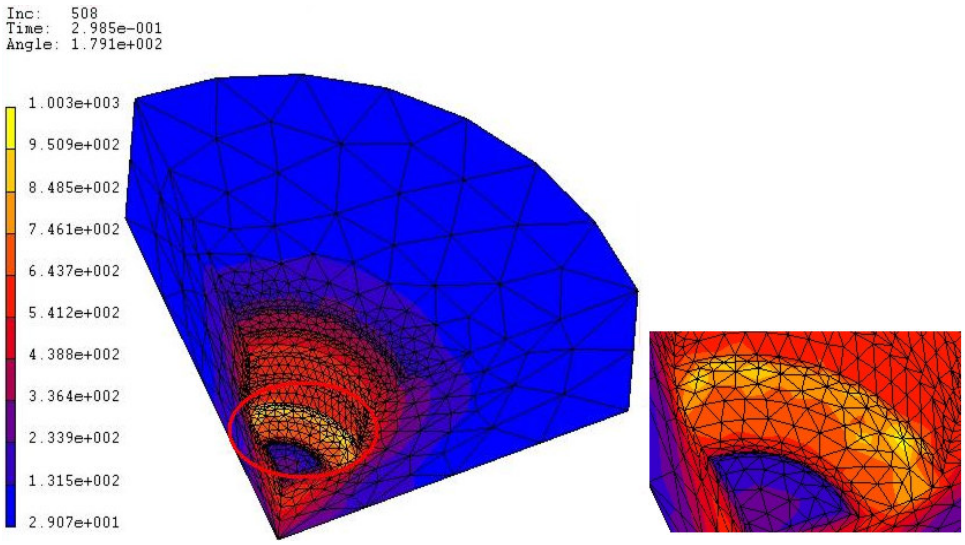


**Figure 4.24 Maximum Equivalent Stress Distribution on Lower Preform Die for Initial Billet Temperature of 400 ºC**

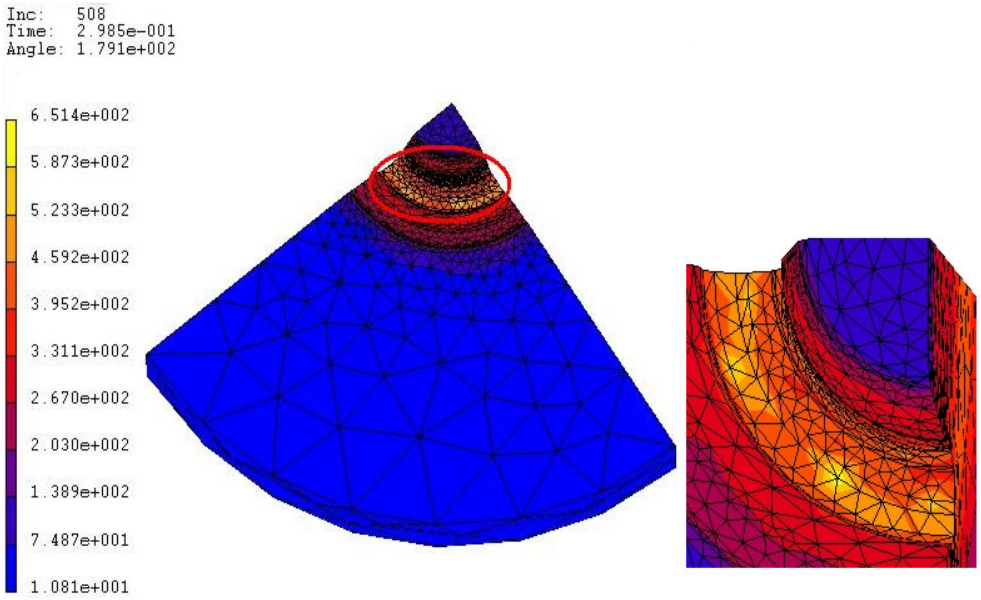


**Figure 4.25 Maximum Equivalent Stress Distribution on Upper Preform Die for Initial Billet Temperature of 400 ºC**

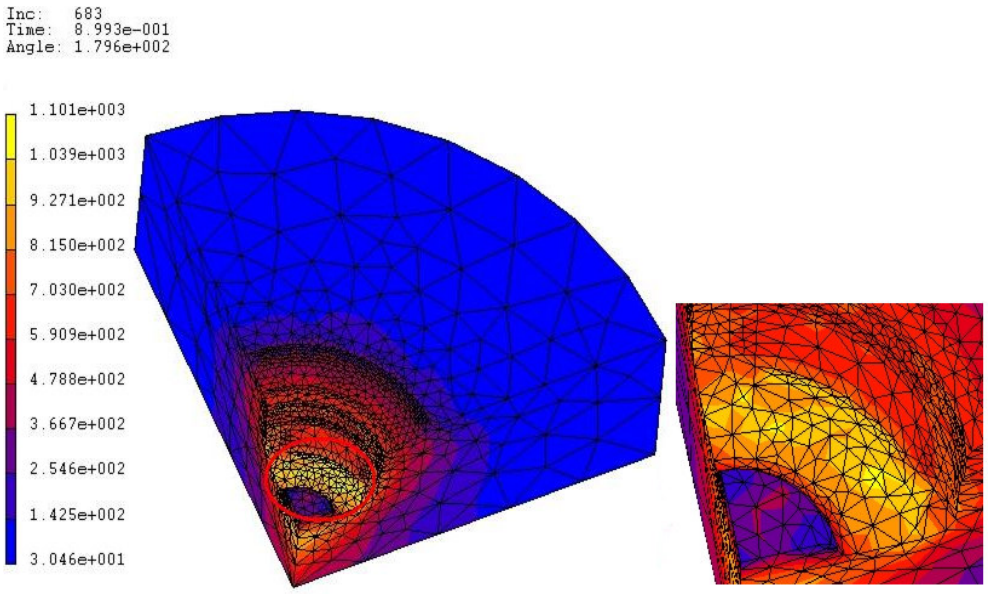


**Figure 4.26 Maximum Equivalent Stress Distribution on Lower Finish Die for Initial Billet Temperature of 400 $^{o}$C**

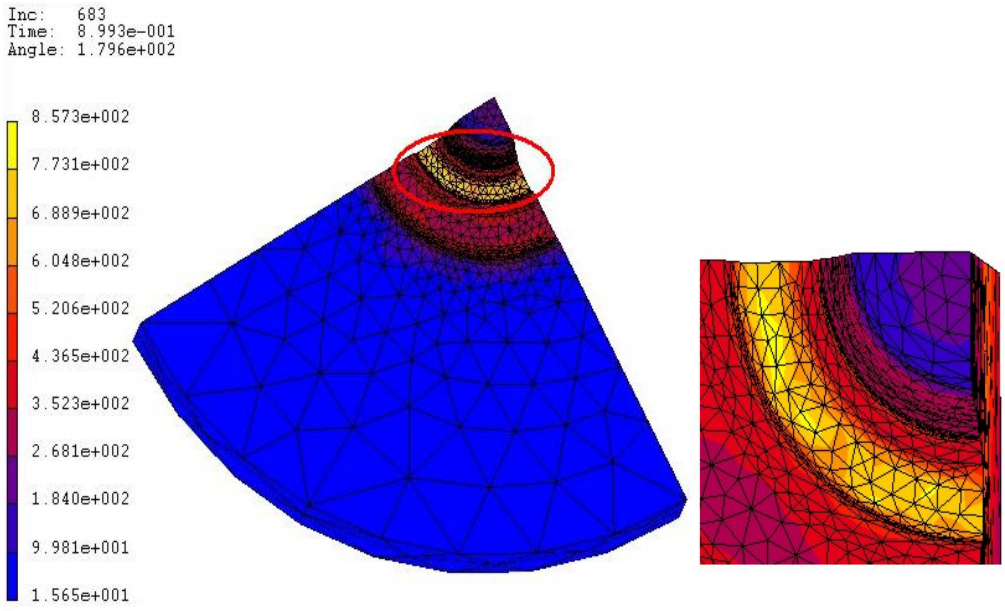


**Figure 4.27 Maximum Equivalent Stress Distribution on Upper Finish Die for Initial Billet Temperature of 400 $^{o}$C**

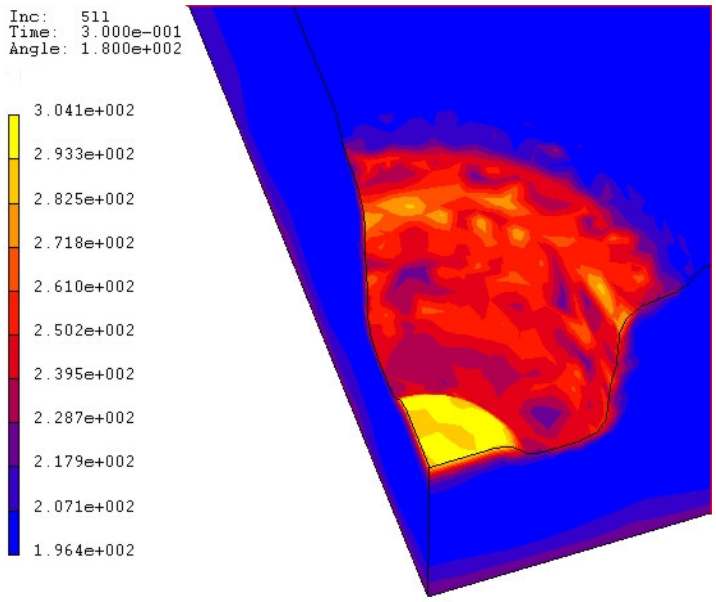


**Figure 4.28 Maximum Temperature Distribution on Lower Preform Die for Initial Billet Temperature of 400 $^{o}$C**

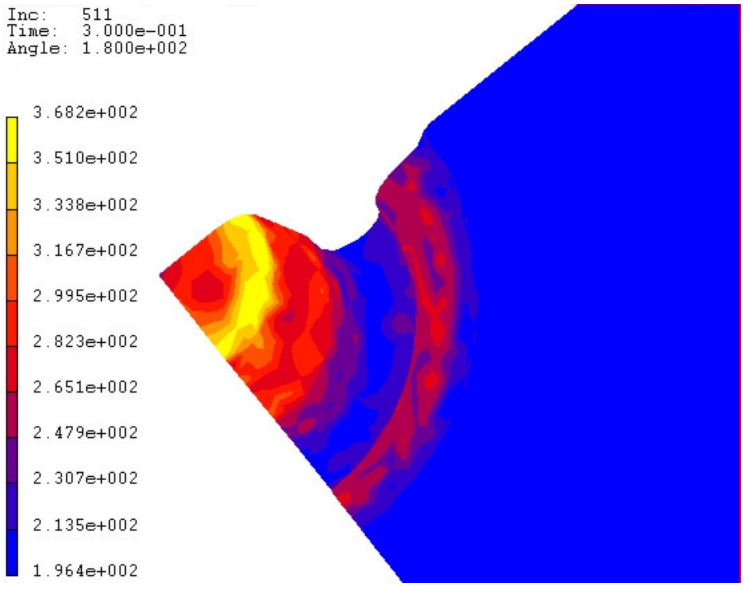


**Figure 4.29 Maximum Temperature Distribution on Upper Preform Die for Initial Billet Temperature of 400 $^{o}$C**

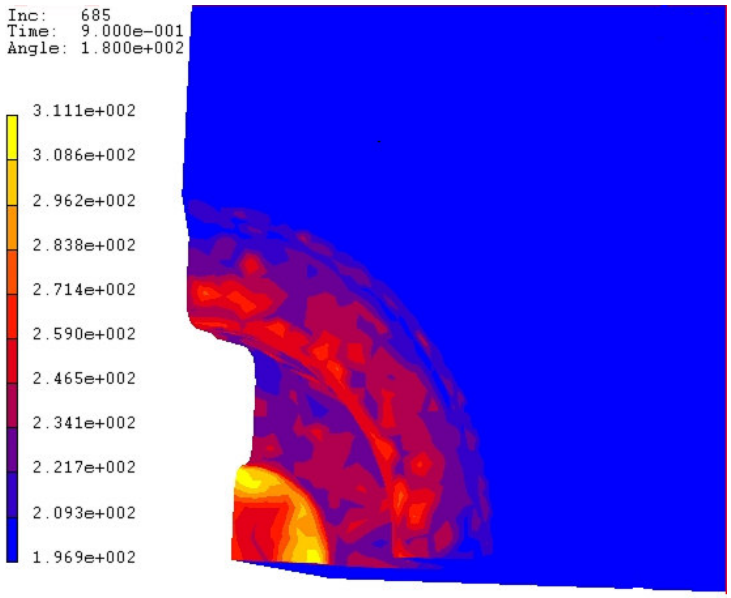


**Figure 4.30 Maximum Temperature Distribution on Lower Finish Die for Initial Billet Temperature of 400 $^{o}$C**

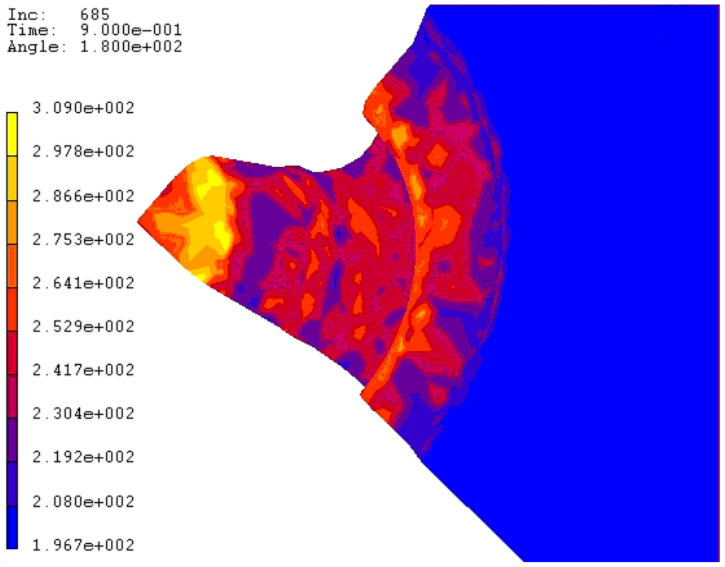


**Figure 4.31 Maximum Temperature Distribution on Upper Finish Die for Initial Billet Temperature of 400 $^{o}$C**

**Table 4.4 Maximum Equivalent Stress and Maximum Temperature Values on Preform and Finish Dies for Initial Billet Temperature of 400 °C**

| | Max. Equiv. Stress (MPa) | Max. Equiv. Plastic Strain | Max. Temp. (°C) | Max. Equiv. Stress. at the Region of Max. Temp. (MPa) | Max. Temp. at the Region of Max. Equiv. Stress (°C) | Angular Pos. of Crank at Max. Equiv. Stress (°) |
|---|---|---|---|---|---|---|
| **Lower Preform Die** | 1003 | 0 | 304 | 235 | 239 | 179.1 |
| **Upper Preform Die** | 651 | 0 | 368 | 240 | 220 | 179.1 |
| **Lower Finish Die** | 1101 | 0 | 311 | 350 | 240 | 179.6 |
| **Upper Finish Die** | 857 | 0 | 309 | 330 | 229 | 179.6 |

The maximum equivalent stresses on the preform dies are about 1003 MPa for the lower preform die and 651 MPa for the upper preform die. The maximum temperatures are about 304 °C for the lower preform die and 368 °C for the upper preform die. The maximum equivalent stress on the lower finish die is about 1101 MPa and the maximum equivalent stress on upper finish die is about 857 MPa. The maximum temperature values are about 311 °C and 309 °C for the lower finish die and the upper finish die, respectively. The values are different than the ones in the case of initial temperature of the billet of 438 °C. Stress values increase and temperature values decrease as expected, but stress and temperature distributions on the dies are very similar. As seen in the figures, the regions where the maximum stresses and temperatures are observed are the same at both temperatures. Again, no plastic deformation occurs on the dies.

The maximum temperature and residual stress values in the preform and finish part for the initial billet temperature of 400 °C are tabulated in Table 4.5.

**Table 4.5 Maximum Temperature and Residual Stress Values on Preform and Finish Part for Initial Billet Temperature of 400 °C**

| | Max. Temp. (°C) | Max. Residual Stress (MPa) | Temp. at the End of Forging (°C) | Angular Position of Crank at Max. Temp. (°) | Time at Max. Temp. (s) |
|---|---|---|---|---|---|
| **Preform Part** | 473 | 90 | 420 | 165.1 | 0.275 |
| **Finish Part** | 441 | 108 | 414 | 172.0 | 0.288 |

Temperature distribution on the preform and the finish part are very similar to the ones in the case of initial temperature of the billet of 438 °C, except the values which decreased as expected. As shown in Table 4.5, the maximum temperatures of the preform and the finish part are about 473 °C and 441 °C, respectively. From the results, it is deduced that no incipient melting occurs for forging temperature of 400 °C; however, maximum temperature that the preform attains is only 3 °C below its solidus temperature. The difference is so small and due to numerical errors, unhomogeneity of the workpiece, etc., it could be said that there is a risk of incipient melting of the workpiece at the initial billet temperature of 400 °C.

The comparison of the results of MSC. SuperForge and MSC. SuperForm for the preform and finish part at the initial billet temperature of 400 °C is given in Appendix B.

### 4.7.3 Results for Initial Billet Temperature of 350 °C

The maximum equivalent stress and the maximum temperature distributions on the preform and finish dies for the initial billet temperature of 350 °C are given in Figures 4.32–4.35. The maximum values are tabulated in Table 4.6.

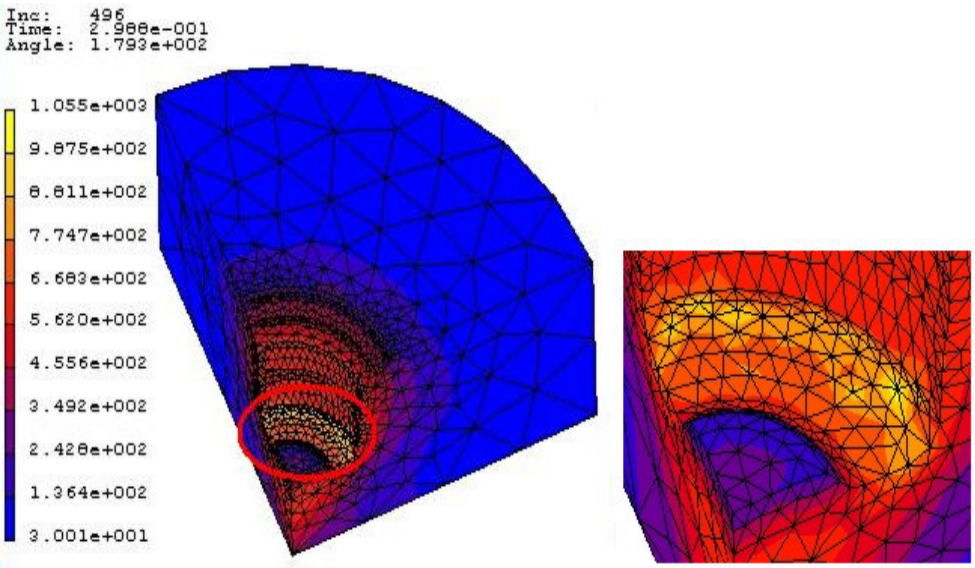


**Figure 4.32 Maximum Equivalent Stress Distribution on Lower Preform Die for Initial Billet Temperature of 350 $^{o}$C**

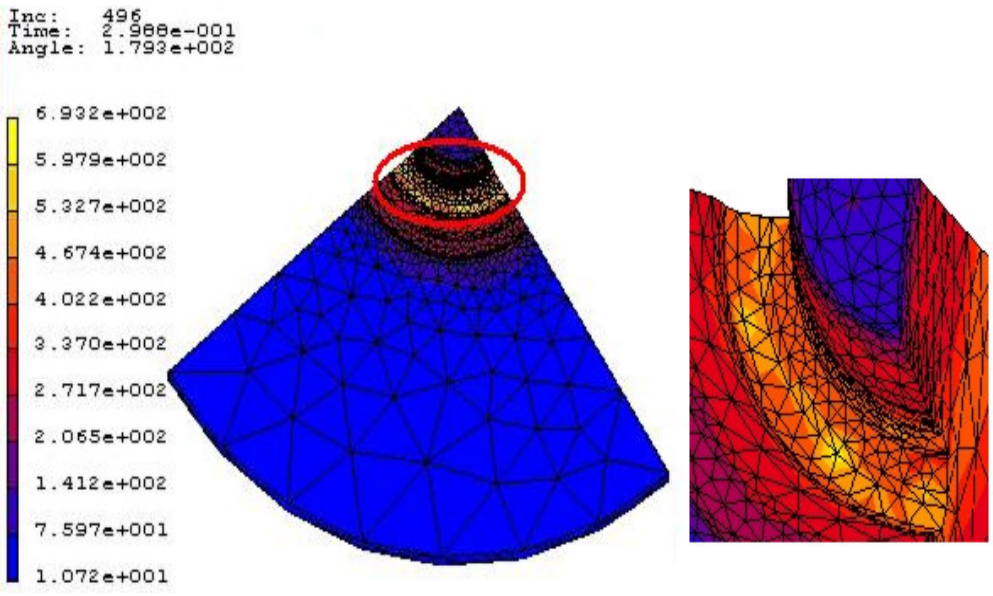


**Figure 4.33 Maximum Equivalent Stress Distribution on Upper Preform Die for Initial Billet Temperature of 350 $^{o}$C**

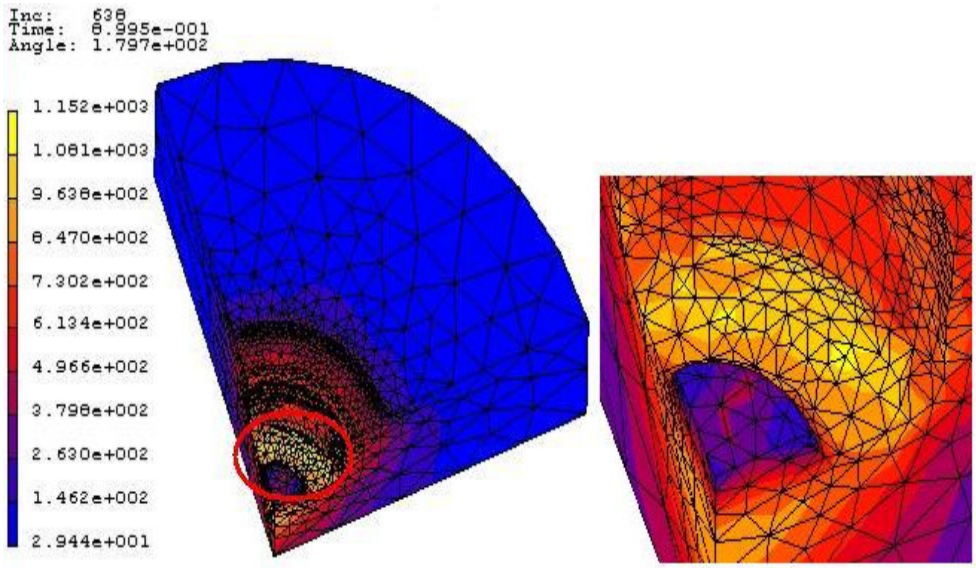


**Figure 4.34 Maximum Equivalent Stress Distribution on Lower Finish Die for Initial Billet Temperature of 350 $^{o}$C**

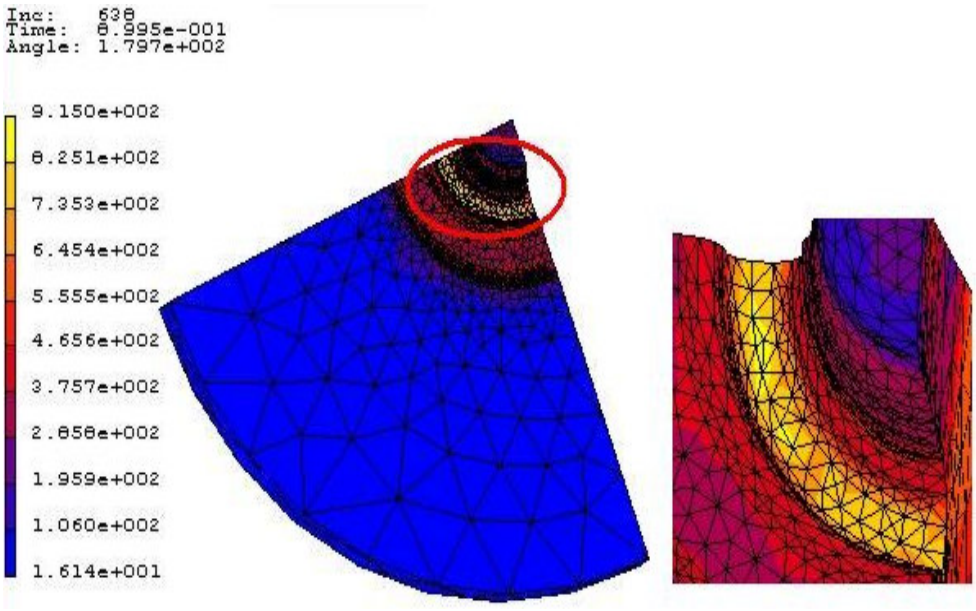


**Figure 4.35 Maximum Equivalent Stress Distribution on Upper Finish Die for Initial Billet Temperature of 350 $^{o}$C**

**Table 4.6 Maximum Equivalent Stress and Maximum Temperature Values on Preform and Finish Dies for Initial Billet Temperature of 350 °C**

| | Max. Equiv. Stress (MPa) | Max. Equiv. Plastic Strain | Max. Temp. (°C) | Max. Equiv. Stress. at the Region of Max. Temp. (MPa) | Max. Temp. at the Region of Max. Equiv. Stress (°C) | Angular Pos. of Crank at Max. Equiv. Stress (°) |
|---|---|---|---|---|---|---|
| **Lower Preform Die** | 1055 | 0 | 283 | 245 | 223 | 179.3 |
| **Upper Preform Die** | 693 | 0 | 338 | 290 | 217 | 179.3 |
| **Lower Finish Die** | 1152 | 0 | 300 | 379 | 225 | 179.7 |
| **Upper Finish Die** | 915 | 0 | 295 | 376 | 220 | 179.7 |

The maximum equivalent stresses on the preform dies are about 1055 MPa for the lower preform die and 693 MPa for the upper preform die. The maximum equivalent stresses on the lower finish die and the upper finish die are about 1152 MPa and 915 MPa, respectively. The maximum stress values on the dies increase; but still dies do not deform plastically when the initial billet temperature is decreased to 350 °C.

The maximum temperature and the residual stress values in the preform and finish part for the initial billet temperature of 350 °C are tabulated in Table 4.7.

**Table 4.7 Maximum Temperature and Residual Stress Values on Preform and Finish Part for Initial Billet Temperature of 350 °C**

| | Max. Temp. (°C) | Max. Residual Stress (MPa) | Temp. at the End of Forging (°C) | Angular Position of Crank at Max. Temp. (°) | Time at Max. Temp. (s) |
|---|---|---|---|---|---|
| **Preform Part** | 442 | 127 | 400 | 165.6 | 0.276 |
| **Finish Part** | 425.6 | 117 | 394 | 174.3 | 0.290 |

The temperature distribution on the preform and the finish part are very similar to the ones in the case of initial temperature of the billet of 400 °C, except the values which decreased. The maximum temperature of the workpiece during forging process is about 442 °C which is 34 °C lower than the solidus temperature of aluminum alloy 7075; therefore it can be concluded that no incipient melting of workpiece is expected when the initial billet temperature is decreased to 350 °C.

### 4.7.4 Results for Initial Billet Temperature of 300 °C

The maximum equivalent stress, the maximum equivalent plastic strain and the maximum temperature distributions on the preform and finish dies for the initial billet temperature of 300 °C are given in Figures 4.36–4.41. The maximum values are tabulated in Table 4.8.

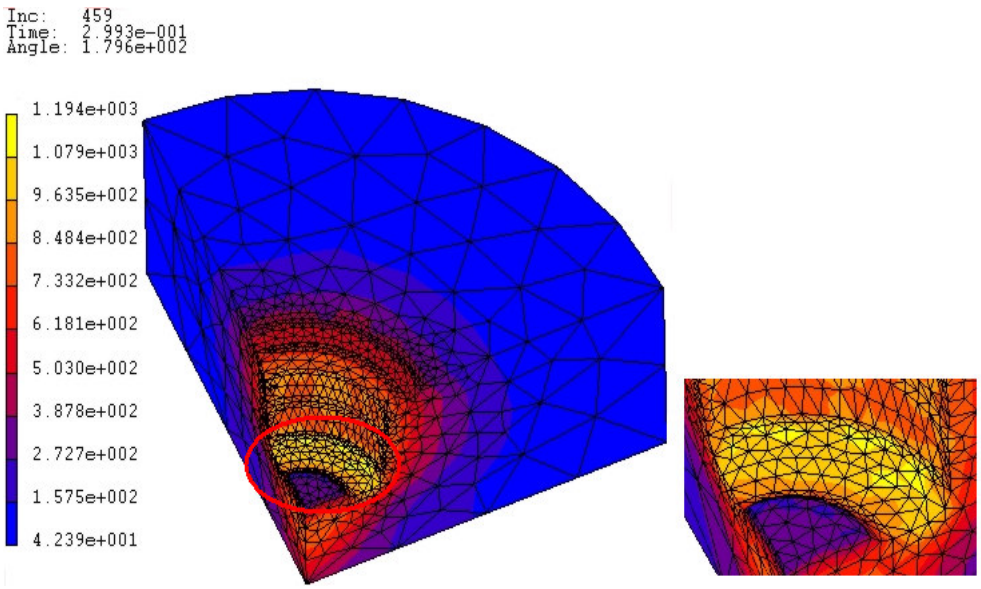


**Figure 4.36 Maximum Equivalent Stress Distribution on Lower Preform Die for Initial Billet Temperature of 300 $^{o}$C**

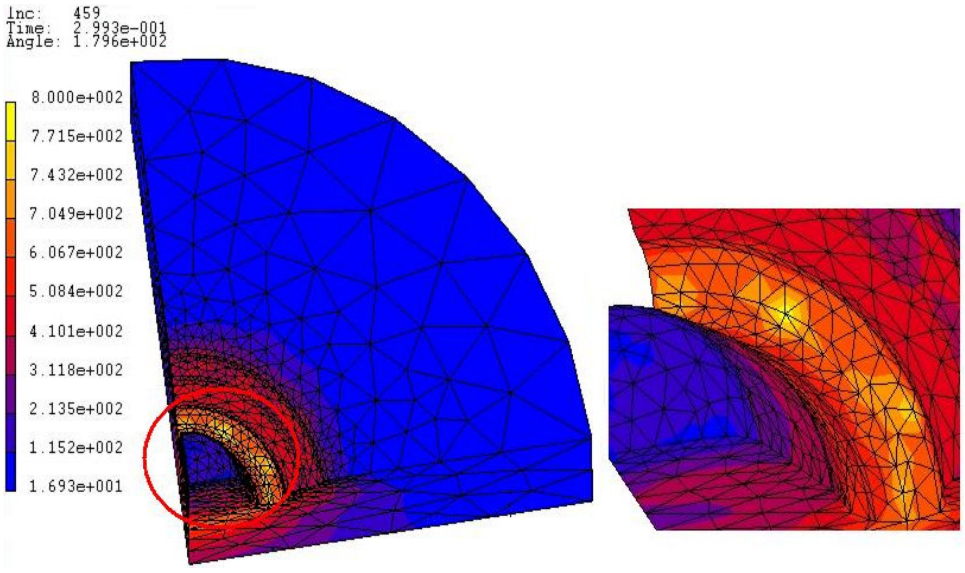


**Figure 4.37 Maximum Equivalent Stress Distribution on Upper Preform Die for Initial Billet Temperature of 300 $^{o}$C**

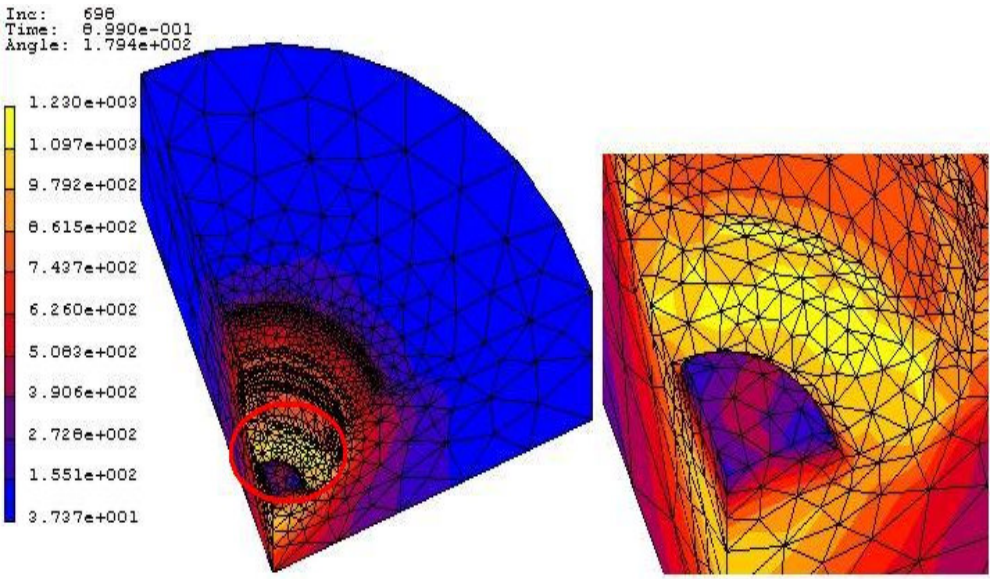


**Figure 4.38 Maximum Equivalent Stress Distribution on Lower Finish Die for Initial Billet Temperature of 300 $^{o}$C**

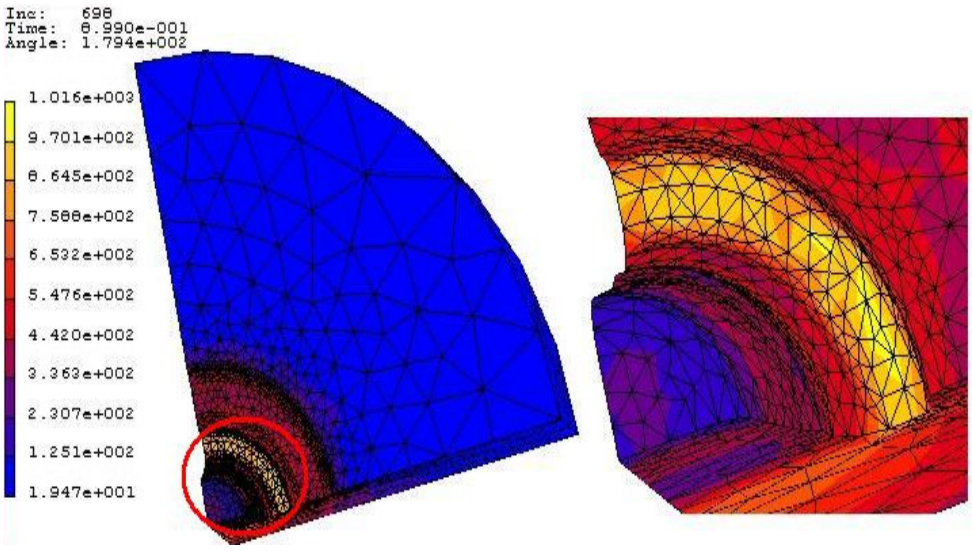


**Figure 4.39 Maximum Equivalent Stress Distribution on Upper Finish Die for Initial Billet Temperature of 300 $^{o}$C**

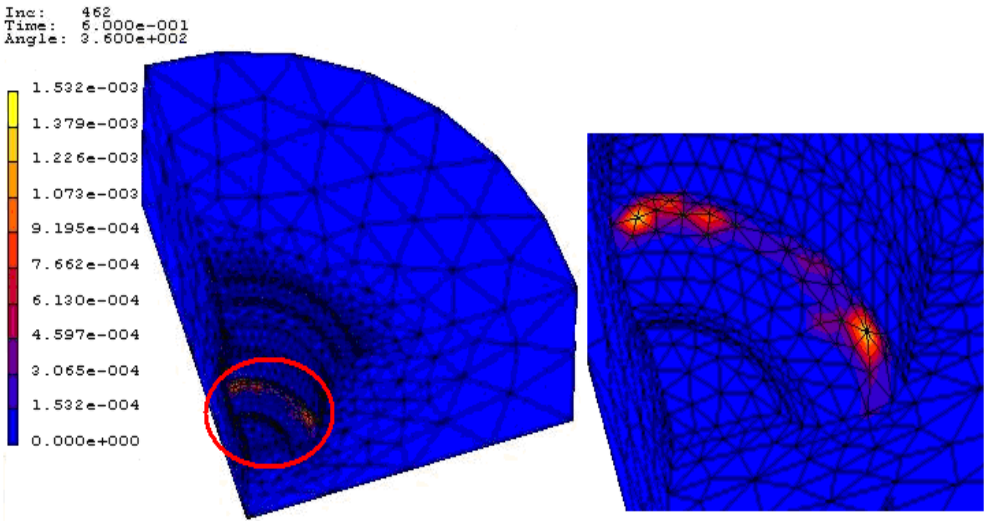


**Figure 4.40 Maximum Equivalent Plastic Strain Distribution on Lower Preform Die for Initial Billet Temperature of 300 $^{o}$C**

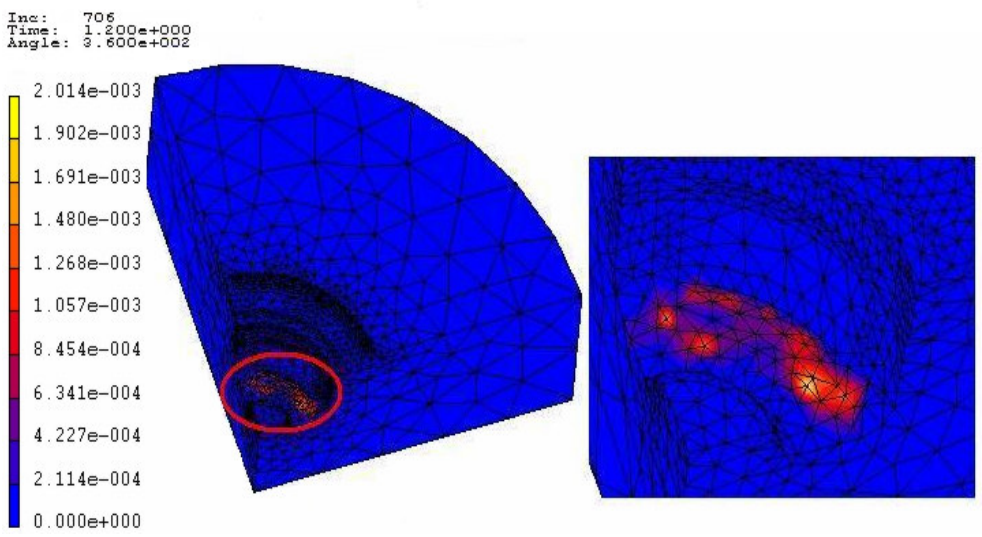


**Figure 4.41 Maximum Equivalent Plastic Strain Distribution on Lower Finish Die for Initial Billet Temperature of 300 $^{o}$C**

**Table 4.8 Maximum Equivalent Stress, Maximum Equivalent Plastic Strain and Maximum Temperature Values on Preform and Finish Dies for Initial Billet Temperature of 300 $^{o}$C**

| | Max. Equiv. Stress (MPa) | Max. Equiv. Plastic Strain | Max. Temp. (°C) | Max. Equiv. Stress. at the Region of Max. Temp. (MPa) | Max. Temp. at the Region of Max. Equiv. Stress (°C) | Angular Pos. of Crank at Max. Equiv. Stress (°) |
|---|---|---|---|---|---|---|
| **Lower Preform Die** | 1194 | $1.53 \times 10^{-3}$ | 255 | 272 | 214 | 179.6 |
| **Upper Preform Die** | 800 | 0 | 313 | 315 | 211 | 179.6 |
| **Lower Finish Die** | 1230 | $2.01 \times 10^{-3}$ | 271 | 420 | 217 | 179.4 |
| **Upper Finish Die** | 1016 | 0 | 280 | 430 | 214 | 179.4 |

The maximum equivalent stresses on the preform dies are about 1194 MPa for the lower preform die and 800 MPa for the upper preform die. The maximum equivalent stresses on the lower finish die and upper finish die are about 1230 MPa and 1016 MPa, respectively. The maximum stress values increase and maximum temperature values decrease as expected but the locations are similar to the ones that are given for higher initial billet temperatures. Also as seen from the results, the increase in the maximum stress values is greater when initial billet temperature is reduced to 300 $^{o}$C. On the lower preform and finish dies, local plastic strains are observed at the region where the maximum stresses occur. The maximum equivalent plastic strains for the lower preform die and the lower finish die are about $1.53 \times 10^{-3}$ and $2.01 \times 10^{-3}$, respectively. The plastic strain starts to occur on the lower preform die at the crank's angular position of 178° and on the lower finish die at the crank's angular position of 177.9°.

The residual stresses and the temperature distributions on the preform and finish part are very similar to the ones that are given for higher initial billet temperatures, except the values which are given in Table 4.9.

**Table 4.9 Maximum Temperature and Residual Stress Values on Preform and Finish Part for Initial Billet Temperature of 300 °C**

| | Max. Temp. (°C) | Max. Residual Stress (MPa) | Temp. at the End of Forging (°C) | Angular Position of Crank at Max. Temp. (°) | Time at Max. Temp. (s) |
|---|---|---|---|---|---|
| **Preform Part** | 425 | 131 | 365 | 165.7 | 0.276 |
| **Finish Part** | 394.3 | 126 | 362 | 174.5 | 0.290 |

### 4.7.5 Results for Initial Billet Temperature of 250 °C

The maximum equivalent stress, the maximum plastic strain and the maximum temperature distributions on the preform and finish dies for the initial billet temperature of 250 °C are given in Figures 4.42–4.47. The maximum values are tabulated in Table 4.10.

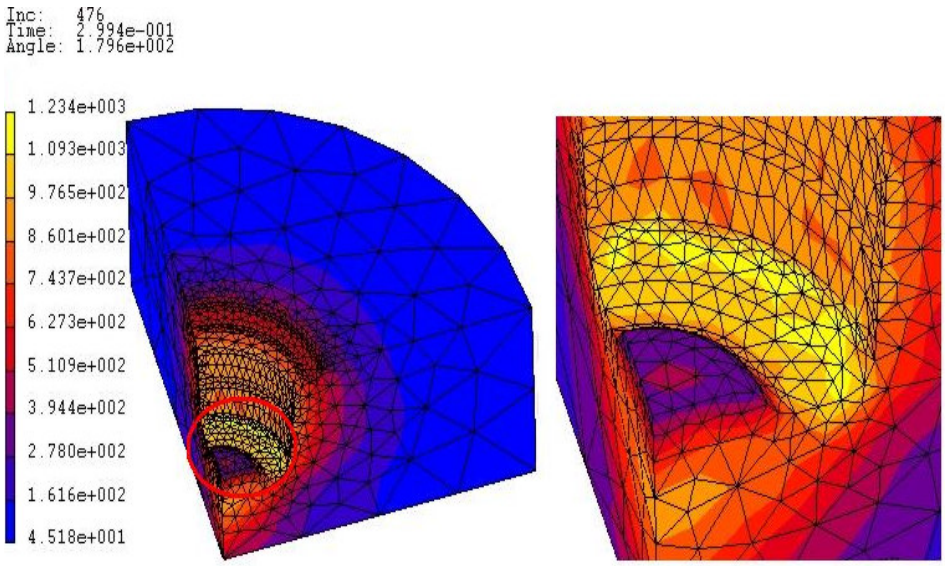


**Figure 4.42 Maximum Equivalent Stress Distribution on Lower Preform Die for Initial Billet Temperature of 250 $^{o}$C**

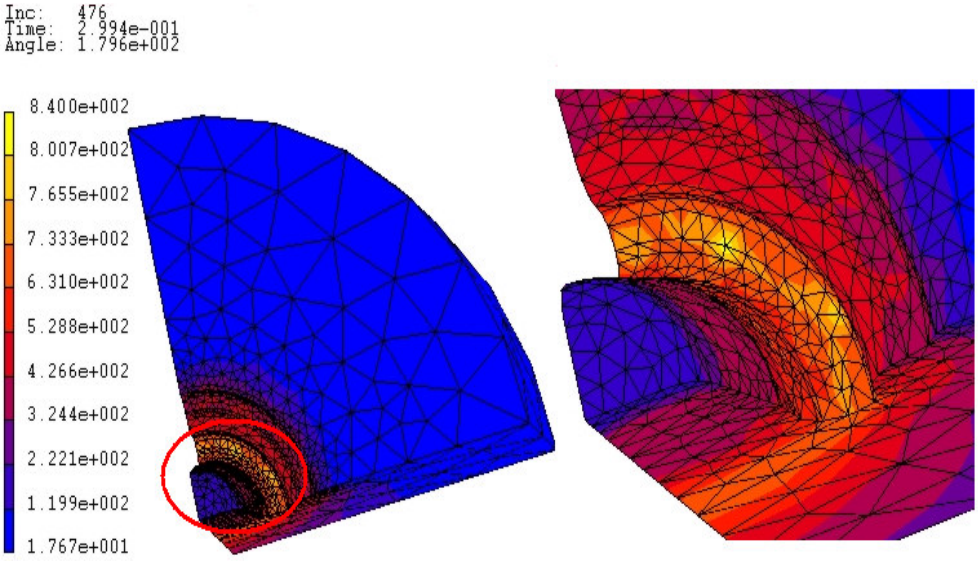


**Figure 4.43 Maximum Equivalent Stress Distribution on Upper Preform Die for Initial Billet Temperature of 250 $^{o}$C**

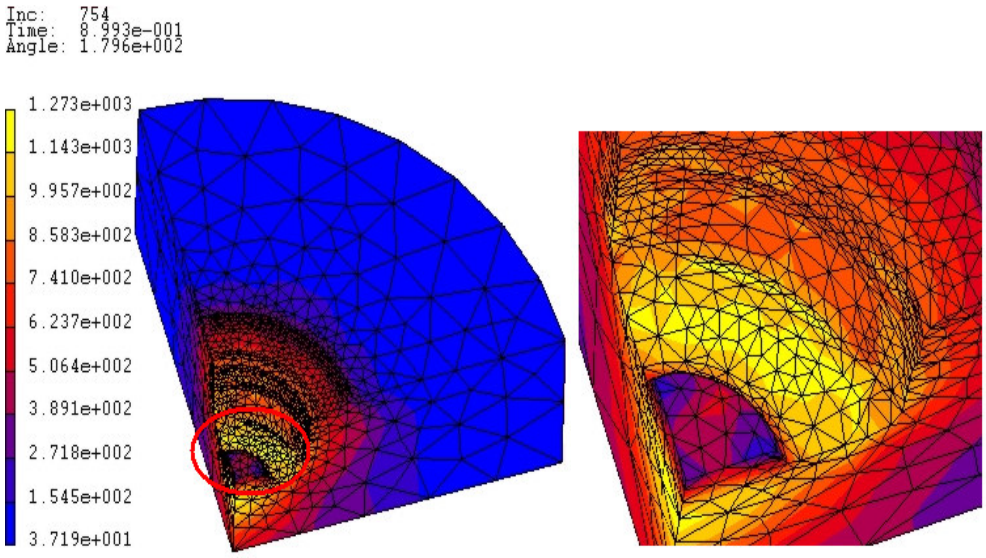


**Figure 4.44 Maximum Equivalent Stress Distribution on Lower Finish Die for Initial Billet Temperature of 250 $^{o}$C**

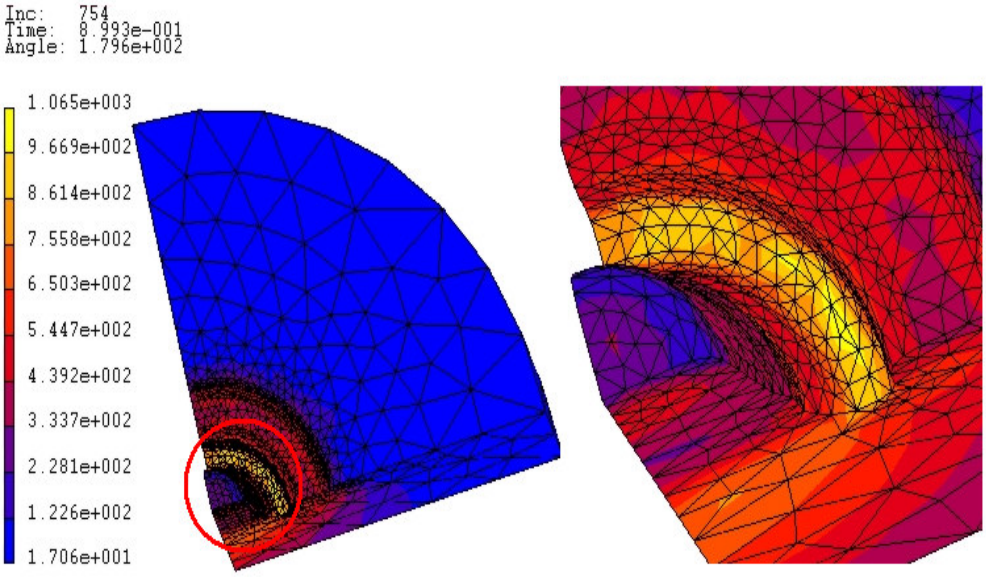


**Figure 4.45 Maximum Equivalent Stress Distribution on Upper Finish Die for Initial Billet Temperature of 250 $^{o}$C**

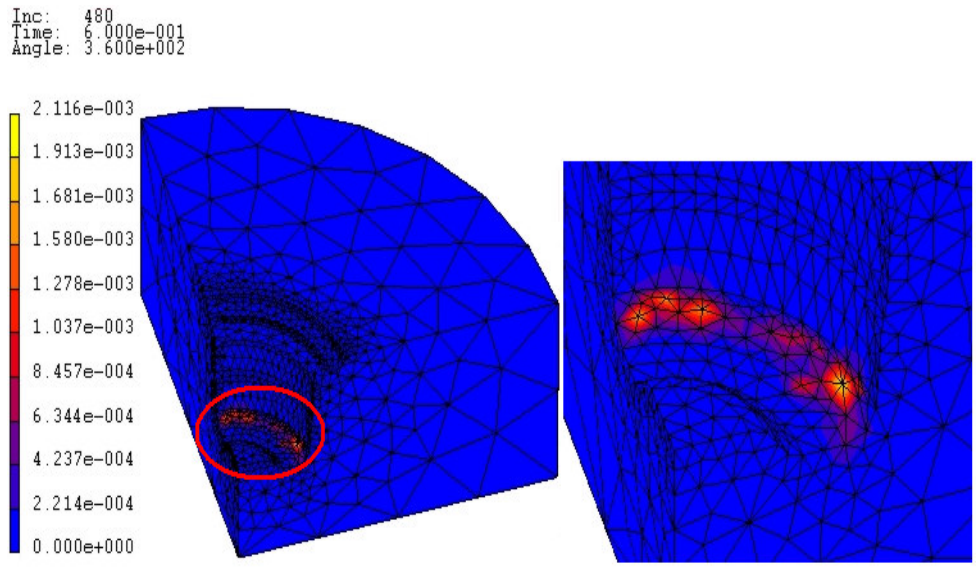


**Figure 4.46 Maximum Equivalent Plastic Strain Distribution on Lower Preform Die for Initial Billet Temperature of 250 $^{o}$C**

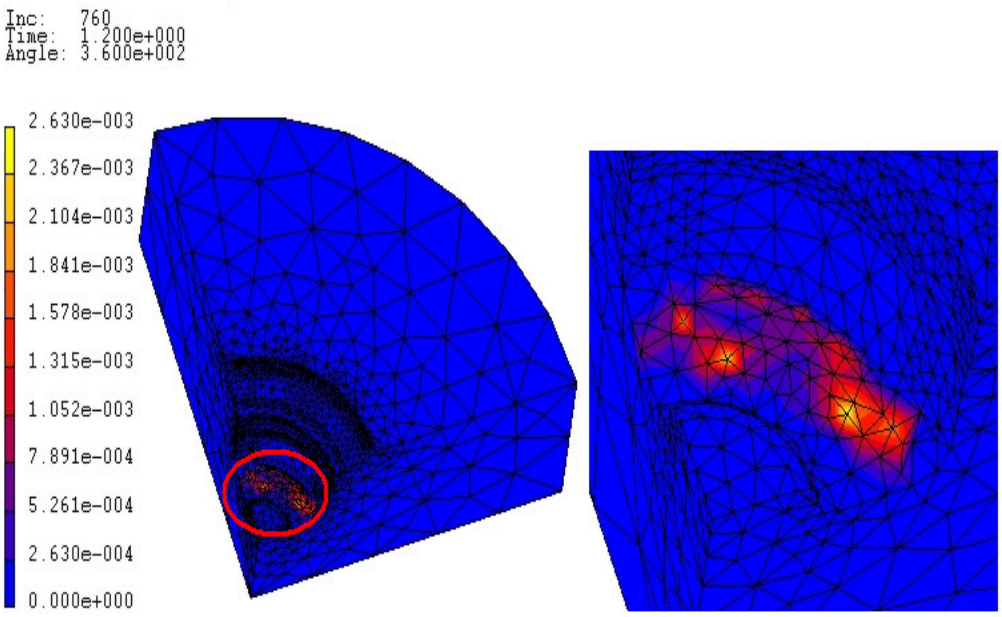


**Figure 4.47 Maximum Equivalent Plastic Strain Distribution on Lower Finish Die for Initial Billet Temperature of 250 $^{o}$C**

**Table 4.10 Maximum Equivalent Stress, Maximum Equivalent Plastic Strain and Maximum Temperature Values in Preform and Finish Dies for Initial Billet Temperature of 250 $^{o}$C**

| | Max. Equiv. Stress (MPa) | Max. Equiv. Plastic Strain | Max. Temp. (°C) | Max. Equiv. Stress. at the Region of Max. Temp. (MPa) | Max. Temp. at the Region of Max. Equiv. Stress (°C) | Angular Pos. of Crank at Max. Equiv. Stress (°) |
|---|---|---|---|---|---|---|
| **Lower Preform Die** | 1234 | $2.11 \times 10^{-3}$ | 241 | 300 | 207 | 179.6 |
| **Upper Preform Die** | 840 | 0 | 298 | 343 | 203 | 179.6 |
| **Lower Finish Die** | 1273 | $2.63 \times 10^{-3}$ | 260 | 443 | 210 | 179.6 |
| **Upper Finish Die** | 1065 | 0 | 268 | 469 | 206 | 179.6 |

The maximum equivalent stresses on the preform dies are about 1234 MPa for the lower preform die and 840 MPa for the upper preform die. The maximum equivalent stresses on the lower finish die and upper finish die are about 1273 MPa and 1065 MPa, respectively. The maximum stress values increase and the maximum temperature values decrease as expected but the locations are similar to the ones that are given for higher initial billet temperatures. On the lower preform and finish dies local plastic strains are observed at the regions of where maximum stresses occur. The maximum equivalent plastic strains for the lower preform die and the lower finish die are about $2.11 \times 10^{-3}$ and $2.63 \times 10^{-3}$, respectively. The plastic strain starts to occur on the lower preform die at the crank's angular position of 177.3° and on the lower finish die at the crank's angular position of 177.1°.

**Table 4.11 Maximum Temperature and Residual Stress Values in Preform and Finish Part for Initial Billet Temperature of 250 °C**

| | Max. Temp. (°C) | Max. Residual Stress (MPa) | Temp. at the End of Forging (°C) | Angular Position of Crank at Max. Temp. (°) | Time at Max. Temp. (s) |
|---|---|---|---|---|---|
| **Preform Part** | 403.5 | 161 | 328.7 | 165.4 | 0.275 |
| **Finish Part** | 362 | 179 | 330 | 174.6 | 0.291 |

The residual stresses and the temperature distributions on the preform and finish part are very similar to the ones that are given for higher billet temperatures, except the values which are given in Table 4.11.

In Table 4.12, the maximum forces applied on the dies are given for the initial billet temperature of 250 °C. As seen in Table 4.12, maximum die forces are about $3.50 \times 10^5$ N for the lower preform die, $3.13 \times 10^5$ N for the upper preform die, $1.20 \times 10^6$ N for the lower finish die and $1.12 \times 10^6$ N for the upper finish die.

**Table 4.12 Maximum Die Forces for Initial Billet Temperature of 250 °C**

| | **Maximum Die Load (N)** |
|---|---|
| **Lower Preform Die** | $3.50 \times 10^5$ |
| **Upper Preform Die** | $3.13 \times 10^5$ |
| **Lower Finish Die** | $1.20 \times 10^6$ |
| **Upper Finish Die** | $1.12 \times 10^6$ |

### 4.8 Discussion of the Finite Element Simulations

In the simulation results, it is observed that the maximum equivalent stress values on the dies increase as the initial billet temperature is reduced. However, the locations on the upper and lower dies where the maximum equivalent stresses occur are very similar for all the simulations.

In the simulation results, for the initial billet temperatures of 438 $^{o}$C, 400 $^{o}$C and 350 $^{o}$C, no plastic deformation occurs on the dies. However, for the initial billet temperatures of 300 $^{o}$C and 250 $^{o}$C, the plastic strains are observed on the lower preform and lower finish dies. At initial billet temperature of 300 $^{o}$C, the maximum equivalent plastic strains are about $1.53x10^{-3}$ and $2.01x10^{-3}$ for the lower preform die and the lower finish die, respectively and average plastic strains are about $9x10^{-4}$ for the lower preform die and $1.2x10^{-3}$ for the lower finish die. At initial billet temperature of 250 $^{o}$C, the maximum equivalent plastic strains are about $2.11x10^{-3}$ and $2.63x10^{-3}$ for the lower preform die and the lower finish die, respectively and average plastic strains are about $1.2x10^{-3}$ for the lower preform die and $1.5x10^{-3}$ for the lower finish die.

In the results, it is seen that for the initial billet temperature of 438 $^{o}$C, temperature of the workpiece exceeds its solidus temperature during the forging process that means incipient melting of the workpiece occurs. Since according to the literature, incipient melting can be resulted in rupture, cracks and permanently damage of the workpiece, it can be said that the part should not be forged at the initial billet temperature of 438 $^{o}$C. For the initial billet temperature of 400 $^{o}$C, although the maximum temperature of the workpiece does not exceed its solidus temperature, it reaches very close its solidus temperature value. For this reason, forging at the initial billet temperature of 400 $^{o}$C should also be avoided.

The temperature distribution at the increment of the maximum equivalent stress is similar for all simulations but the numerical values are different. The locations

where the temperature reaches to its peak values are the ones which are in contact with the workpiece for a longer duration. The peak values of the temperature on the dies decrease as the initial billet temperature is reduced.

Although in Table 2.2 recommended temperature range for forging aluminum alloy 7075 is given within 382 $^{o}$C and 438 $^{o}$C, from the finite element simulations, it can be concluded that the particular part can be forged at 350 $^{o}$C because no plastic deformation occurs on the dies at this initial billet temperature. Forging temperature can be reduced up to 250 $^{o}$C however, local plastic strains are observed on the lower preform and lower finish dies. Although observed plastic strains are negligible, to obtain smooth parts forging at the initial billet temperatures of 300 $^{o}$C and 250 $^{o}$C is not recommended. This study also showed that, to determine the most appropriate forging temperature of the particular part, more finite element analyses between the initial forging temperatures of 350 $^{o}$C and 300 $^{o}$C must be performed.

In the experiments, the initial forging temperature of the billet will be reduced up to 250 $^{o}$C. Since maximum die load at the initial billet temperature of 250 $^{o}$C is about $1.2x10^{6}$ N, it is concluded that the capacity of 1000 ton SMERAL mechanical press available in METU-BILTIR Center Forging Research and Application Laboratory will be enough to forge the particular part at the initial billet temperature of 250 $^{o}$C.

# CHAPTER 5

# MANUFACTURING OF THE DIES AND EXPERIMENTATION

In this chapter, manufacturing of the dies and the results of the experiments which have been conducted according to the previously realized finite element analyses will be explained.

## 5.1 Dimensional Features of the Press, the Die Holders and the Dies

In the experiments, 1000 ton SMERAL mechanical press which is available in METU-BILTIR Center Forging Research and Application Laboratory has been used. The photograph of the available press can be seen in Figure 5.1. The dies have been manufactured according to the dimensional limitations of this press. The press has a ram stroke of 220 mm and has a shut height of 620 mm, which is the distance between the ram and the anvil when the ram is at its bottom dead position. When the die holders which are given in Figures 5.2 and 5.3 are mounted and the ram is at its bottom dead position, the distance between the die locating surfaces of the upper and lower die holders is 200 mm. That distance gives the total allowable height of the upper and lower dies when there is no flash formation. So the sum of the heights of the dies and the die facial clearance must be equal to 200 mm in order to prevent collision of the dies during the forging stroke. In the experiments, the facial clearance for the preform stage has been given as 1.8 mm, so the total height of preform dies has become 198.2 mm, while for the finish stage facial clearance (i.e. flash thickness) is 1.5 mm, so the total height of finish dies has become 198.5 mm.


**Figure 5.1 1000-ton SMERAL Mechanical Press Available in METU-BILTIR Center Forging Research and Application Laboratory [18]**

The lower die holder has three sections for three different die sets. For the upper die holder, the same arrangement exists. So that up to three die sets can be used according to the number of stages in the forging process.

As shown in Figure 5.2, the middle section of the die holder has the largest diameter which is 222 mm and the other sections have diameters of 197 mm.

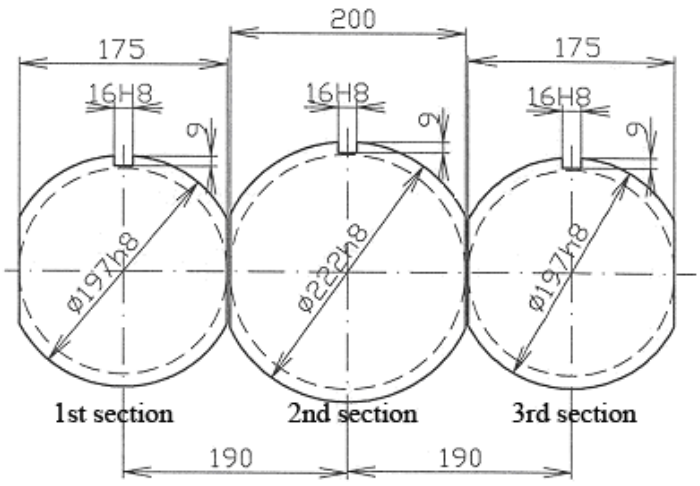


**Figure 5.2 Top View of Circular Dies [40]**

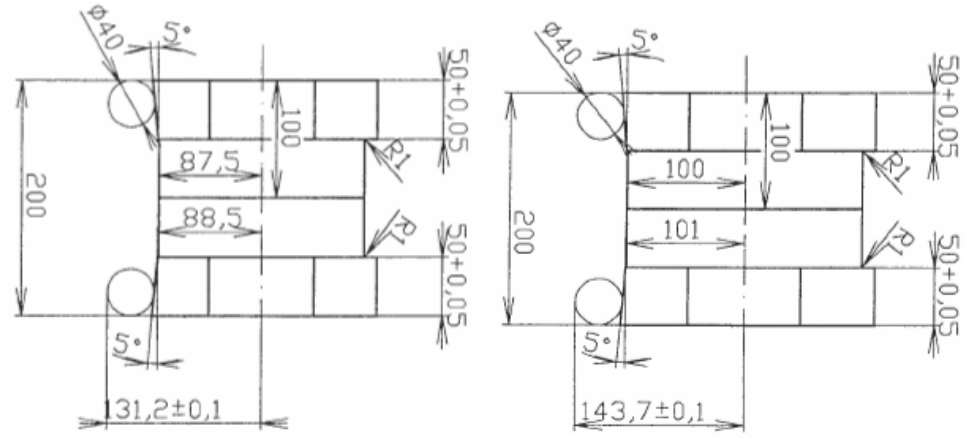


**Figure 5.3 Front View of the Circular Dies [40]**

## 5.2 Manufacturing of the Dies

The dies have been manufactured in METU-BILTIR Center Forging Research and Application Laboratory. Firstly, the outside die diameters have been machined to the required dimensions in the universal turning machine then they

have been milled to their final shapes in MAZAK Variaxis 630-5X High-Speed Vertical Milling Machine available in the laboratory. The G-Codes required to manufacture the dies have been obtained by using Pro-Engineer Wildfire III. The dies have been modeled in the CAD module of the program, than G-Codes have been created according to these models in the CAM module of the program. These codes have been transferred to MAZAK Variaxis 630-5X High-Speed Vertical Milling Machine. The dies have been turned and milled from the die steel of DIEVAR in the soft annealed condition because machining is easy in this condition, and then the dies have been sent for heat treatment. Heat treatment is necessary to improve performance of the dies by increasing their strength and other desirable characteristics.

The photographs of the manufactured preform and finish dies are given in Figure 5.4 and Figure 5.5, respectively. The engineering drawings of the preform and the finish dies are given in Appendix D.

**Figure 5.4 View of Lower and Upper Preform Dies**

**Figure 5.5 View of Lower and Upper Finish Dies**

## 5.3 Preparation of Experiments

During the preparation of experiments, first of all, the billets have been prepared for forging process. For this purpose, the Ø37 mm cylindrical bar which has been supplied from the aluminum supplier has been cut into the pieces with the length of 46 mm length at the sawing machine available in the laboratory. Billets have been measured in length, and each of them have been marked and given a number. The lengths of the billets have been measured using digital compass having an accuracy of ±0.01 mm. The length of each billet has been measured three times to decrease the risk of wrong measurement and the average value has been recorded.

After billets have been cut, manufactured dies have been fastened to the press. In the set up of the dies, the upper dies have been located to the die holders by the help of the hydraulic jack as shown in Figure 5.6 and then fastened by the clamping elements.

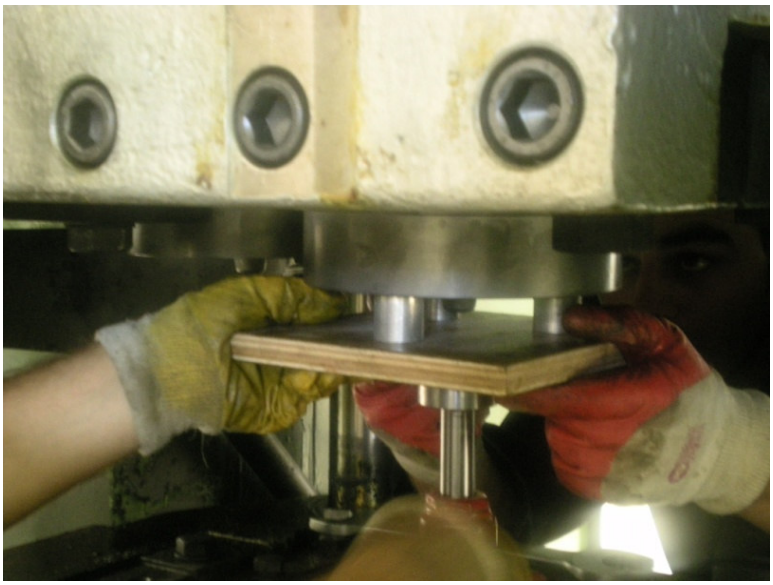

**Figure 5.6 View of Lifting of the Upper Finish Die by Hydraulic Jack**

Like the upper dies, the lower dies have been mounted to the die holder by using the clamping elements and the bolts as shown in Figure 5.7. Then the reliability of fastening has been checked by operating the press in unloaded position.

**Figure 5.7 View of Clamping of Lower Finish Die**

After mounting of the dies, the billets have started to be heated to the required temperature in PROTHERM standard chamber electric furnace available in the laboratory. The volume of the chamber is 25 liters, so few billets can be inserted into the furnace at once. Although the furnace has this disadvantage, it has been preferred instead of INDUCTOTERM 125 KVA induction heater available in the laboratory for heating the billets because temperature control of the billets at the induction heater is very difficult and since the temperatures which the aluminum alloy billets are heated to are very close to their solidus temperature, heating at induction heater can cause incipient melting of aluminum alloys. The temperature range of the experiments has been between 250 $^{o}$C and 438 $^{o}$C, so the temperature of the billets in the furnace has been kept within these limits. Photograph of PROTHERM standard chamber electric furnace is given in Figure 5.8. Photograph of the billets in the furnace is shown in Figure 5.9.


**Figure 5.8 View of PROTHERM Standard Chamber Electric Furnace in METU-BILTIR Center**


**Figure 5.9 View of Billets in Electric Furnace**

As the billets have been kept at the target temperature in the furnace, pre-heating of the dies has been started. The main reason for preheating is to decrease the temperature difference between the dies and the heated billets during forging and by this way to reduce thermal shocks on the dies and to prevent cooling of the workpiece. The dies have been preheated approximately to 200 $^{o}$C by two LPG heater flame gun which have been located at different positions for homogenous temperature distribution as much as possible. The temperature of the dies has been measured by the optical pyrometer at every ten minutes. The photograph of preheating of the dies is shown in Figure 5.10.

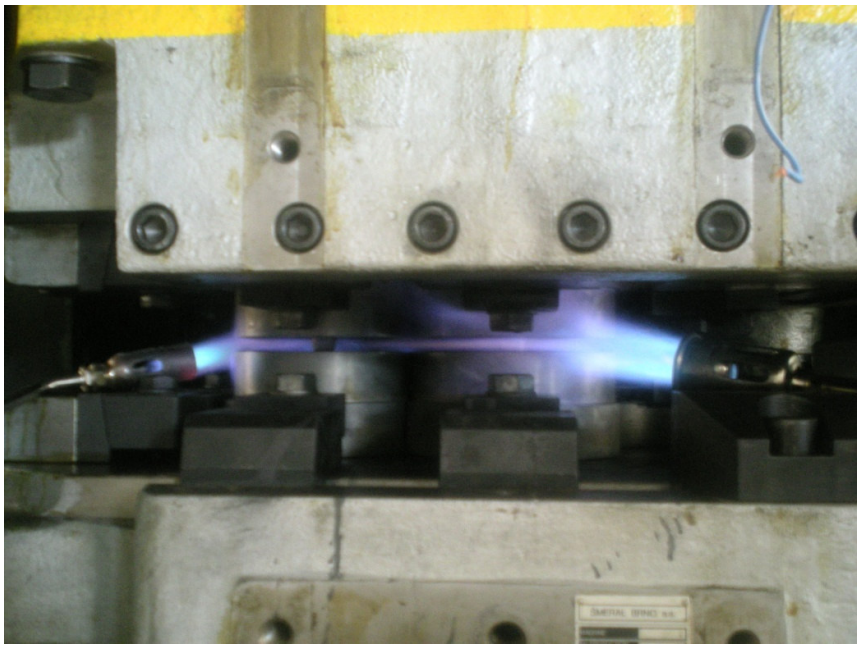

**Figure 5.10 View of Preheating of the Dies**

## 5.4 Experimentation

After pre-heating of the dies has been completed, lubricant has been applied on the die cavity surfaces. As soon as lubricant has been applied forging operation has been started. In Figure 5.11 to Figure 5.15, the photographs of the stages of the operation after the pre-heating of the dies can be seen.

During the experiments, the data related to the billet and considered to be important have been measured and recorded. These data are listed below and tabulated in Table 5.1.

- Billet temperature at the exit of the furnace
- Billet temperature before the preform forging
- Billet temperature after the preform forging
- Billet temperature after the finish forging

**Figure 5.11 View of Billet before the Preform Stage**

**Figure 5.12 View of the Preform**

**Figure 5.13 View of Preform before the Finish Stage**

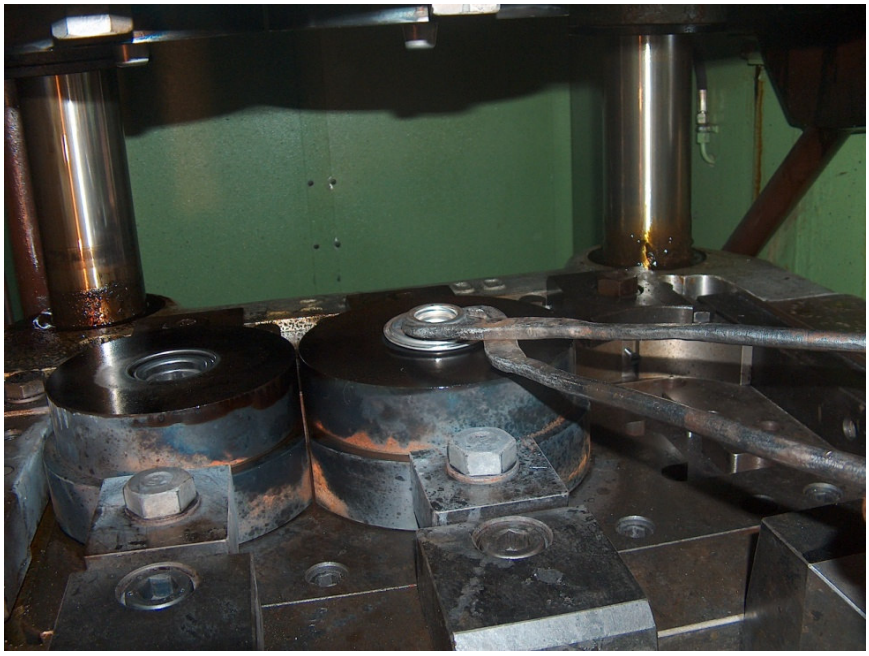

**Figure 5.14 View of Finish Part Taken by Tongs**

**Figure 5.15 View of Finish Parts after the Forging Process**

During the experiments, the data related to the dies and considered to be important have been measured and recorded. The data are listed below and tabulated in Table 5.2.

- Temperature of the lower preform die before forging
- Temperature of the upper preform die before forging
- Temperature of the lower preform die after forging
- Temperature of the upper preform die after forging
- Temperature of the lower finish die before forging
- Temperature of the upper finish die before forging
- Temperature of the lower finish die after forging
- Temperature of the upper finish die after forging

Forging of samples 5, 17 and 27 have been stopped after the preform stage in order to inspect the preform parts. So for these samples the data related to the finish stage are not available in Table 5.1, Table 5.2 and Table 5.3.

**Table 5.1 Experimental Data of the Billet**

| Sample No | Av. Billet Length (mm) | Billet Temp. at Furnace Exit (°C) | Billet Temp. Before Forging (°C) | Preform Temp. (°C) | Finish Part Temp. (°C) |
|---|---|---|---|---|---|
| **1** | 46.05 | 469 | 442 | 456 | 435 |
| **2** | 45.45 | 438 | 403 | 430 | 400 |
| **3** | 45.61 | 442 | 401 | 433 | 406 |
| **4** | 45.42 | 444 | 394 | 421 | 408 |
| **5** | 46.01 | 439 | 397 | 421 | – |
| **6** | 45.45 | 430 | 387 | 413 | 395 |
| **7** | 45.91 | 433 | 381 | 415 | 388 |
| **8** | 45.99 | 428 | 375 | 400 | 381 |
| **9** | 45.89 | 426 | 368 | 403 | 375 |
| **10** | 45.54 | 430 | 354 | 393 | 356 |
| **11** | 46.03 | 424 | 341 | 359 | 343 |
| **12** | 45.91 | 427 | 336 | 361 | 352 |
| **13** | 45.85 | 430 | 327 | 360 | 334 |
| **14** | 46.04 | 405 | 329 | 380 | 375 |
| **15** | 45.93 | 388 | 323 | 368 | 341 |
| **16** | 46.02 | 376 | 320 | 346 | 325 |
| **17** | 46.07 | 370 | 327 | 350 | – |
| **18** | 45.97 | 356 | 326 | 337 | 328 |
| **19** | 45.95 | 344 | 309 | 341 | 338 |
| **20** | 45.81 | 342 | 313 | 349 | 336 |
| **21** | 46.03 | 335 | 302 | 341 | 332 |
| **22** | 45.94 | 330 | 305 | 339 | 337 |
| **23** | 45.97 | 322 | 294 | 333 | 326 |
| **24** | 46.02 | 319 | 293 | 337 | 327 |
| **25** | 46.04 | 321 | 286 | 332 | 320 |
| **26** | 46.05 | 317 | 285 | 334 | – |
| **27** | 46.03 | 305 | 271 | 309 | 313 |
| **28** | 46.00 | 301 | 262 | 301 | 308 |
| **29** | 45.99 | 298 | 258 | 300 | 295 |
| **30** | 46.02 | 293 | 251 | 290 | 288 |

**Table 5.2 Experimental Data of the Dies**

| Sample No | Lower Preform Die Temp. Before Forging (°C) | Upper Preform Die Temp. Before Forging (°C) | Lower Finish Die Temp. Before Forging (°C) | Upper Finish Die Temp. Before Forging (°C) | Lower Preform Die Temp. After Forging (°C) | Upper Preform Die Temp. After Forging (°C) | Lower Finish Die Temp. After Forging (°C) | Upper Finish Die Temp. After Forging (°C) |
|---|---|---|---|---|---|---|---|---|
| **1** | 240 | 223 | 235 | 215 | 252 | 244 | 249 | 226 |
| **2** | 233 | 214 | 223 | 202 | 247 | 239 | 242 | 228 |
| **3** | 218 | 205 | 219 | 216 | 237 | 229 | 237 | 214 |
| **4** | 200 | 185 | 204 | 195 | 218 | 213 | 225 | 205 |
| **5** | 185 | 166 | – | – | 191 | 178 | – | – |
| **6** | 180 | 168 | 174 | 170 | 190 | 185 | 191 | 181 |
| **7** | 168 | 163 | 174 | 177 | 181 | 193 | 195 | 189 |
| **8** | 222 | 213 | 233 | 218 | 218 | 247 | 251 | 233 |
| **9** | 217 | 209 | 219 | 215 | 226 | 244 | 242 | 227 |
| **10** | 199 | 205 | 202 | 210 | 214 | 246 | 237 | 222 |
| **11** | 188 | 196 | 190 | 199 | 186 | 210 | 205 | 200 |
| **12** | 177 | 184 | 190 | 185 | 186 | 205 | 199 | 202 |
| **13** | 165 | 172 | 170 | 184 | 173 | 189 | 179 | 180 |
| **14** | 156 | 162 | 168 | 171 | 166 | 185 | 179 | 175 |
| **15** | 210 | 204 | 220 | 213 | 222 | 230 | 237 | 223 |
| **16** | 200 | 197 | 213 | 202 | 213 | 215 | 218 | 220 |
| **17** | 202 | 198 | – | – | 207 | 222 | – | – |
| **18** | 193 | 190 | 188 | 190 | 205 | 220 | 193 | 185 |
| **19** | 190 | 188 | 191 | 186 | 200 | 201 | 197 | 190 |
| **20** | 183 | 185 | 180 | 174 | 191 | 213 | 195 | 184 |
| **21** | 182 | 180 | 175 | 169 | 183 | 199 | 185 | 184 |
| **22** | 177 | 179 | 170 | 162 | 181 | 197 | 182 | 169 |
| **23** | 221 | 209 | 226 | 219 | 230 | 238 | 230 | 218 |
| **24** | 220 | 207 | 218 | 210 | 231 | 233 | 209 | 206 |
| **25** | 209 | 199 | 202 | 196 | 216 | 212 | 198 | 202 |
| **26** | 207 | 200 | – | – | 210 | 212 | – | – |
| **27** | 198 | 201 | 192 | 190 | 209 | 228 | 205 | 201 |
| **28** | 195 | 203 | 186 | 180 | 195 | 224 | 189 | 182 |
| **29** | 200 | 208 | 209 | 213 | 206 | 215 | 202 | 220 |
| **30** | 202 | 203 | 199 | 204 | 208 | 229 | 210 | 211 |

After the experiments, the dimensions of the finish part considered to be important have been measured and recorded. The dimensions which have been measured are listed below and the values are tabulated in Table 5.3.

- Height of the part (by digital compass)
- Flange diameter of the part (by digital compass)
- Flange height of the part (by digital compass)
- Plug thickness (by digital compass)
- Flash thickness (by digital compass)

**Table 5.3 Measured Dimensions of the Finish Part**

| Sample No | Height of the Part (mm) | Flange Diameter of the Part (mm) | Flange Height of the Part (mm) | Plug Thickness (mm) | Flash Thickness (mm) |
|---|---|---|---|---|---|
| **1** | 36.07 | 67.65 | 6.96 | 2.51 | 1.52 |
| **2** | 36.09 | 67.75 | 7.05 | 2.53 | 1.55 |
| **3** | 36.12 | 67.76 | 7.04 | 2.54 | 1.57 |
| **4** | 36.14 | 67.74 | 7.01 | 2.53 | 1.57 |
| **5** | 39.83 | 56.90 | 10.05 | 8.35 | – |
| **6** | 36.12 | 67.75 | 7.04 | 2.56 | 1.53 |
| **7** | 36.09 | 67.73 | 7.01 | 2.52 | 1.54 |
| **8** | 36.11 | 67.73 | 7.01 | 2.54 | 1.53 |
| **9** | 36.13 | 67.74 | 7.02 | 2.56 | 1.56 |
| **10** | 36.12 | 67.72 | 7.04 | 2.55 | 1.52 |
| **11** | 36.16 | 67.75 | 7.06 | 2.58 | 1.55 |
| **12** | 36.14 | 67.74 | 7.05 | 2.56 | 1.54 |
| **13** | 36.16 | 67.76 | 7.06 | 2.56 | 1.56 |
| **14** | 36.14 | 67.74 | 7.04 | 2.55 | 1.57 |
| **15** | 36.17 | 67.77 | 7.08 | 2.58 | 1.55 |
| **16** | 36.16 | 67.76 | 7.08 | 2.56 | 1.57 |
| **17** | 39.00 | 57.20 | 9.90 | 8.50 | – |
| **18** | 36.15 | 67.76 | 7.05 | 2.57 | 1.55 |
| **19** | 36.17 | 67.78 | 7.09 | 2.57 | 1.58 |
| **20** | 36.16 | 67.76 | 7.09 | 2.58 | 1.57 |
| **21** | 36.17 | 67.78 | 7.08 | 2.59 | 1.55 |
| **22** | 36.17 | 67.79 | 7.10 | 2.61 | 1.56 |
| **23** | 36.18 | 67.81 | 7.10 | 2.60 | 1.57 |
| **24** | 36.20 | 67.80 | 7.11 | 2.59 | 1.59 |
| **25** | 36.20 | 67.81 | 7.13 | 2.60 | 1.59 |
| **26** | 39.01 | 57.00 | 9.20 | 8.02 | – |
| **27** | 36.22 | 67.82 | 7.13 | 2.59 | 1.59 |
| **28** | 36.20 | 67.81 | 7.12 | 2.60 | 1.60 |
| **29** | 36.21 | 67.80 | 7.12 | 2.61 | 1.63 |
| **30** | 36.23 | 67.82 | 7.14 | 2.64 | 1.62 |

## 5.5 Discussion of the Results of the Experiments

After the forging operation, the parts have been inspected by eyes carefully and it has been seen that there are no forging defects like folds, laps, etc. except sample 1 which is shown in Figure 5.15 from different views. In Chapter 4, it has been observed that the material temperature plus the temperature rise during forging has exceeded the solidus temperature in the finite element simulation which has been done at the initial billet temperature of 438 $^{o}$C and it has been said that this would lead incipient melting of the part that would be resulted in severe cracks on the part. In the experiments, when the billet has been forged at the initial billet temperature of 442 $^{o}$C, wide cracks as shown in Figure 5.15 have been occurred that means workpiece temperature has exceeded its solidus temperature during forging process which is a consistent result with the result of finite element simulation. At the end of the analyses, it has been stated that forging the billet at the initial billet temperature of 400 $^{o}$C could be risky because during the analyses the part's temperature has reached very close to the its solidus temperature, but in the experiments it has been seen that the billet forged at the initial billet temperature of 403 $^{o}$C, has been obtained without any cracks and distortions, so it can be concluded that part can be forged at 400 $^{o}$C without any failure.

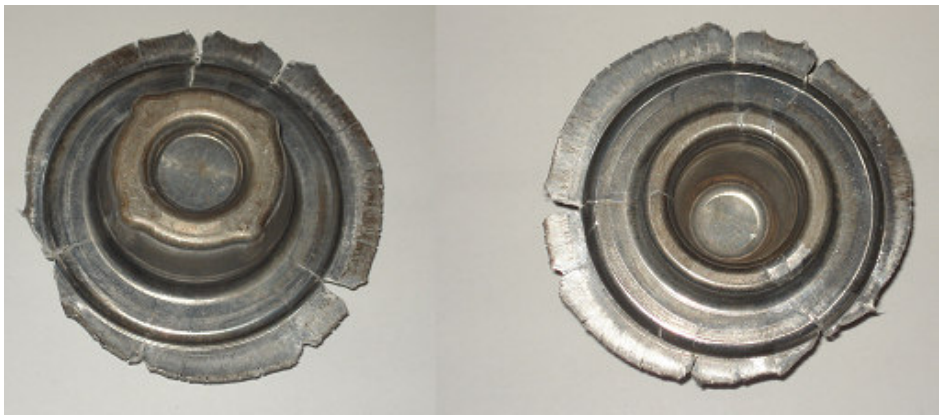

**Figure 5.16 View of Sample 1**

From samples 2 to 30, the dimensions that have been measured after forging process are within the tolerances of the dimensions of the part whose engineering drawing is given in Appendix C. The dimensions of the height of the parts are within the range of 36.07–36.23 mm which satisfy the tolerance 36.1±0.3 mm. The dimensions of the flange diameter of the parts are within the range of 67.65–67.82 mm which satisfy the tolerance 67.7±0.3 mm. The dimensions of the flange height of the parts are within the range of 6.96-7.14 mm which satisfy the tolerance 7.0±0.3 mm. So according to these results it can be concluded that required accuracy and tolerances are obtained.

The flash formation during the experiments is similar to the simulations which have been done in previous chapters. The flash diameter on the finish part has been measured in the range of 75.55–77.5 mm, which has been designed to be 76.7 mm. This difference has resulted from using smaller and greater billets then the desired one. Also it has been seen that flash has been distributed nonuniformly in some samples. The reason is that, in those samples the billets have not been located into the lower dies properly. The flash thicknesses on the finish parts have been measured in the range of 1.52–1.63 mm, which has been designed to be 1.5 mm. The reason of the difference in some samples may be the change of the facial clearance between the dies after certain strokes. In preform stage, no flash has formed which is a consistent result with the simulation result.

The temperature measurements that have been taken on the billets at different stages of the process show that, the temperature of the workpieces has decreased considerably between the electric furnace and the press. This cooling has been due to the convection and radiation between the workpiece and the ambient air. Besides, the temperature of the some workpieces has decreased during forging operation, again due to convection and conduction.

In the analyses, the initial die temperatures have been taken as 200 $^{o}$C, however, in the experiments, the temperatures of the dies just before forging have been between 175 $^{o}$C and 246 $^{o}$C. The first reason for this difference is that it is very

difficult to heat the dies to desired temperature by LPG heater flame. The second reason is that during the experiments lots of data have been recorded and photos have been taken and during this period the temperature of the dies has reduced by convection. Intermediate heating may be applied to the dies to prevent the cooling of the dies.

In the experiments, it has been observed that in some samples, the temperature of the dies after forging have been lower than the temperatures before forging. In reality, it has been expected that there would be heat transfer from the billet to the dies and there would be heat generation because of deformation that would result in an increase in the die temperatures after forging. The reason is that it has not been possible to measure the die temperatures just after forging, and the dies have cooled down by convection during that period, therefore, some lower temperature measurements have been taken on the dies after forging.

Moreover, during the finite element simulations it has been observed that the temperatures of the dies have reached up to 381 $^{o}$C locally. However, as mentioned, the temperatures of the preform and finish dies are in the range of 163 $^{o}$C to 243 $^{o}$C during the experiments. There are some reasons for that difference. First of all, the software used in the analyses can calculate the peak temperatures during forging, but in the experiments the measurements have been taken just after the part has been forged and taken away from the dies. During this time period, the dies have cooled down considerably by convection. The other reason is that, the temperature measurements on the dies have been made by optical pyrometer at different points and it has not been always possible to focus on the actual local point where the temperature has been at its peak value.

Consistent with the literature, in the experiments it has been seen that the lubrication is very critical element for aluminum alloy forging. While forging some samples, dies have not been lubricated or poorly lubricated. As a result, some samples have adhered to the lower or upper preform dies. Although the samples have been separated from the dies by the help of tongs, some of them

have distorted. In Figure 5.17 a view of the preform which is adhered to the upper preform die can be seen.

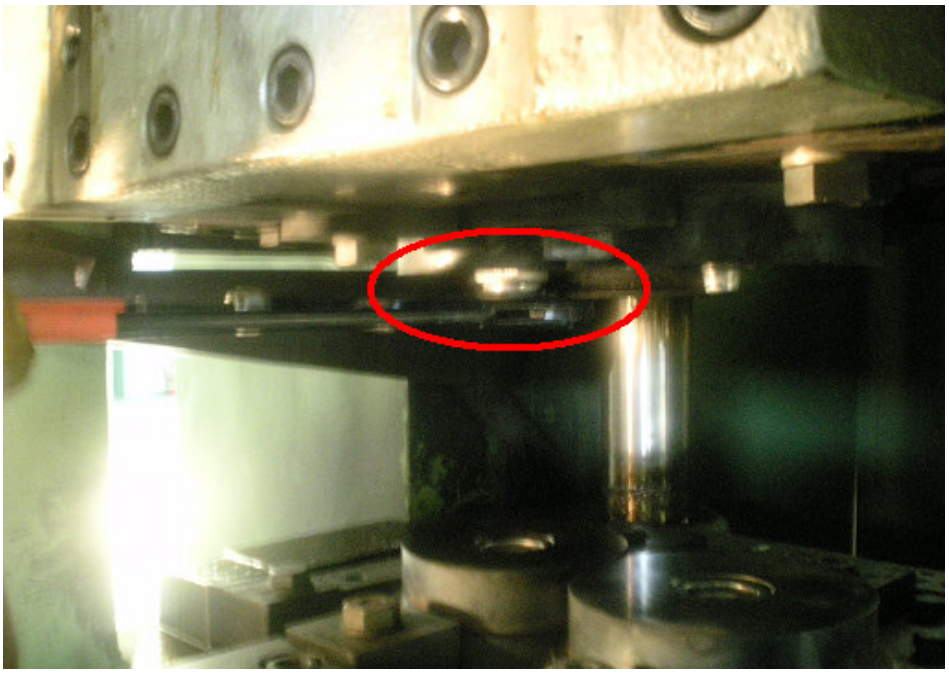

**Figure 5.17 View of Preform Adhered to the Upper Preform Die**

# CHAPTER 6

# CONCLUSION AND FUTURE WORK

## 6.1 Conclusions

In this study, a particular part which is made of 7075 aluminum alloy and which is currently produced by machining operation in industry has been produced by forging operation. First, the forging process sequence has been designed by using a commercially available finite volume program as described in Chapter 3. Then designed process has been simulated by using FEM in order to analyze the workpiece and the stresses and strains and temperature distributions on the dies, as explained in detail in Chapter 4. Finally, the experimental study has been carried out in METU-BILTIR Center Forging Research and Application Laboratory out as explained in detail in Chapter 5. At the end of this study following general results have been obtained:

In the finite element analyses, it has been observed that the maximum equivalent stress values on the dies have increased and the maximum temperature values on the dies have decreased as the initial billet temperature has been reduced. Also it has been observed that the locations where the temperature has reached its maximum values have been the ones which have been in contact with the workpiece longest time. However, the locations on the upper and lower dies where the maximum equivalent stress and maximum temperature values occur have not changed for all the simulations.

In the finite element analyses, for the initial billet temperatures of 300 $^{o}$C and 250 $^{o}$C, plastic deformation have occurred on the lower preform and finish dies. At the initial billet temperature of 300 $^{o}$C, the maximum equivalent plastic strains are about $1.53 \times 10^{-3}$ and about $2.01 \times 10^{-3}$ for the lower preform die and the

lower finish die, respectively and the average plastic strains are about $9x10^{-4}$ for the lower preform die and about $1.2x10^{-3}$ for the lower finish die. At the initial billet temperature of 250 $^{o}$C, the maximum equivalent plastic strains are about $2.11x10^{-3}$ and about $2.63x10^{-3}$ for the lower preform die and the lower finish die, respectively and the average plastic strains are about $1.2x10^{-3}$ for the lower preform die and about $1.5x10^{-3}$ for the lower finish die. Although in literature [1] the recommended temperature range for forging aluminum alloy 7075 is 382–438 $^{o}$C, it is observed that the particular part can also be forged at the initial billet temperature of 350 $^{o}$C because no plastic deformation occurs on the dies during the finite element simulations at this temperature. It should be also noted that no failure has been observed about this temperature during the experiments.

In the simulations, at the forging temperature of 438 $^{o}$C, it has been observed that temperature of the part during forging has exceeded its solidus temperature that would result in incipient melting of the part. Incipient melting can cause wide and serious cracks on the part and can make the forging useless. In the experiments, wide cracks and distortions have been observed on the sample which has been forged at the forging temperature of 442 $^{o}$C that means workpiece temperature has exceeded its solidus temperature during forging process which is a consistent result with the simulation result.

In the experiments, after measuring and inspecting the parts, it has been seen that, there have been no forging defects like unfilled regions, folds, laps, surface cracks, except sample 1, which is a consistent result with the analyses results.

From samples 2 to 30, the dimensions that have been measured after forging process are within the tolerances of the dimensions of the part whose engineering drawing is given in Appendix C. The dimensions of the height of the parts are within the range of 36.07–36.23 mm which satisfy the tolerance 36.1±0.3 mm. The dimensions of the flange diameter of the parts are within the range of 67.65–67.82 mm which satisfy the tolerance 67.7±0.3 mm. The

dimensions of the flange height of the parts are within the range of 6.96–7.14 mm which satisfy the tolerance 7.0±0.3 mm. So according to these results it can be concluded that required accuracy and tolerances are obtained and a successful forging process design has been achieved.

The flash formation during the experiments is similar to the simulations which have been done in previous chapters. The flash diameter on the finish part has been measured in the range of 75.55–77.5 mm, which has been designed to be 76.7 mm. This difference has resulted from using smaller and greater billets then the desired one. Also it has been seen that flash has been distributed nonuniformly in some samples. The reason is that, in those samples the billets have not been located into the lower dies properly. The flash thicknesses on the finish parts have been measured in the range of 1.52–1.63 mm, which has been designed to be 1.5 mm. The reason of the difference in some samples may be the change of the facial clearance between the dies after certain strokes. In preform stage, no flash has formed which is a consistent result with the simulation result.

In the experiments, it has been decided that die lubrication is very critical element for aluminum forging. When the dies have not been lubricated or poorly lubricated, the billet has generally adhered to the dies.

## 6.2 Future Works

The followings may be suggested as future works of this particular study;

- Different parts which are made of aluminum alloy 7075 and which have different geometries can be analyzed.
- This study can be extended by using aluminum alloys from different series, for instance 2000 or 6000 series, instead of 7075.
- Precision forging of an aluminium alloy part can be studied.

- Cold forging of an aluminium alloy part can be studied.
- Die life and wear analyses can be made for the dies.
- Heating of aluminium alloys by induction heater can be studied.
- Microstructure of aluminum alloy 7075 forgings can be analyzed.

## REFERENCES

[1] T. Altan, F. W. Boulger, J. R. Becker, N. Akgerman, H. J. Henning, "Forging Equipment, Materials and Practices", Air Force Materials Laboratory, October 1973.

[2] George E. Totten, D. Scott Mackenzie., "Handbook of Aluminum", Volume 1, USA, 2003.

[3] Wikipedia
http://www.en.wikipedia.org/wiki/Aluminium_alloy
Last access: 10.07.2008

[4] U. Gallade, "Forging Trends in Europe", Proc. of IFC 2005 Japan 18th International Forging Congress, Nagoya, Japan, April 2005, p.9-17.

[5] S. Asahi, " Outlined Situations of Forging Industries in Asia and Oceania", Proc. of IFC 2005 Japan 18th International Forging Congress, Nagoya, Japan, April 2005, p.24-29.

[6] İsbir, S. Ş., "Finite Element Analysis of Trimming", M.S. Thesis, 2002, p.24, Middle East Technical University, Ankara, Turkey, 2002.

[7] Saraç, S., "Design and Thermo-Mechanical Analysis of Warm Forging Process and Dies", M. Sc. Thesis, Middle East Technical University, Ankara, Turkey, 2007.

[8] Vries, E. Ding P., "Simulation of 3D Forging and Extrusion Problems using a Finite Volume Method", MSC Taiwan User Conference, Taipai, 2000.

[9] Gökler, M.İ., "Computer Aided Sequence and Die Design for Hot Upset Forgings", Ph. D. Thesis, University of Birmingham, England, 1983.

[10] Alper, E., “Computer Aided Design of Axi-Symmetric Press Forgings”, M. Sc. Thesis, Middle East Technical University, Ankara, Turkey, 1989.

[11] Elmaskaya, D., “Finite Element Analysis of Effects of Tapered Preforms in Cold Upsetting”, Middle East Technical University, Ankara, Turkey, 1997.

[12] Kutlu, A, E., “Analysis and Design of Preforms for Non-Axisymmetric Press”, M. Sc. Thesis, Middle East Technical University, Ankara, Turkey, 2001.

[13] Karagözler, A, B., “Analysis and Preform Design for Long Press Forgings with Non-Planar Parting Surfaces”, M. Sc. Thesis, Middle East Technical University, Ankara, Turkey, 2003.

[14] Civelekoğlu, B., “Analysis of Forging For Three Different Alloy Steels”, Middle East Technical University, Ankara, Turkey, 2003.

[15] Gülbahar, S. “Preform Design for Forging of Heavy Vehicle Steering Joint”, M. Sc. Thesis, Middle East Technical University, Ankara, Turkey, 2004.

[16] Abachi, S., “Wear Analysis of Hot Forging Dies”, M. Sc. Thesis, Middle East Technical University, Ankara, Turkey, 2004.

[17] Aktakka, G., “Analysis of Warm Forging Process”, Middle East Technical University, Ankara, Turkey, 2006.

[18] Maşat, M. “ Design and Implementation of Hot Precision Forging Die for a Spur Gear”, M. Sc. Thesis, Middle East Technical University, Ankara, Turkey, 2007.

[19] “Metals Handbook-Forging and Casting”, Vol. 5, 8th Edition, ASM Handbook Commitee, USA, 1971.

[20] Jensrud, O., Pedersen, K., “Cold Forging of High Strength Aluminum Alloys and the Development of New Thermomechanical Processing”, J. Mater. Process. Technol. 1998, p.156–160.

[21] Tanner, D., A., Robinson, J., S., “Reducing Residual Stress in 2014 Aluminum Alloy Die Forgings”, 2007.

[22] Yoshimura, H., Tanaka, K., “Precision Forging of Aluminum and Steel”, J. Mater. Process. Technol. 2000, p.196-204.

[23] “Metals Handbook-Forming and Forging”, Vol. 14, 9th Edition, ASM Handbook Committee, USA, 1988.

[24] Thomas A. “Forging Handbook”, Drop Forging Res. Assoc. UK, 1980.

[25] FNSS Defense Systems Inc.

[26] J.R. Davis. “Aluminum and Aluminum Alloys”, ASM Specialty Handbook. USA, 1993.

[27] John E. Hatch. “Aluminum Properties and Physical Metallurgy”, American Society for Metals, Ohio, 1984.

[28] Pro/Engineer Wildfire 3.0

[29] Efunda

http://www. efunda.com/processes/metal_processing/forging

Last access: 20.08.2008

[30] MSC SuperForge 2005

[31] MSC SuperForge User Manual

[32] MSC. SuperForm 2005

[33] MSC SuperForm Userguide Manual

[34] MSC. MARC User Manual

[35] MSC PATRAN 2005

[36] MSC PATRAN User Manual

[37] Assab Korkmaz Company
http://www.assabkorkmaz.com
Last Access: 29.06.2008

[38] Personal communication with MSC SuperForm developing authorities from Femutec Company, Germany.

[39] Farmingdale State College
http://www.info.lu.farmingdale.edu/depts/met/met205/annealingstages.html
Last access: 02.09.2008

[40] Smeral QLZK UC Die Holder Manual

[41] "Aluminum Forging Design Manual", 2nd Edition The Aluminum Association, 2004.

[42] A. M. Sabroff, F. W. Boulger, H.J. Henning "Forging Materials and Practices" 1968, New York, Reinhold Book Corp.

[43] Alcoa
http://www.alcoa.com/gcfp/catalog/pdf/alcoa_alloy_7075.pdf
Last Access: 29.06.2008

# APPENDIX A

## ALUMINUM AND ALUMINUM ALLOYS

Aluminum has many advantages some of which are tabulated in Table A.1.

**Table A.1 Advantages of Aluminum**

| | Properties | Details |
|---|---|---|
| **1** | Very Light | The specific gravity of aluminum is about 2.7 ~ 2.8, which is about 36% of iron or stainless steel. Therefore it is a particularly suitable metal for making light weight vehicles, vessels and other structures. |
| **2** | Good Corrosion Resistance | Aluminum naturally produces a fine oxidized surface film which protects it from corrosion and by artificially thickening the oxidized film (anodized aluminum) it is possible to make aluminum perfectly corrosion prove. |
| **3** | Suitable for Further Processing | Because of its property of easy thinning and lengthening, aluminum is a suitable material for molding, machining and welding. By pushing it out of a cast it is possible to make aluminum pieces with any cross section shape. |
| **4** | Strong Under Various Conditions | The strength-weight ratio is good. According to the requirements, desired strength and properties can be obtained by alloying and heat-treatment. Further, different from steel, aluminum is not fragile in low temperature, thus possible to be used in cold districts. |

**Table A.1 Advantages of Aluminum (Continued)**

| | Properties | Details |
|---|---|---|
| **5** | Suitable for Various Surface Treatment | In harsh environment when the natural surface protection film of aluminum is not enough, thickening the oxidized film (anodized aluminum) by the anode oxidization treatment gives abrasion resistance. Various surface treatments are used and the technologies of plating have been recently developed. |
| **6** | Not Fragile at Low Temperature | The properties of aluminum, makes it resistant to ultra low temperatures. Therefore it is suitable for LNG transportations, making storage tanks and other structures or equipments for low temperature plants. |
| **7** | High Electric and Heat Conductivity | Second to copper, aluminum has a high electric conductivity. Since the electric conductivity of pure aluminum exceeds 60% of that of copper's, to be used as leads it has to be slightly thicker than copper leads. However, it is advantageous when weight reduction is required. Further, second to copper, aluminum also has excellent heat conductivity, thus together with its suitability for reprocessing and joining quality, it is often used for making heat exchangers. |
| **8** | High Recycling Value | Aluminum is seemingly rather expensive; however, its scrap price is high and has a high recycling value. |
| **9** | Beautiful Appearance | It has a beautiful silver color and unlike iron, red rust would not appear damaging its clean appearance. |
| **10** | Good Shock-Absorption Nature | Small elastic coefficient of aluminum brings about good shock absorption effects. It also has the advantage of reducing the stress caused by heat. |

**Aluminum Alloys**

It is convenient to divide aluminum alloys into two major categories which are wrought compositions and casting compositions. A further differentiation for each category is based on the primary mechanism of property development.

International Alloy Designation System is the most widely accepted naming schema for wrought alloys. Each alloy is given a four digit number and the first digit indicates the alloy group as follows [26]:

- 1000 series are essentially pure aluminum with a minimum 99% aluminum content by weight and can be work hardened. They are primarily used in electrical and chemical industries.
- 2000 series are alloyed with copper can be precipitation hardened to strengths comparable to steel. They were once the most common aerospace alloys, but were susceptible to stress corrosion and are increasingly replaced by 7000 series in new designs.
- 3000 series are alloyed with manganese, and can be work hardened. They are used in architectural applications and various products.
- 4000 series are alloyed with silicon. They are used in welding rods and brazing sheet.
- 5000 series are alloyed with magnesium, derive most of their strength from solution hardening, and can also be work hardened to strengths comparable to steel.
- 6000 series are alloyed with magnesium and silicon, are easy to machine, and can be precipitation hardened, but not to the high strengths that 2000, 5000 and 7000 can reach. They are used for architectural extrusions.

- 7000 series are alloyed with zinc, and can be precipitation hardened to the highest strengths of any aluminum alloy. They are used in aircraft structural components and other high-strength applications.

- 8000 series are a miscellaneous category.

Wrought aluminum alloys' % weight compositions is tabulated in Table A.2. [3]

**Table A.2 Some Wrought Aluminum Alloys' % Weight Compositions [3]**

| Alloy | Si | Fe | Cu | Mn | Mg | Cr | Zn | V | Ti | Ga |
|---|---|---|---|---|---|---|---|---|---|---|
| **1100** | 0.95 Si+Fe | | 0.050-0.200 | 0.05 | | | 0.10 | | | |
| **2014** | 0.50-1.20 | 0.70 | 3.90-5.00 | 0.40-1.20 | 0.20-0.80 | 0.10 | 0.25 | | 0.15 | |
| **2024** | 0.50 | 0.50 | 3.80-4.90 | 0.30-0.90 | 1.20-1.80 | 0.10 | 0.25 | | 0.15 | |
| **3003** | 0.60 | 0.70 | 0.05-0.20 | 1.00-1.50 | | | 0.10 | | | |
| **3004** | 0.30 | 0.70 | 0.25 | 1.00-1.50 | 0.80-1.30 | | 0.25 | | | |
| **3102** | 0.40 | 0.70 | 0.10 | 0.05-0.40 | | | 0.30 | | 0.10 | |
| **4043** | 4.50-6.00 | 0.80 | 0.30 | 0.05 | 0.05 | | 0.10 | | 0.20 | |
| **5052** | 0.25 | 0.40 | 0.10 | 0.10 | 2.20-2.80 | 0.15-0.35 | 0.10 | | | |
| **5083** | 0.40 | 0.40 | 0.10 | 0.40-1.00 | 4.00-4.90 | 0.05-0.25 | 0.25 | | 0.15 | |
| **5086** | 0.40 | 0.50 | 0.10 | 0.20-0.70 | 3.50-4.50 | 0.05-0.25 | 0.25 | | 0.15 | |
| **5154** | 0.25 | 0.40 | 0.10 | 0.10 | 3.10-3.90 | 0.15-0.35 | 0.20 | | 0.20 | |
| **5356** | 0.25 | 0.40 | 0.10 | 0.10 | 4.50-5.50 | 0.05-0.20 | 0.10 | | 0.06-0.20 | |
| **6060** | 0.30-0.60 | 0.10-0.30 | 0.10 | 0.10 | 0.35-0.60 | 0.50 | 0.15 | | 0.10 | |
| **6061** | 0.40-0.80 | 0.70 | 0.15-0.40 | 0.15 | 0.80-1.20 | 0.04-0.35 | 0.25 | | 0.15 | |
| **6063** | 0.20-0.60 | 0.35 | 0.10 | 0.10 | 0.45-0.90 | 0.10 | 0.10 | | 0.10 | |
| **6070** | 1.00-1.70 | 0.50 | 0.15-0.40 | 0.40-1.00 | 0.50-1.20 | 0.10 | 0.25 | | 0.15 | |
| **6082** | 0.70-1.30 | 0.50 | 0.10 | 0.40-1.00 | 0.60-1.20 | 0.25 | 0.20 | | 0.10 | |

**Table A.2 Some Wrought Aluminum Alloys' % Weight Compositions [3] (Continued)**

| Alloy | Si | Fe | Cu | Mn | Mg | Cr | Zn | V | Ti | Ga |
|---|---|---|---|---|---|---|---|---|---|---|
| **6162** | 0.40-0.80 | | 0.50 | 0.20 | 0.10 | 0.70-1.10 | 0.10 | 0.25 | | 0.10 |
| **7072** | 0.70 Si+Fe | 0.10 | 0.10 | 0.10 | | 0.80-1.30 | | | | |
| **7075** | 0.40 | 0.50 | 1.20-2.00 | 0.30 | 2.10-2.90 | 0.18-0.28 | 5.10-6.10 | | 0.20 | |
| **7116** | 0.15 | 0.30 | 0.50-1.10 | 0.05 | 0.80-1.40 | | 4.20-5.20 | 0.05 | 0.05 | 0.03 |

Aluminum alloys are also classified as heat treatable and non-heat treatable alloys. Heat treatable aluminum alloys are those that can be strengthened by a controlled cycle of heating and cooling. Some alloys, usually in the 2000, 6000 and 7000 series can be strengthened by heating and then quenching [26]. Non-heat treatable aluminum alloys are hardenable by cold working, but not by heat treatment. Some alloys in 1000, 3000, and 4000 and 5000 series gain their strengths only by cold working which is denoted by H tempers.

# APPENDIX B

## COMPARISON OF RESULTS OF MSC. SUPERFORGE AND MSC. SUPERFORM AT THE INITIAL BILLET TEMPERATURE OF 400 $^{o}$C

MSC. SuperForge and MSC. SuperForm are based on two different methods; MSC. SuperForge is based on FVM where MSC. SuperForm is based on FEM. These softwares are two of the most preferred programs in forging simulations. In Figures B1–B6, the results of the forging simulation of the case part for the initial billet temperature of 400 $^{o}$C are given in MSC. SuperForge and MSC. SuperForm to compare the results of these two softwares. Temperature distribution of preform, temperature distribution of finish part, effective stress distribution of preform, effective stress distribution of finish part, effective plastic strain distribution of preform and effective plastic strain distribution of finish part for the initial billet temperature of 400 $^{o}$C in MSC. SuperForge and MSC. SuperForm are given in Figure B.1, Figure B2, Figure B3, Figure B4, Figure B5 and Figure B6, respectively. The maximum values in MSC. SuperForge and MSC. SuperForm are tabulated in Table B.1.

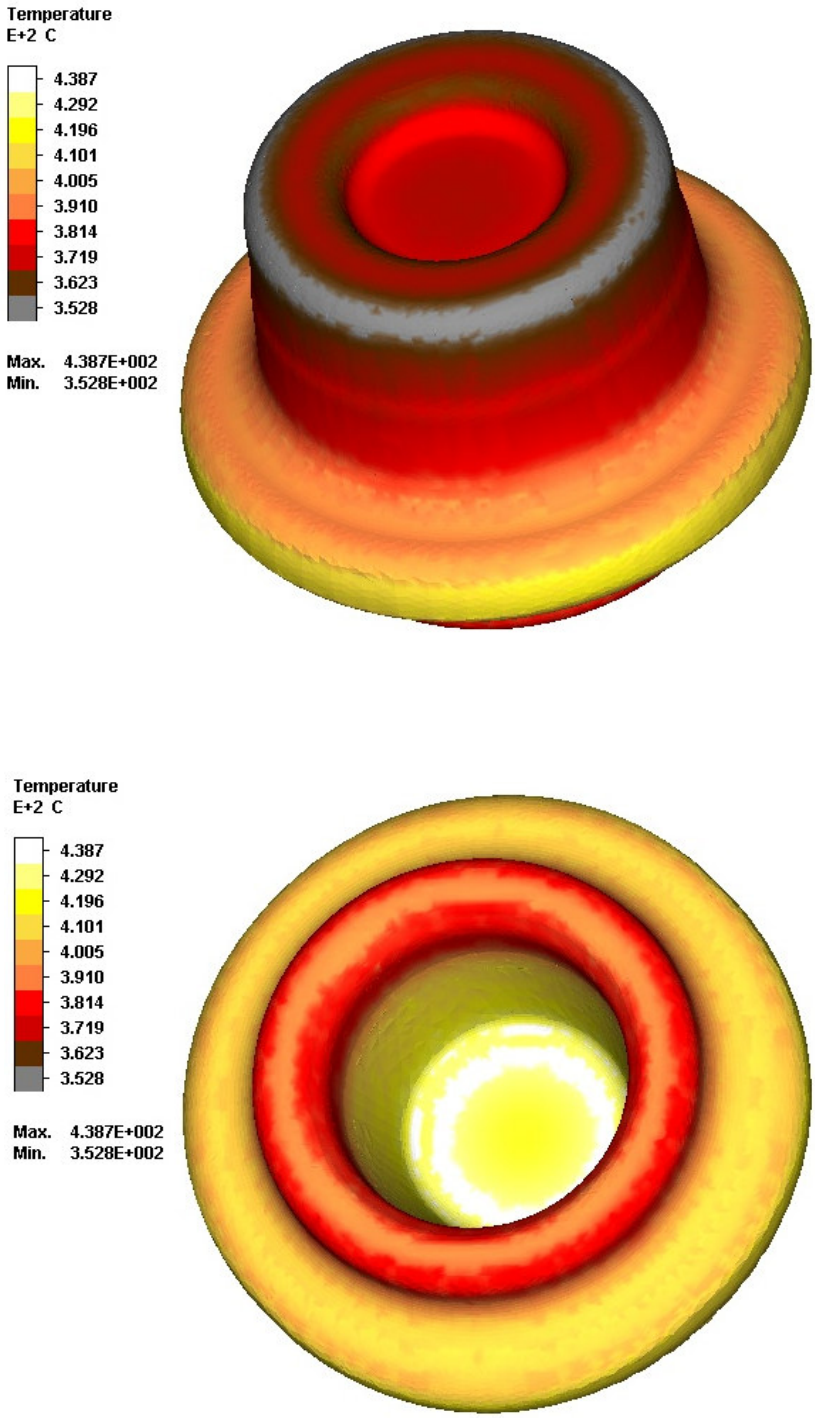
Temperature
E+2 C
4.387
4.292
4.196
4.101
4.005
3.910
3.814
3.719
3.623
3.528
Max. 4.387E+002
Min. 3.528E+002
Temperature
E+2 C
4.387
4.292
4.196
4.101
4.005
3.910
3.814
3.719
3.623
3.528
Max. 4.387E+002
Min. 3.528E+002

**(a)**

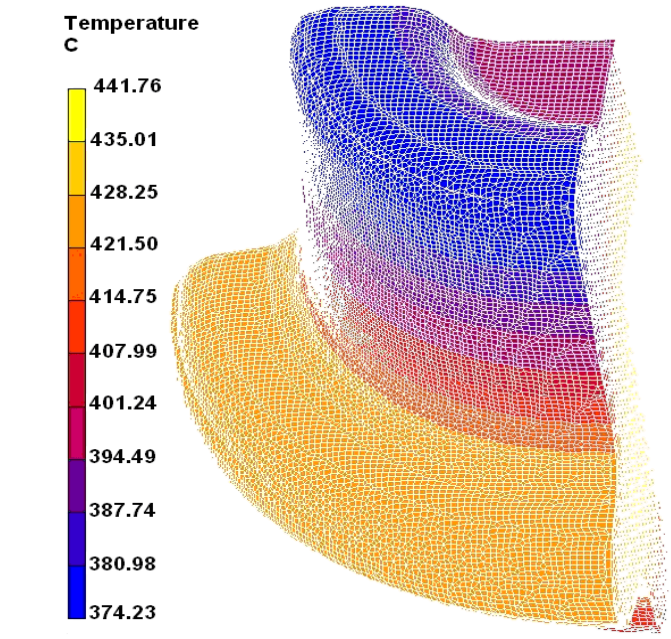


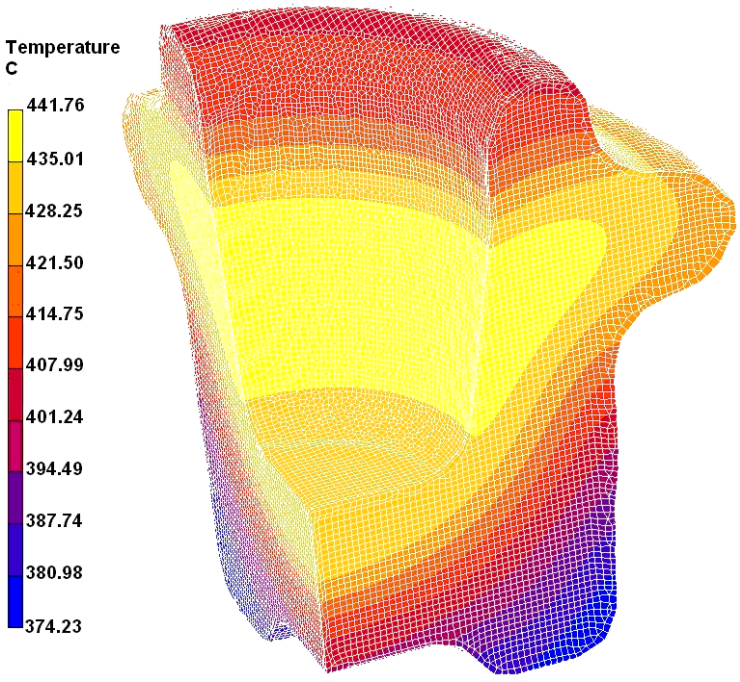


**(b)**

**Figure B.1 Temperature Distribution of Preform in (a) MSC. SuperForge (b) MSC. SuperForm for Initial Billet Temperature of 400 $^{o}$C**

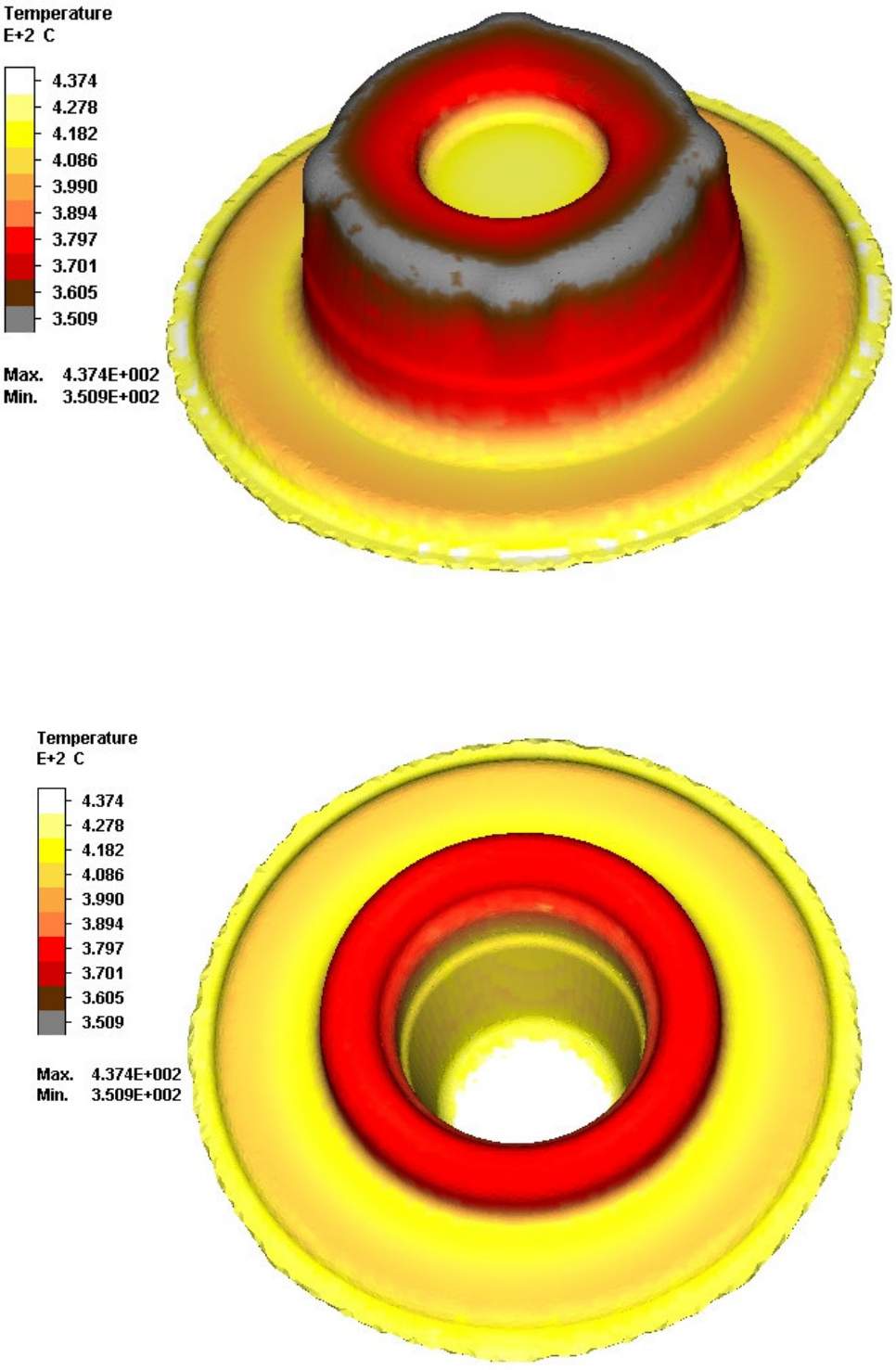
Temperature
E+2 C
4.374
4.278
4.182
4.086
3.990
3.894
3.797
3.701
3.605
3.509
Max. 4.374E+002
Min. 3.509E+002
Temperature
E+2 C
4.374
4.278
4.182
4.086
3.990
3.894
3.797
3.701
3.605
3.509
Max. 4.374E+002
Min. 3.509E+002

**(a)**

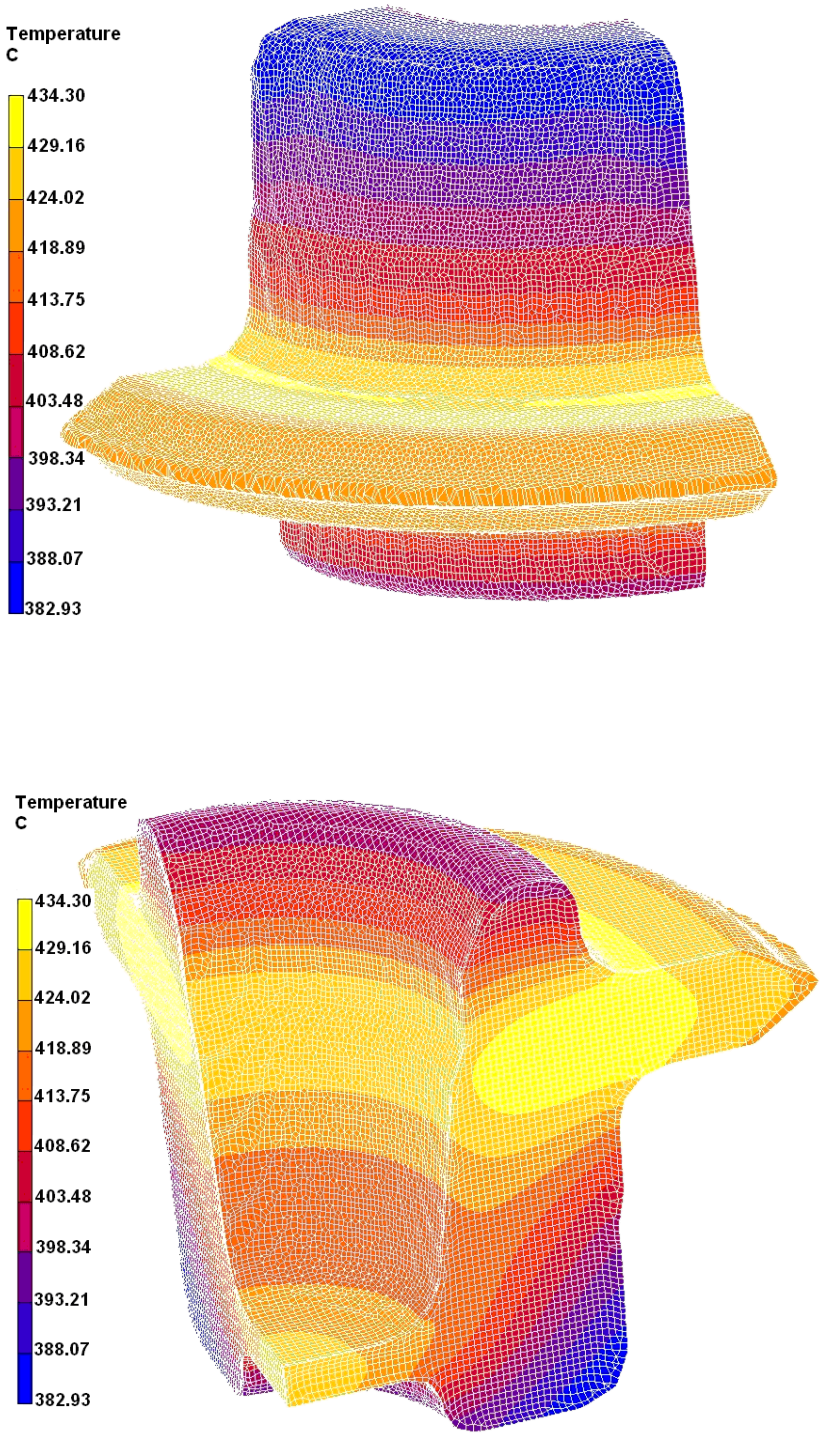


**(b)**

**Figure B.2 Temperature Distribution of Finish Part in (a) MSC. SuperForge (b) MSC. SuperForm for Initial Billet Temperature of 400 $^{o}$C**

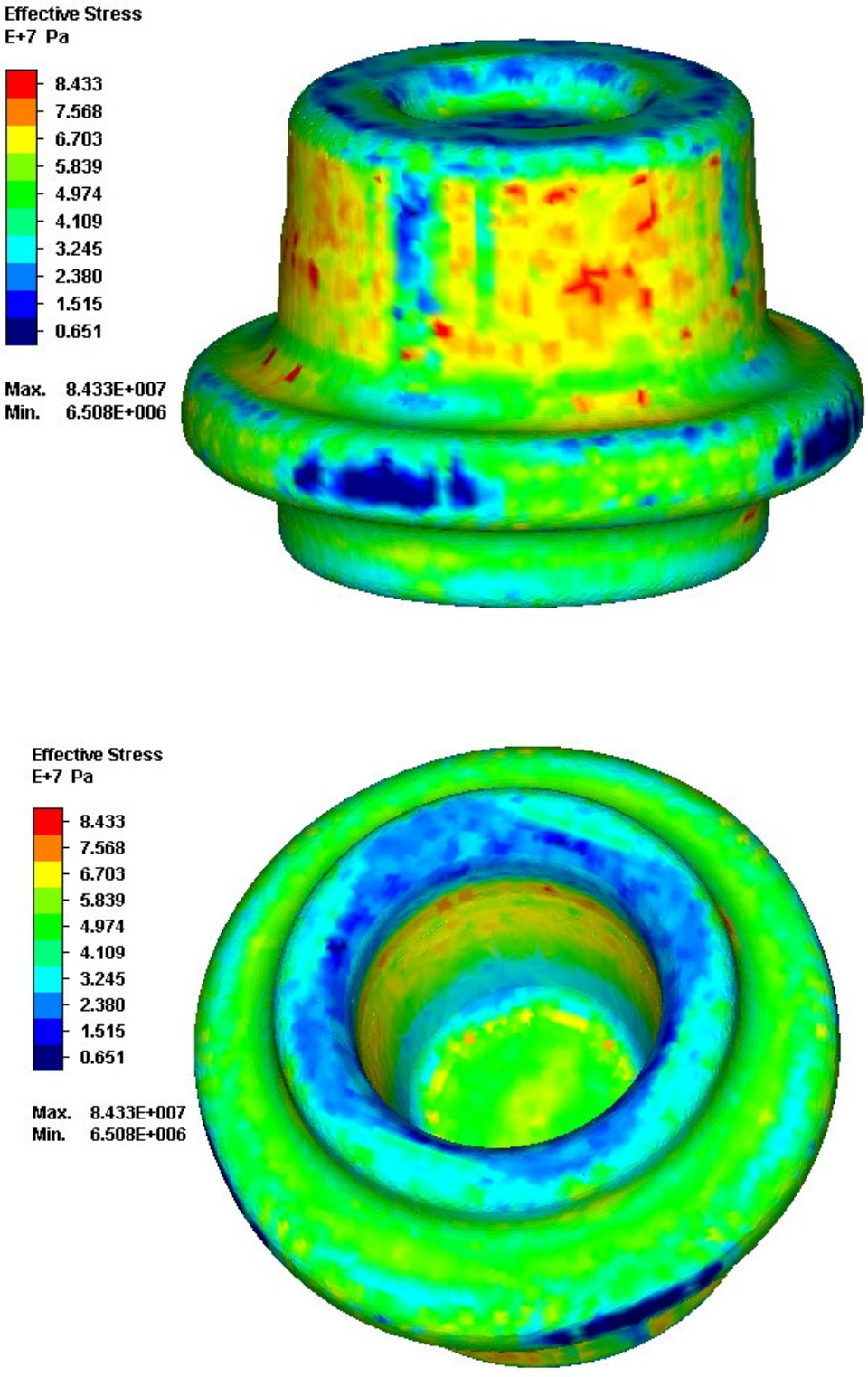
Effective Stress
E+7 Pa
8.433
7.568
6.703
5.839
4.974
4.109
3.245
2.380
1.515
0.651
Max. 8.433E+007
Min. 6.508E+006
Effective Stress
E+7 Pa
8.433
7.568
6.703
5.839
4.974
4.109
3.245
2.380
1.515
0.651
Max. 8.433E+007
Min. 6.508E+006

**(a)**

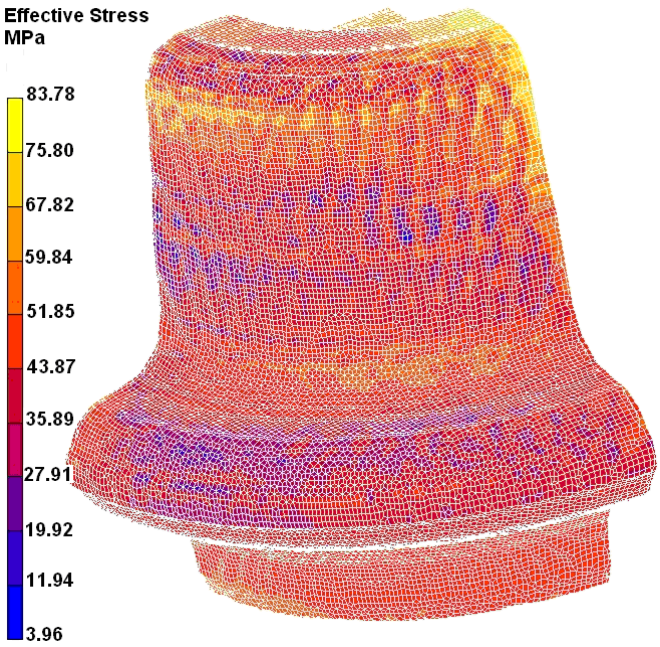


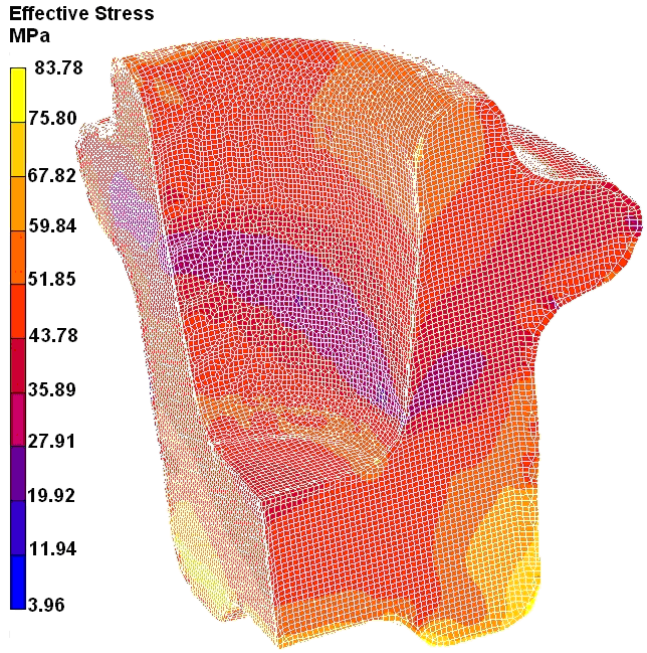


**(b)**

**Figure B.3 Effective Stress Distribution of Preform in (a) MSC. SuperForge (b) MSC. SuperForm for Initial Billet Temperature of 400 °C**

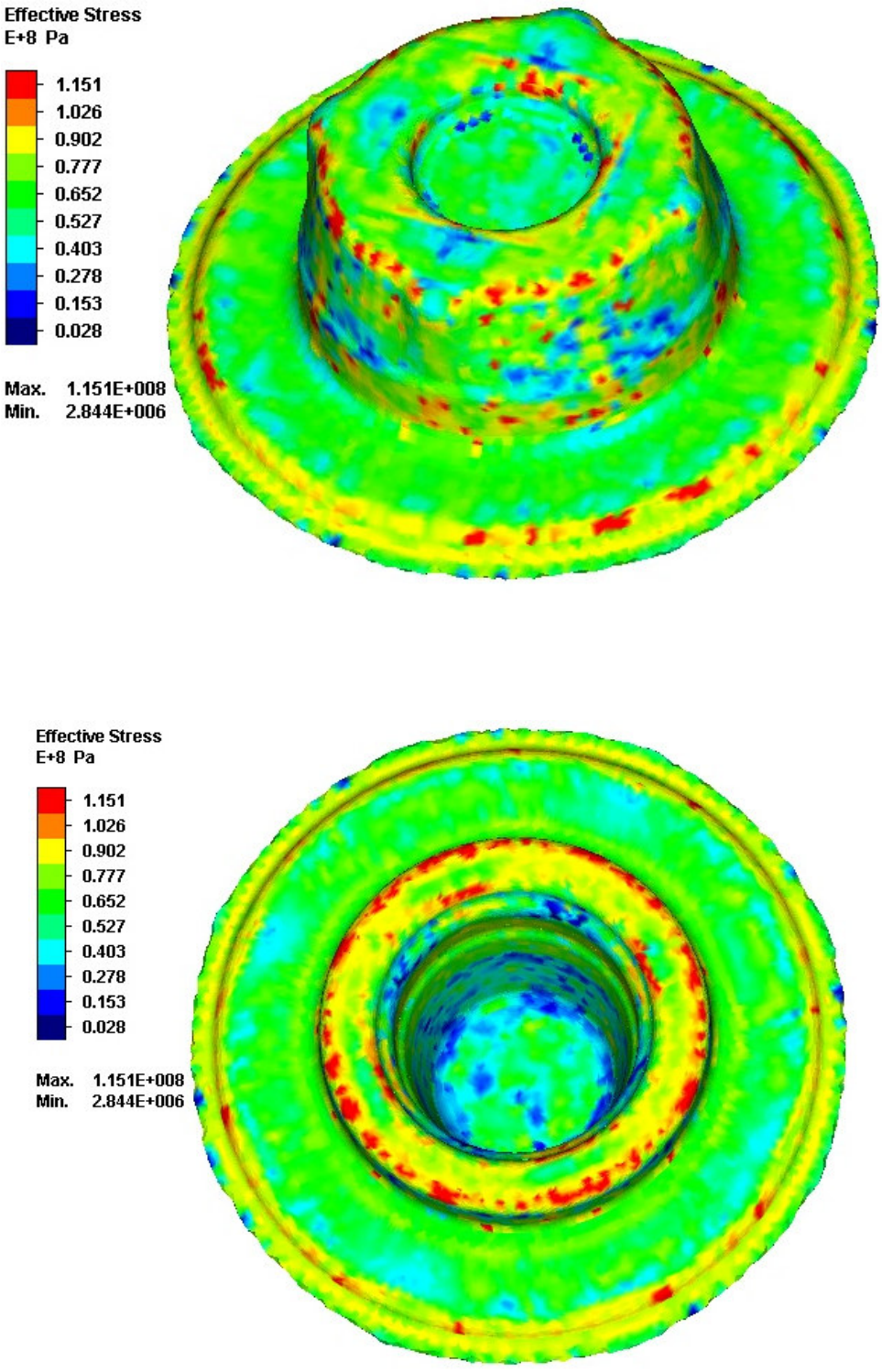
Effective Stress
E+8 Pa
1.151
1.026
0.902
0.777
0.652
0.527
0.403
0.278
0.153
0.028
Max. 1.151E+008
Min. 2.844E+006
Effective Stress
E+8 Pa
1.151
1.026
0.902
0.777
0.652
0.527
0.403
0.278
0.153
0.028
Max. 1.151E+008
Min. 2.844E+006

**(a)**

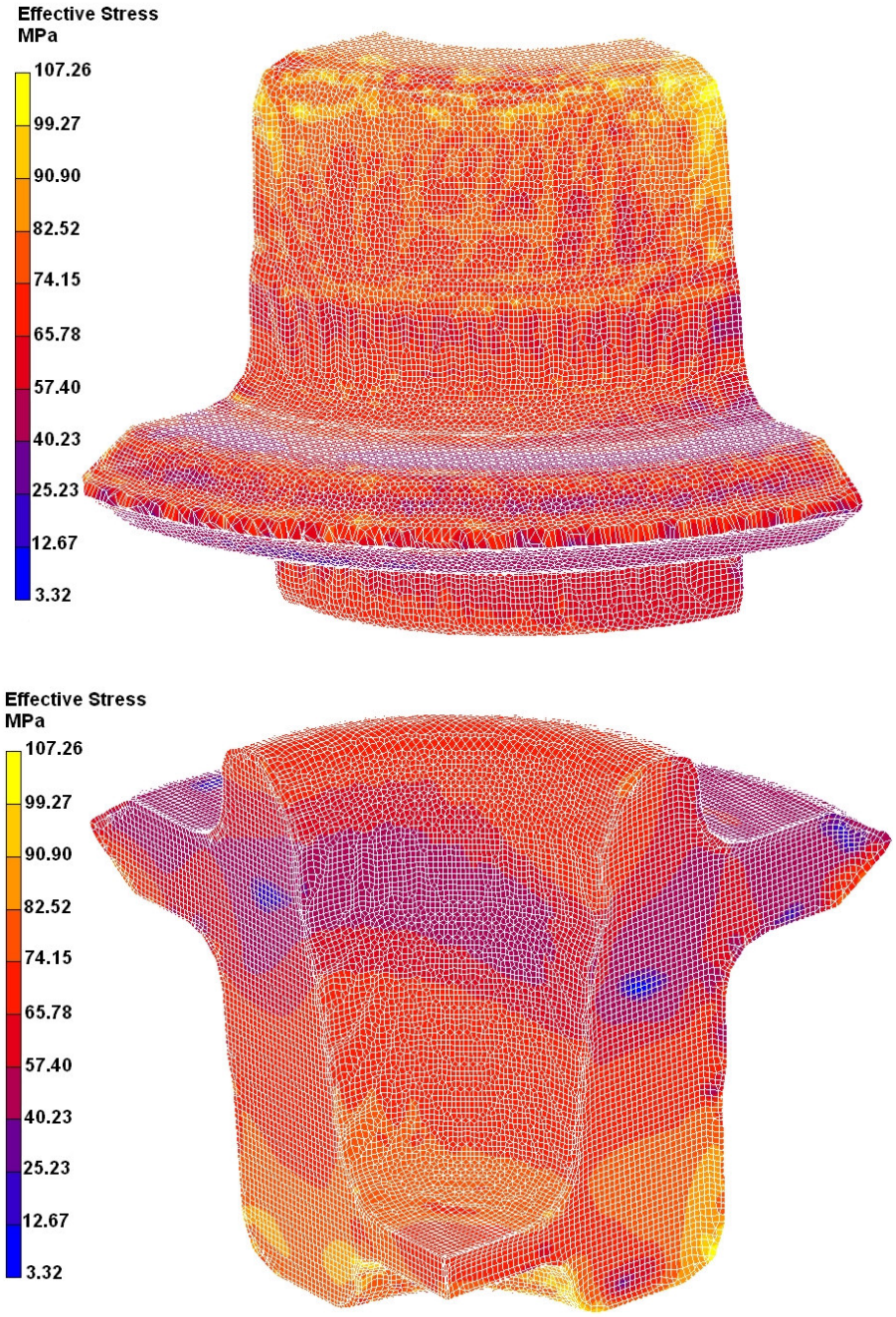


**(b)**

**Figure B.4 Effective Stress Distribution of Finish Part in (a) MSC. SuperForge (b) MSC. SuperForm for Initial Billet Temperature of 400 $^{o}$C**

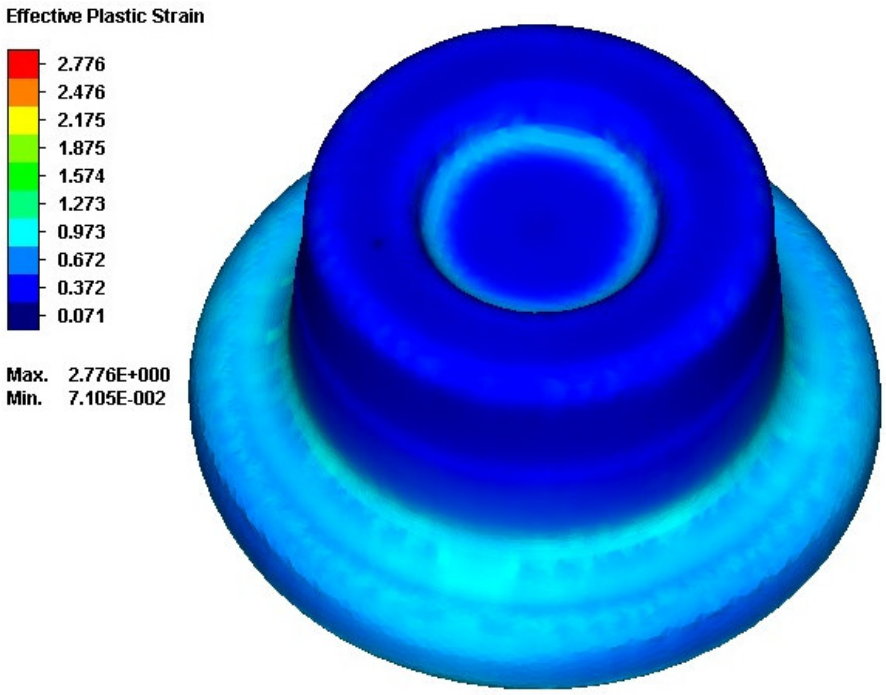
Effective Plastic Strain
2.776
2.476
2.175
1.875
1.574
1.273
0.973
0.672
0.372
0.071
Max. 2.776E+000
Min. 7.105E-002

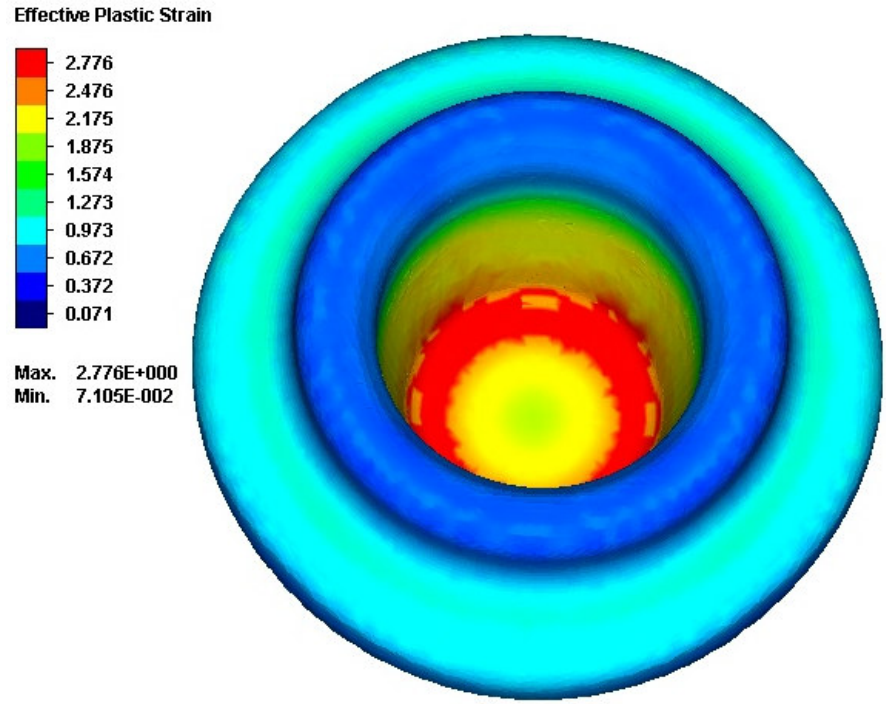
Effective Plastic Strain
2.776
2.476
2.175
1.875
1.574
1.273
0.973
0.672
0.372
0.071
Max. 2.776E+000
Min. 7.105E-002

**(a)**

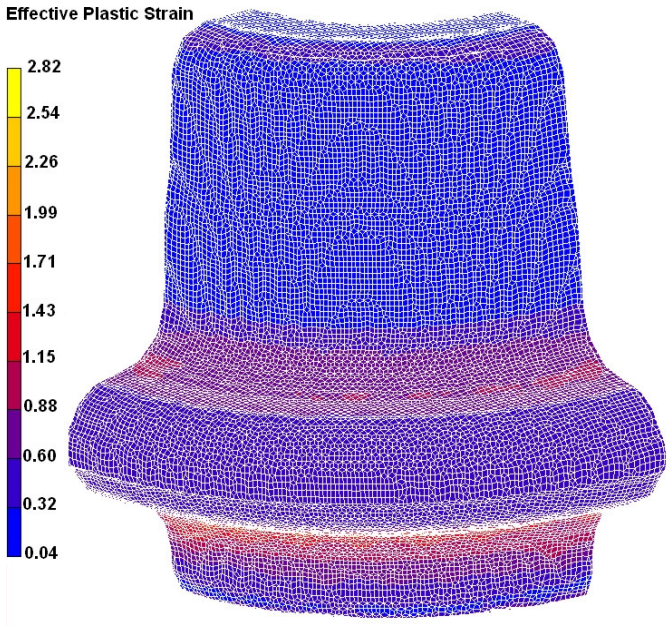


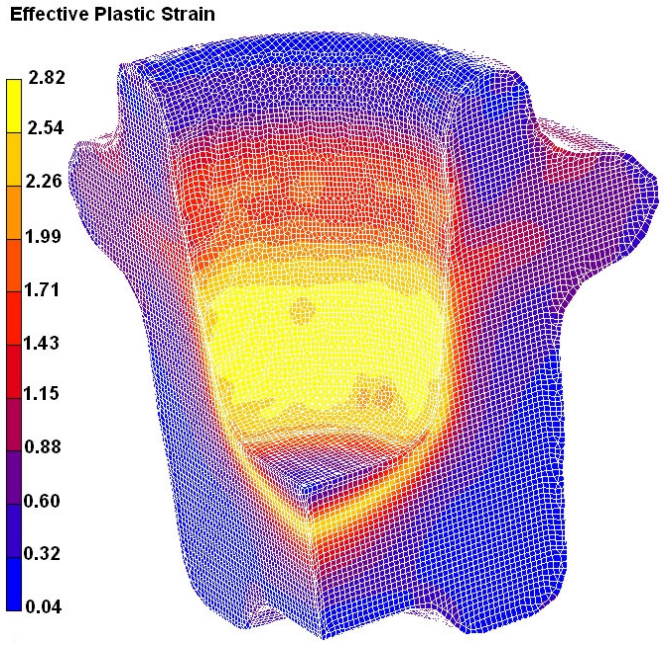


**(b)**

**Figure B.5 Effective Plastic Strain Distribution of Preform in (a) MSC. SuperForge (b) MSC. SuperForm for Initial Billet Temperature of 400 $^{o}$C**

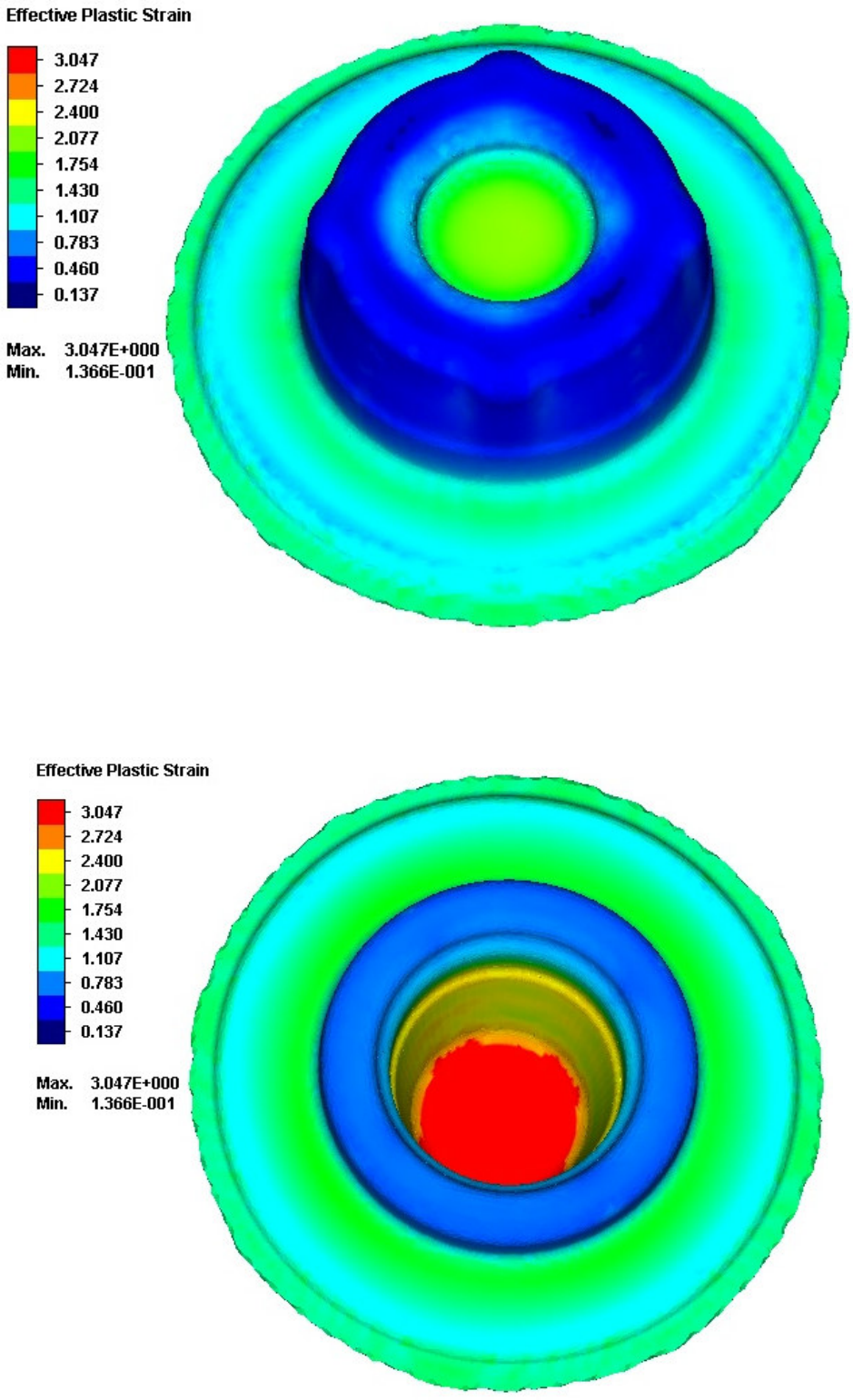
Effective Plastic Strain
3.047
2.724
2.400
2.077
1.754
1.430
1.107
0.783
0.460
0.137
Max. 3.047E+000
Min. 1.366E-001
Effective Plastic Strain
3.047
2.724
2.400
2.077
1.754
1.430
1.107
0.783
0.460
0.137
Max. 3.047E+000
Min. 1.366E-001

**(a)**

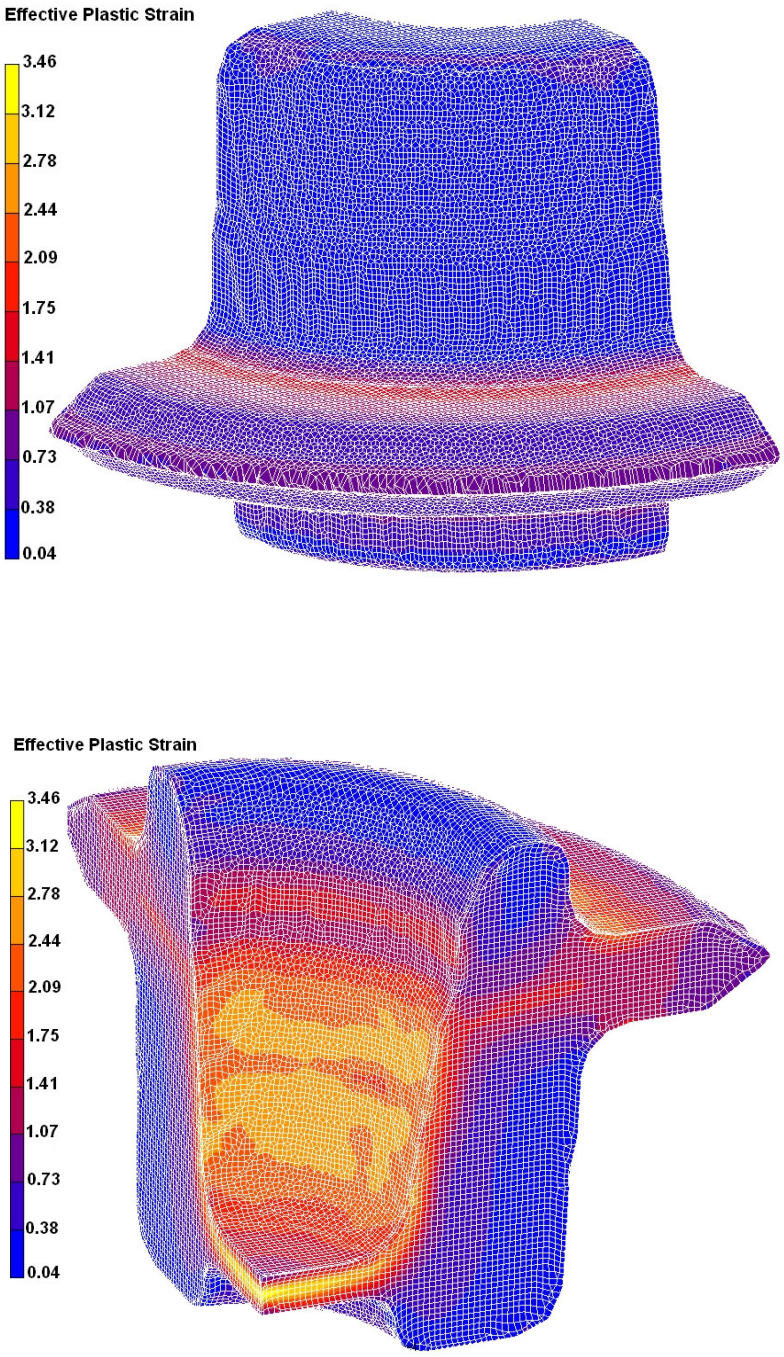


**(b)**

**Figure B.6 Effective Plastic Strain Distribution of Finish Part in (a) MSC. SuperForge (b) MSC. SuperForm for Initial Billet Temperature of 400 $^{o}$C**

**Table B.1 Maximum Temperature, Effective Stress, Effective Strain and Die Load Values in MSC. SuperForge and MSC. SuperForm for Initial Billet Temperature of 400 $^{o}$C**

| | Max. Temp. of Preform (°C) | Max. Temp. of Finish Part (°C) | Max. Effec. Stress in Preform (MPa) | Max. Effec. Stress in Finish Part (MPa) | Max. Effec. Plastic Strain in Preform | Max. Effec. Plastic Strain in Finish Part | Max. Die Load in Preform Stage (N) | Max. Die Load in Finish Stage (N) |
|---|---|---|---|---|---|---|---|---|
| **MSC. SuperForge** | 438.70 | 437.40 | 84.33 | 115.10 | 2.776 | 3.047 | 2.106 x$10^5$ | 7.765 x$10^5$ |
| **MSC. SuperForm** | 441.76 | 434.30 | 83.78 | 107.26 | 2.820 | 3.460 | 2.432 x$10^5$ | 7.963 x$10^5$ |

Although MSC. SuperForge and MSC. SuperForm are based on two different methods, as shown in Figures B1-B6; temperature, effective stress and effective plastic strain distributions on the preform and finish parts for the initial billet temperature of 400 $^{o}$C are similar. Also as shown in Table B.1, maximum values of temperature, effective stress and effective strain on the preform and finish part are very close to each other.

# APPENDIX C

## ENGINEERING DRAWING THE PART

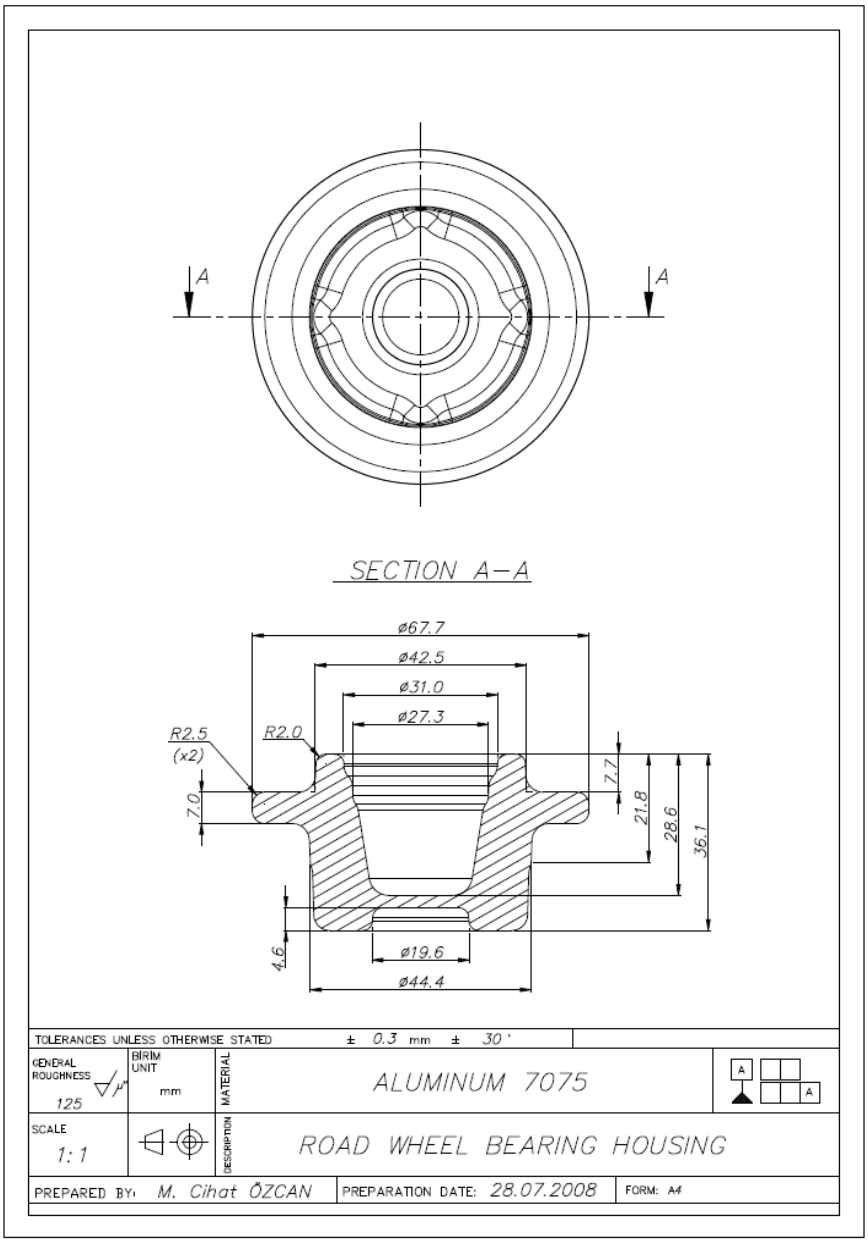


**Figure C.1 Engineering Drawing of the Road Wheel Bearing Housing**

## APPENDIX D

## ENGINEERING DRAWING THE DIES

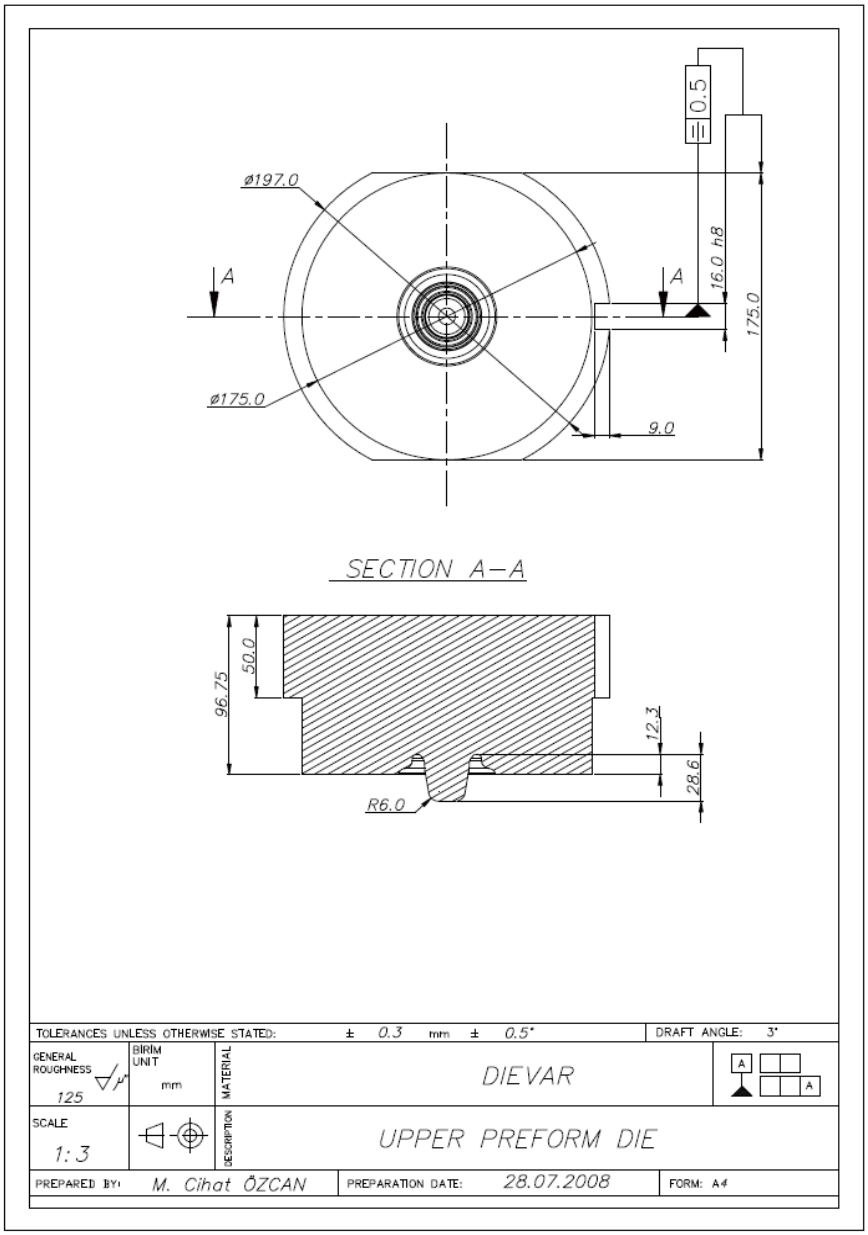


**Figure D. 1 Engineering Drawing of the Upper Preform Die**

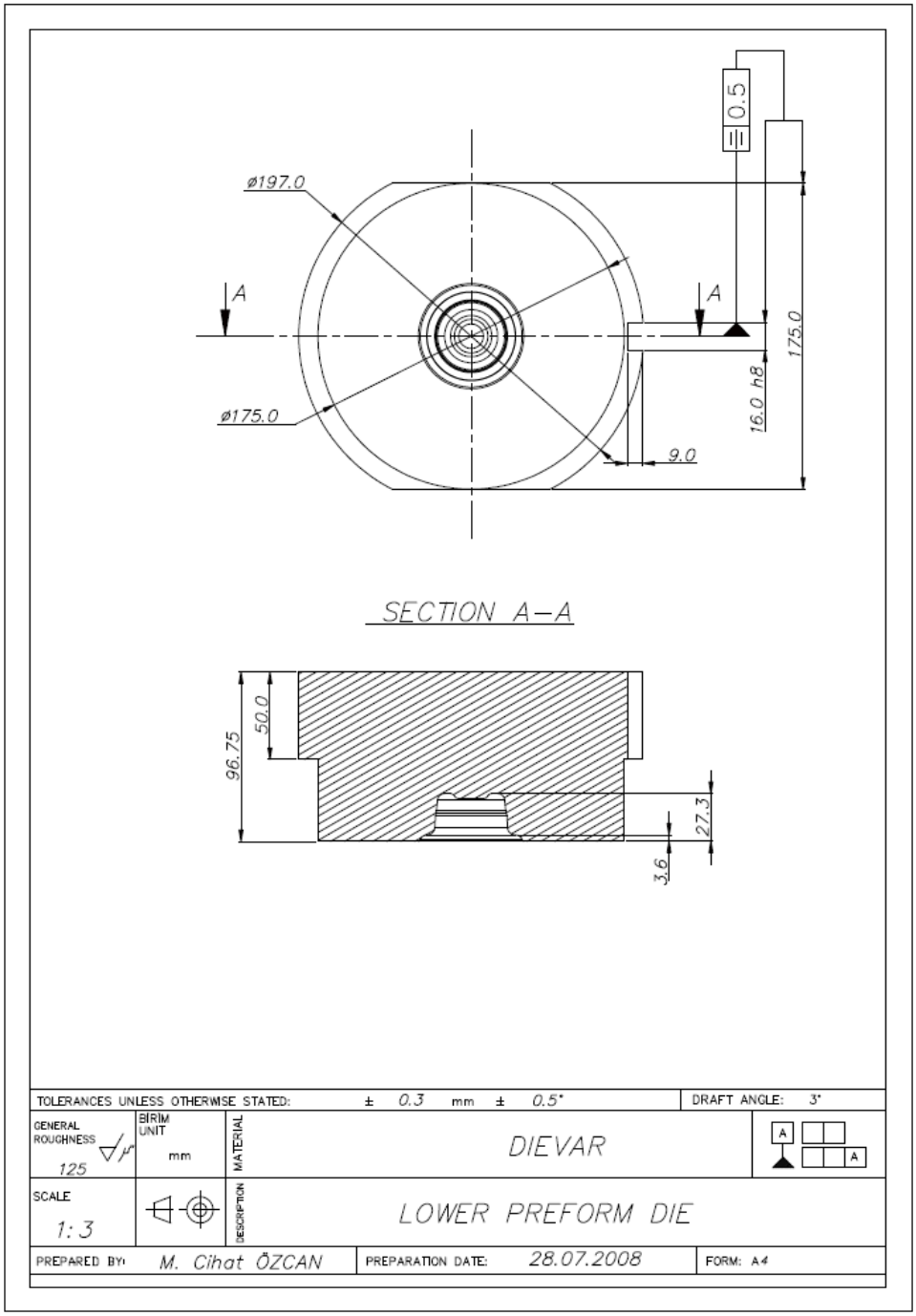


**Figure D. 2 Engineering Drawing of the Lower Preform Die**

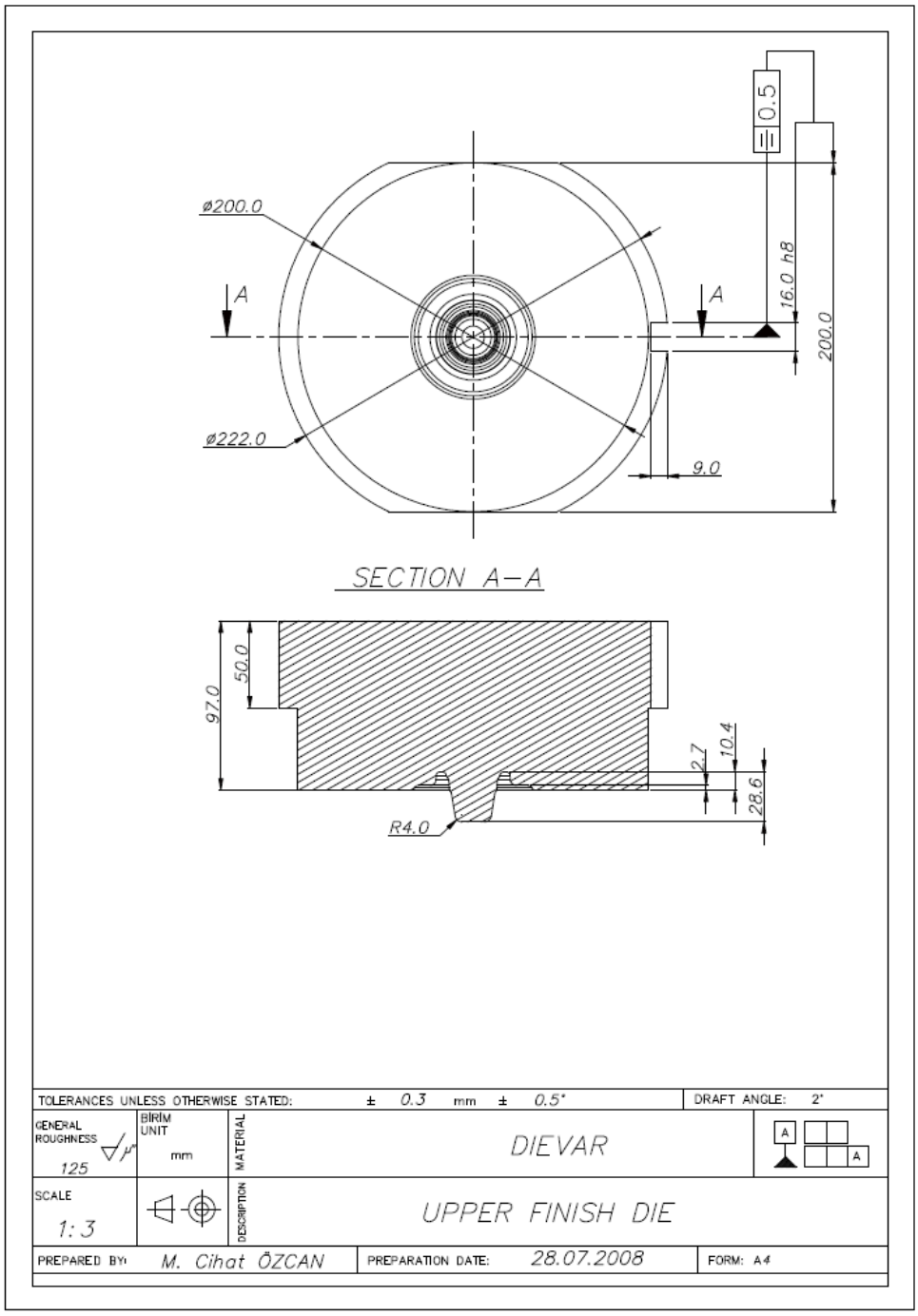


**Figure D.3 Engineering Drawing of the Upper Finish Die**

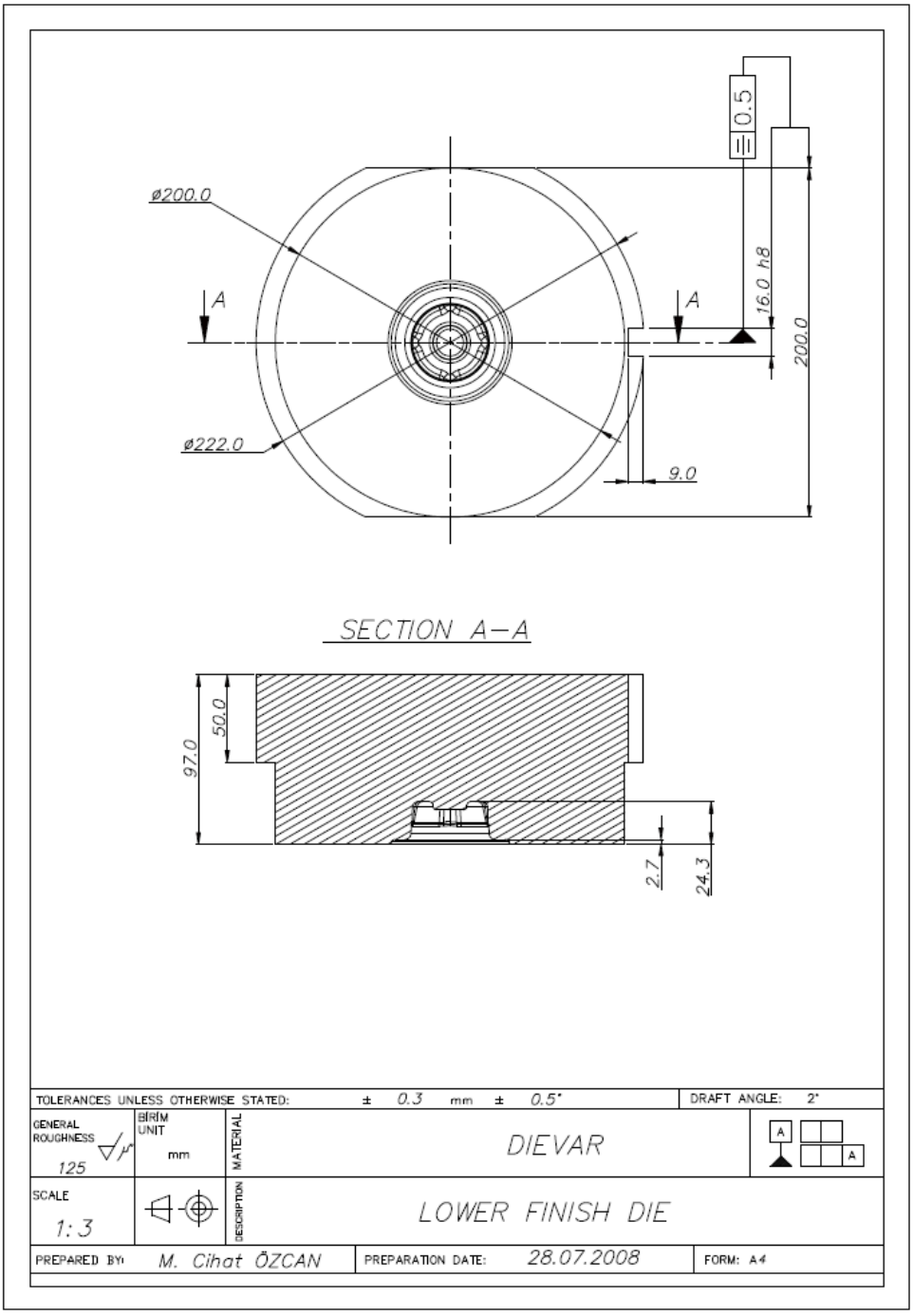


**Figure D. 4 Engineering Drawing of the Lower Finish Die**

## APPENDIX E

## TECHNICAL DATA OF 1000 TON SMERAL MECHANICAL PRESS

| | |
|---|---|
| Nominal Forming Force | : 10 MN |
| Ram Stroke | : 220 mm |
| Shut Height | : 620 mm |
| Ram Resetting | : 10 mm |
| Rod Length | : 750 mm |
| Crank Radius | : 110 mm |
| Number of Strokes at Continuous Run | : 100 $min^{-1}$ |
| Press Height | : 4840 mm |
| Press Height above Floor | : 4600 mm |
| Press Width | : 2540 mm |
| Press Depth | : 3240 mm |
| Press Weight | : 48000 kg |
| Die Holder Weight | : 3000 kg |
| Main Motor Input | : 55 kW |
| Max. Stroke of the Upper Ejector (without die holder) | : 40mm |
| Max. Stroke of the Lower Ejector (without die holder) | : 50 mm |
| Max. Force of the Upper Ejector | : 60 kN |
| Max. Force of the Lower Ejector | : 150 kN |